Elucidating the role of macrophages and $CD4^+CD25^+$ regulatory T cells on colorectal cancer cell invasion

Maria Helena Cristiano Brigas
Master in Cellular and Molecular Biology
Department of Biology
2014/2015

Supervisor
Maria José Cardoso Oliveira, Assistant Researcher, I3S/INEB

Co-Supervisor
Marta Isabel Abreu Oliveira, Assistant Researcher, INL

Todas as correções determinadas pelo júri, e só essas, foram efetuadas.
O Presidente do Júri,

Porto, _____/_____/_____

Acknowledgments

A primeira pessoa a quem tenho de agradecer é à minha orientadora Maria José Oliveira. És das melhores pessoas que conheço. Muito obrigada por teres acreditado em mim e por me teres deixado participar nesta grande aventura. Foi um grande privilégio teres-me confiado um projeto de raiz. Obrigada por todo o conhecimento científico e orientação que me deste na construção e realização deste projeto. Tenho imensa admiração por ti e pelo teu trabalho.

Quero agradecer à minha co-orientadora, Marta Oliveira, que desenhou este projeto e me deu todas as condições para o realizar. Obrigada pelo otimismo, estímulo, compreensão e orientação assim como por todas as contribuições preciosas que deste para este trabalho.

Marta, foste o meu anjinho. Nunca te agradecerei o suficiente por toda ajuda e apoio que me deste. Obrigada por teres estado comigo em toda esta caminhada com toda a tua paciência, disponibilidade e carinho. Ajudaste-me sempre a ver as coisas com mais clareza. Obrigada por todo o conhecimento cientifico e laboratorial que me deste.

Ana, muito obrigada por teres ajudado no planeamento de experiências e teres discutido comigo os resultados. Estiveste sempre disponível para me ajudar quando eu precisava.

Flávia, muito obrigada pelo conhecimento que partilhaste comigo e por todas as discussões científicas que tiveste comigo. Agradeço teres sido sempre sincera e crítica relativamente ao meu trabalho.

Hugo, obrigada pela tua amizade. Obrigada pelo apoio que me deste e por teres tornado os momentos menos fáceis em momentos cheios de alegria (e de comida e de café). A tua paixão pela ciência é contagiante, obrigada.

Mãe, obrigada por seres sempre carinhosa, mas ao mesmo tempo exigente. Deste-me a oportunidade de chegar onde cheguei. Pai, muito obrigada por todo o apoio e preocupação que sempre demonstraste. Obrigada, por acreditares em mim e por me estimulares a dar sempre o melhor de mim. Agradeço ao meu irmão e à minha irmã por acreditarem mais em mim do que qualquer outra pessoa. Obrigado por me terem apoiado em todos os momentos stressantes e por estarem sempre prontos para me ajudar.

Gustavo, tenho de te agradecer por todas os conselhos que me deste e todo amor, compreensão e paciência que tiveste comigo durante este ano. Muito obrigada.

Abstract

Solid tumours became malignant when cancer cells invade the surrounding tissues, becoming prone to intravasate blood and lymph vessels and to metastasize. In solid tumours, tumour-associated macrophages (TAMs) and regulatory T cells (Tregs) are reported to favour tumour progression. However, in colorectal cancer (CRC) their intratumour infiltration often correlates with good prognosis. Depending on the tumour microenvironment, TAMs may polarize into a pro- or an anti-inflammatory profile, modulating cancer cell activities and participating in tumour progression. On their turn, Tregs may steer macrophage differentiation, modulating macrophage inflammatory profile and functions within the tumour microenvironment.

This study aims to elucidate how TAM-$CD4^+CD25^+$ Treg crosstalk affects macrophage phenotype, clarifying the role of Treg-educated macrophages on cancer cell invasion, as well as dissecting the underlying invasion-related pathways. Therefore, macrophage precursors and $CD4^+CD25^+$ T cells were co-cultured at 1:1 and 2:1 ratios, for 3 or 7 days. The monocyte-macrophage profile was then assessed through the analysis of specific cell surface receptor expression and cytokine secretion. The impact of $CD4^+CD25^+$ T cells-educated macrophages on RKO and SW620 CRC cell invasion was evaluated through 3D-matrigel-invasion-assays and through analysis of the matrix metalloproteinases (MMPs) proteolytic profile. Phosphorylation of epidermal growth factor receptor (EGFR) and of its downstream regulators was also evaluated as part of the invasion-related pathway. Furthermore, FoxP3-positive cell infiltration on human CRC specimens was characterized by immunohistochemistry.

Our results evidenced that $CD4^+CD25^+$ Treg-educated macrophages lost CD80 maintaining the expression of CD163 and displaying a mixed pro- and anti-inflammatory cytokine secretion profile. Only RKO cell invasion was significantly promoted by soluble factors produced by macrophages and macrophage/$CD4^+CD25^+$ Treg co-cultures, but not by Tregs alone. At 2:1 ratio co-cultures, macrophage pro-invasive properties were enhanced. This effect was concomitant with increased pro-MMP9 activity and with the activation of EGFR (at the residue Y^{1086}). In addition, using histopathological sections derived from human CRC specimens, we observed that FoxP3-positive cells infiltrate preferentially at the tumour nest and at the invasive front.

In conclusion, our *in vitro* results suggest that $CD4^+CD25^+$ T cells modulate macrophages toward a more anti-inflammatory profile and that, at 2:1 ratio, they promoted

macrophage pro-invasive activities. The higher FoxP3 infiltration found at the tumour nest and at the invasive front of CRC patient surgical resections are supported by previous reports. In the future, we intent to cross CRC FoxP3^{+} subpopulation characterization and TAMS differentiation profile with patients' clinicopathological information. This research will elucidate the modulatory role of Tregs on macrophage pro-tumour properties, contributing to the design of novel therapeutic strategies targeting macrophages and/or Tregs.

Keywords: *Tumour microenvironment; M1-like pro-inflammatory macrophages; M2-like anti-inflammatory macrophages; Regulatory T cells; Colorectal cancer cell invasion; Invasion-related EGFR pathway; Matrix metalloproteinases*

Resumo

Os tumores sólidos tornam-se malignos quando as células tumorais ultrapassam os limites dos tecidos, tornando-se capazes de entrar nos vasos sanguíneos e linfáticos e metastisar. Nos tumores sólidos, os macrófagos associados ao tumor (TAMs) e os linfócitos T reguladores (Tregs) estão descritos como promotores da progressão tumoral. No entanto, no cancro colorretal (CRC) a sua elevada infiltração intratumoral está geralmente associada a bom prognóstico. De acordo com o microambiente tumoral, os macrófagos podem diferenciar-se em pró- ou anti-inflamatórios, modelando a atividade das células tumorais e participando na progressão tumoral. Por sua vez, os Tregs podem modelar a diferenciação dos macrófagos, modelando o seu perfil inflamatório e as suas funções dentro do microambiente tumoral.

Com este projeto pretende-se elucidar como é que a interação TAM-$CD4^+CD25^+$ Treg afeta o fenótipo dos macrófagos, regulando a sua capacidade de estimular a invasão das células tumorais, bem como identificar as vias de sinalização envolvidas nessa atividade. Para tal, os precursores dos macrófagos (monócitos) e as células T $CD4^+CD25^+$ foram co-cultivados nos rácios 1:1 e 2:1, durante 3 ou 7 dias. O perfil de diferenciação monócito-macrófago foi assim caraterizado através da análise da expressão de recetores celulares de membrana específicos e da produção de citocinas. O impacto dos macrófagos, diferenciados na presença de células T $CD4^+CD25^+$, na invasão das linhas colorectais RKO e SW620 foi avaliado por ensaios de invasão 3D em Matrigel e por análise do perfil proteolítico de metaloproteases da matriz (MMPs). A fosforilação do recetor do fator de crescimento epidérmico (EGFR) e dos seus reguladores a jusante foram avaliadas, como parte de uma via de sinalização associada à invasão. Por último, a infiltração de células FoxP3 positivas nos tumores de doentes com cancro colorectal foi caraterizada por imunohistoquímica.

Os nossos resultados demonstram que os macrófagos diferenciados na presença de células T reguladoras $CD4^+CD25^+$ perderam a expressão de CD80, mantendo a expressão de CD163 e apresentando um perfil inflamatório misto com secreção de citocinas pró- e anti-inflamatórias. Os macrófagos e as co-culturas de macrófagos/$CD4^+CD25^+$ Tregs, mas não as Tregs sozinha, produziram fatores solúveis que estimularam apenas a invasão das células RKO. No entanto, a capacidade pró-invasiva dos macrófagos foi maior no rácio 2:1. Este efeito foi concomitante com o aumento da atividade da pró-MMP9 e da ativação do EGFR (no resíduo Y^{1086}). Recorrendo a cortes histopatológicos provenientes de

amostras de pacientes com cancro colorrectal, observámos que as células FoxP3-positivas estão preferencialmente infiltradas na região intratumoral e na frente invasiva.

Concluindo, os nossos resultados *in vitro* sugerem que as células T $CD4^+CD25^+$ modelam os macrófagos para um perfil mais anti-inflamatório e que, no rácio 2:1, promovem as propriedades pró-invasivas dos mesmos. O nível elevado de células FoxP3 positivas, encontradas no centro do tumor e na frente invasiva de recidivas cirúrgicas de pacientes com CRC, está de acordo com a literatura. No futuro, pretendemos cruzar a caracterização das populações $FoxP3^+$ com o perfil de diferenciação dos macrófagos nas amostras de CRC e com a informação clinico-patológica dos pacientes. Esta investigação permitirá elucidar o papel Tregs na modelação das propriedades pró-tumorais dos macrófagos, contribuindo para o planeamento de novas estratégias terapêuticas que tenham como alvo os macrófagos e/ou os Tregs.

Palavras-chave: Microambiente tumoral; Macrófagos pró-inflamatórios tipo-M1; Macrófagos anti-inflamatórios tipo-M2; Linfócitos T reguladores; Invasão das células de cancro colorretal; Invasão mediada pela via do EGFR; Metaloproteases da matriz.

Contents

List of figures and tables

List of Abbreviations

ACF – Aberrant crypt focus

Akt – v-AKT murine thymoma viral oncogene homologue

APC – Antigen-presenting cells

APC – Allophycocyanin

ATCC – American type culture collection

aTreg – Activated regulatory T cell

Avidin-HRP D – Horseradish peroxidase avidin D

CAC – Colitis-associated colorectal cancer

$CaCl_2$ – Calcium chloride

cAMP – Cyclic adenosine monophosphate

CCL – Chemokine ligand

CD – Cluster of differentiation

Cdc42 – Cell division cycle protein 42

CM – Conditioned media

CO_2 – Carbon dioxide

CpG – Cytosine-phosphate-Guanine

CRC – Colorectal cancer

CSF-1 – Colony stimulating factor-1

c-Src – Cellular Homologue of Rous sarcoma virus protein

CTL – Cytotoxic T lymphocyte

CTLA-4 – Cytotoxic T-lymphocyte antigen 4

CXCL – Chemokine (C-X-C motif) ligand

DAPI – 6-diamidino-2-phenylindole

DC – Dendritic cell

DNA – Deoxyribonucleic acid

ECM – Extracellular matrix

EDTA – Ethylenediaminetetraacetate

EGF – Epidermal growth factor

EGFR – Epidermal growth factor receptor

ELISA – Enzyme-linked immunosorbent assay

EMT – Epithelial-mesenchymal transition

ERK1/2 – Extracellular regulated MAP kinase1/2

FAP – Familial adenomatous polyposis

FACS – Fluorescence-activated cell sorting

FBS – Fetal bovine serum

FITC – Fluorescein isothiocyanate

FSC – Forward scatter

FoxP3 – Forkhead box protein 3

Gab1 – GRB2-associated binding protein-1

GM-CSF – Granulocyte-macrophage colony-stimulating factor

GTP – Guanosine-5'-triphosphate

GITR – Glucocorticoid induced TNFR family-related protein

H_2O_2 – Hydrogen peroxide

HA – Hyaluronic acid

HCl – Hydrochloric acid

HLA-DR – Human leukocyte antigen-D related

HNPCC – Hereditary nonpolyposis colorectal cancer

HRGβ1 – Heregulin β1

IBD – Inflammatory bowel disease
ICC – Immunocytochemistry
IDO – Indoleamine 2,3-dioxygenase
IF – Tumour invasive front
IFN – Interferon
Ig – Immunoglobulin
IL – Interleukin
IL – 2Rα Interleukin-2 receptor α-chain
iNOS2 – Inducible nitric oxide synthetase tyoe 2
iTreg – Induced regulatory T cell
K-RAS – Kirsten rat sarcoma viral oncogene homologue
LPS – Lipopolysaccharide
M1 – M1-like pro-inflammatory macrophage
M2 – M2-like anti-inflammatory macrophage
mAB – Monoclonal antibody
Mac – Macrophage
MCP-1 – Monocyte chemoattractant protein-1
MHC – Major histocompatibility complex
MIP- 1β – Macrophage inflammatory protein-1β
MIP-1α – Macrophage inflammatory protein-1α
MMP – Matrix metalloproteinase
MMR – Mismatch repair
MSI – Microsatellite instability
NaF – Sodium fluoride
NCM – Normal colonic mucosa
NK – Natural killer
nTreg – Natural regulatory T cell
ON – Overnight
P53 – Tumour protein-53
PB – Peripheral blood
PBMC – Peripheral blood mononuclear cell
PBS – Phosphate buffered saline
PDGF – Platelet derived growth factor
PDL1 – Programmed cell death protein 1
PE – Phycoerythrin
PFA – Paraformaldehyde
PGE2 – Prostaglandin E2
PI1-K – Phosphatidylinositol 3-kinase
PIGF – Placental growth factor
PLC-γ – Phospholipase C-gamma
PMF – Phenylmethylsulfonyl fluoride
RAF/MAPK – Raf-mitogen-activated protein Kinase
RANTES – Regulated on activation, normal T cell expressed and secreted
RA
RIPA – Radioimmunoprecipitation assay
RFU – Relative fluorescence units
RhoA – Ras homolog gene family, member A
RT – Room temperature
rTreg – Resting regulatory T cell
SC – Stem cell
SD – Standard deviation
SDF-1 – Stromal-derived factor 1
SDS – Sodium dodecyl sulfate
SMAD – Contraction of Sma and Mad (Mothers against decapentaplegic)
SSC – Side scatter

STAT – Signal transducer and activator of transcription

TAM – Tumour-associated macrophage

Tconv – Conventional T cell

TCR – T cell receptor

TGFBRII – Type II TGFβ receptor

TGF-β – Transforming growth factor-beta

Th – T helper cell

TILs – Tumour-infiltrating lymphocytes

TLR – Toll-like receptor

TMB – 3,3',5,5'-tetramethylbenzidine

TME – Tumour microenvironment

TN – Tumour nest

TNF-α – Tumour necrosis factor-alpha

Tr3 – Type-3 regulatory T cells

Tr1 – Type-1 regulatory T cells

Tregs – Regulatory T cells

TSDR – Treg-specific demethylated region

tTGF-β – Total transforming growth factor-beta

VEGF – Vascular endothelial-growth factor

Introduction

1. Cancer

Cancer is a progressive disease that occurs by a multistep regulated process. Typically, it arises from a series of mutations and epigenetic alterations that encompass gain of function of oncogenes and loss of function of tumour suppressor genes. These series of genetic changes confer growth advantages to proliferating cells and drive normal cells to transform into a neoplasic state. The progression of solid malignancies is reflected in the genetic heterogeneity of tumour cell subpopulations that share a common genetic background within a tumour[1,2]. In fact, only 10% of cancers are linked to germline mutations while the vast majority are caused by somatic mutations and environmental factors[3].

1.1. Colorectal Cancer

1.1.1. Epidemiology

Colorectal cancer (CRC) is the third cause of cancer-related death worldwide[4] and one of the most frequent and deadliest cancer in Portugal (Globocan, 2012), being a major health concern in industrialized and developed countries. Moreover, its incidence is increasing in developing countries, while remaining low in less-developed countries[5]. Environmental risk factors such as an inadequate dietary pattern, obesity, tobacco-smoking, excessive alcohol intake and sedentarism are considered to increase CRC risk[6]. These environmental factors have been associated with intestinal microbiota alterations and modifications on crucial molecular pathways related to CRC tumourigenesis[5]. Besides dietary and lifestyle factors, inherited and somatic mutations, epigenetic changes, as well as chronic intestinal inflammation have also prominent roles in CRC occurrence[5].

Despite advances in CRC diagnosis, knowledge of novel biomarkers and therapies, many patients with advanced or metastatic disease, or with local recurrence following primary tumour resection, will still die from this disease[7]. This stands out the need for early detection, diagnosis and more effective non-invasive treatments.

1.1.2. Pathogenesis

The molecular basis underlying the progression of CRC is still subject of intense research. Typically, CRC is driven by the gradual accumulation of genetic mutations and epigenetic modifications. These modifications induce the activation of oncogenes or loss of function of

tumour suppressor genes in proliferating cells, driving the neoplastic process[9]. Histological changes which result in the transition from normal colon mucosa to adenomas and from adenomas to invasive carcinomas may them occur[8].

The bulk of CRC cases are sporadic (80%) and result from somatic mutations arising during patients' lifetime. The other 20% have a hereditary component, frequently associated with the hereditary nonpolyposis colorectal cancer syndrome (HNPCC or Lynch syndrome) and the familial adenomatous polyposis (FAP), and arise from subtle germ-line mutations[10].

In general, the earliest and most common mutation in CRC is the inactivation of *adenomatous polyposis coli* (*APC*), a tumour-suppressor gene. Consequently, there is an overactivation of the wingless-type(Wnt)/β-catenin signalling pathway, favouring transcription of tumour-promoting genes and cell growth. This mutation underlies the FAP cases, as well as 70–80% of all sporadic CRCs, being frequently found in the aberrant crypt focus (ACF), the first identifiable lesion in CRC formation[10].

Subsequent mutations in other genes, most prominently *K-RAS*, *P53* and *TGFBRII*, are related to colon carcinogenesis. The proto-oncogene *Kirsten rat sarcoma* (*K-RAS*) encodes highly conserved proteins involved in signal transduction. By overactivation of the Raf-mitogen-activated protein Kinase (RAF/MAPK), JNK and phosphatidylinositol 3-kinase (PI3K) pathways[11], K-RAS mutations favour carcinoma growth. This is an early mutational event that underlies the transition from early to intermediate adenoma and occurs in 37-41% of CRCs[11]. Tumour protein-53 (P53) is a tumour suppressor transcription factor which regulates cell-cycle arrest, genomic stability and apoptosis[12]. When mutated, *P53* may foster the malignant transition from intermediate adenoma to carcinoma. Progression of CRC can also involve alteration of the TGF-β signalling pathways through mutations in *type II TGFβ receptor* (*TGFβRII*) gene, that occur in 30% of CRCs[13], or in members of these pathways namely in *SMAD4/2*. Genetic mutations in TGF-β signalling are frequently associated with microsatellite instability (MSI). MSI, characterized by insertion and deletion in repetitive DNA sequences due to the failure of DNA mismatch repair (MMR) mechanisms, gives rise to 15% of sporadic CRC and is highly associated with the HNPCC syndrome.

Epigenetic mechanisms, such as DNA methylation of CpG islands and pos-translational modifications of histones, have also a prominent role in the alteration of chromatin conformation and consequently may favour the transcription of genes that mediate CRC development[14]. Furthermore, specific bacterial pathogens as well as gut microflora and its metabolites can induce DNA damage, cell apoptosis and pro-inflammatory

conditions, thus promoting colon carcinogenesis[15]. In fact, individuals with inflammatory bowel disease (IBD) display an increased incidence of CRC[16].

All of the above mentioned factors can act in concert to promote CRC development and malignant progression, ultimately leading to cancer cell spreading and dissemination to distant organs, primarily to the liver[17].

2. The tumour microenvironment

Typically, tumour formation comprises collaborative interactions between neoplastic cells and the surrounding host microenvironment. This intercellular communication occurs through a complex and dynamic network of cytokines, chemokines and matrix remodelling enzymes that will dictate the tumour fate[18]. In general, when solid tumours emerge, the immune system initiates an anti-tumour response that actively eliminates antigen-expressing tumour cells, characteristic of a T helper (Th)1-like inflammatory response. However, over time, tumour cells elicit several changes in the surrounding stroma and escape the host response, shifting the immune environment from a Th1- towards a Th2-type[19]. In this way, malignant cells can instruct non-malignant stroma elements to support and promote tumour growth, survival, spread and even to affect response to treatment[20,21]. Therefore, together with cancer cells, immune cells, fibroblasts, pericytes, extracellular matrix (ECM) components, blood and lymphatics vessels constitute the tumour microenvironment (TME) (Figure 1)[21]. The immune infiltrate found at the TME can include multiple cell types. These populations can display both pro- and anti-tumour functions and can vary in their activation status, density and localization within the tumour[22]. Macrophages and regulatory T cells (Tregs) are key mediators between tumour cells and stroma components and are highly represented in most neoplastic tissues, including CRC[23,24]. The complete understanding of the tumour biology encompasses the study of cellular and molecular interactions in the TME that will open novel avenues for enhanced therapeutics and better clinical outcomes[21].

3. Macrophages

Mononuclear phagocytes play an essential role in innate immunity and regulate adaptive responses[25]. Tissue macrophages derive from embryonic haematopoietic progenitors that persist and maintain the macrophage pool into adulthood[26]. However, in tissues that are exposed to microbiota (e.g. skin and gut) or under extensive inflammatory conditions, blood

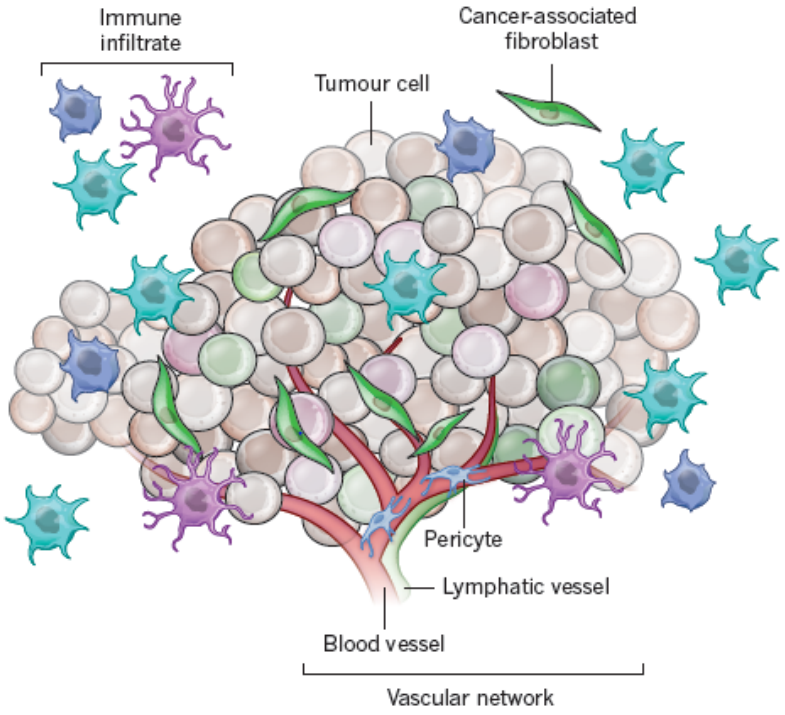

Figure 1. The tumour microenvironment. Tumours are highly complex niches composed by tumour cells, host cells such as pericytes, immune cells and fibroblasts, vascular network (blood and lymph vessels) and extracellular matrix components. The molecular crosstalk established between tumour cells and the surrounding microenvironment dictates tumour fate. Adapted from Junttila et al. (2013) *Nature Reviews*.

monocytes can differentiate into tissue macrophages [27]. Macrophages are highly diverse cells capable of undergoing phenotypic switches depending on environmental cues and on the milieu found at the tissue site[28]. Macrophages may undergo a classical M1-like activation (stimulated by IFN (interferon), IFN/LPS (lipopolysaccharide) and Toll-like receptor (TLR) ligands or an alternative M2-like activation (induced by IL-10, IL-4/IL-13, IL-33, IL-21)[29-31]. These states mirror the Th1/Th2 dichotomy of T cells and represent two extremes of a continuum spectrum of activation. M1-like macrophages express high levels of co-stimulatory receptors for lymphocytes (CD86/CD80, CD40), antigen-presenting molecules (MHC-class II such as human leukocytes antigen-D related protein [HLA-DR]) and produce high levels of pro-inflammatory cytokines (e.g. interleukin (IL)-6, tumour necrosis factor-alpha (TNF-α), IL-12, IL-23 and IL-1β). They target infectious agents or damaged cells, promoting cytotoxic activities[28,29]. Alternatively, M2-like macrophages display high phagocytic activity, high expression of the hemoglobin-scavenger receptor (CD163) and of the mannose receptor (CD206) and secrete anti-inflammatory cytokines (e.g. IL-10 and transforming growth factor-beta (TGF-β))[29,32]. This macrophage subtype contributes to

parasite clearance[33], tissue remodelling[34], tumourigenesis[28,32] and tumour progression[35]. The distinct functional profile of M1/M2 subsets is further reflected in the selective recruitment of other immune cells, such as T cells. While M1-like macrophages induce the recruitment of helper (Th1 and Th17) and cytotoxic T lymphocytes (CTL), by producing CXCL9 and CXCL10, M2-like macrophages recruit Th2 and regulatory T cells (Tregs), by releasing CCL17, CCL22 and CCL24[36,37]. In established tumours, the presence of pro-inflammatory Th1, Th17 cells and CTL within the tumour is associated with an anti-tumour immune response, whereas the presence of Th2 and Tregs is frequently linked to anti-tumour immune escape[38].

3.1. Macrophages and cancer

In the majority of the solid tumours, macrophages dominantly infiltrate the tumour microenvironment and are frequently associated with tumour initiation, progression and metastasis (Figure 2)[3,39-41]. Macrophage-mediated tumourigenesis is tightly related with an inflammatory microenvironment, which promotes mutagenesis and growth of tumour cells[3]. In a developing primary tumour, macrophages hamper the adaptive immune system, particularly T cells' response, and promote angiogenesis, tumour cell migration, invasion and intravasation[39,42]. At the metastatic site, macrophages induce tumour cell extravasation, survival and growth[39]. Different subpopulations of macrophages underlie each of these pro-tumour activities, highlighting these cells as attractive targets for anticancer therapies[39].

Typically, blood monocytes are chemoattracted from the periphery to the tumour site by growth factors (colony stimulating factor-1 (CSF-1), vascular endothelial-growth factor (VEGF), placental growth factor (PIGF)) and/or by potent chemoattractant chemokines (macrophage inflammatory protein-1α [MIP-1α] (CCL3), MIP-1β (CCL4), regulated on activation, normal T cell expressed and secreted [RANTES] (CCL5), macrophage-derived chemokine (CCL22))[40,43,44]. Once within the tissues, monocytes differentiate into tumour-associated macrophages (TAMs) that share functional features with M2-like (anti-inflammatory) macrophages, reflecting the Th2-like anti-inflammatory response found at the tumour site[25]. M2-like macrophage polarization can be induced by IL-4, released from tumour cells or $CD4^+$ T cells[42], as well as by tumour cell-derived growth factors, like tumour granulocyte-macrophage colony-stimulating factor (GM-CSF) and colony-stimulating factor type 1 (CSF1)[45]. During tumour progression, TAMs levels are maintained by the proliferation of recruited monocytes or of resident macrophages and by their retention at the tumour site[46].

3.1.1. Tumour cell survival and growth

In general, TAMs and lymphocytes produce IL-6, which is described as promoting tumourigenesis, tumour cell survival and growth[47]. The excess of this pro-inflammatory cytokine activates the transcription factor signal transducer and activator of transcription 3 (STAT3)[48], one of the major components of cancer-related inflammation[47]. The loss of the anti-inflammatory cytokine IL-10, that acts through STAT3, also enhanced carcinogen-induced tumourigenesis in the intestine[15]. Increased activation of STAT3 is also linked to enhanced tumour cell growth and survival, invasion, metastasis, and modulation of tumour-promoting T-cell subtypes[49]. At high concentrations tumour necrosis factor-alpha (TNF-α), one of the major mediators of inflammation, is also able to induce tumourigenesis[50].

3.1.2. Tumour cell invasion

The ability of cancer cells to cross tissue boundaries and invade neighbouring areas is what confers them malignancy. In breast cancer, macrophages were described as obligate partners in cancer cell migration, invasion and metastasis[35]. Cancer cell-derived CSF1 was described to induce macrophage secretion of epidermal growth factor (EGF), which in turn activates cancer cell EGF receptor (EGFR), stimulating tumour cell migration and invasion[51-54]. Moreover, it was described that macrophages are able to induce an angiogenic switch[55] and that tumour cell intravasation occurred in association with perivascular macrophages[52]. The relevance of this CSF1-EGF loop was further confirmed when ablation of macrophages, through depletion of CSF1, decreased circulating tumour cells and metastasis[52]. Further, the use of CSF1R antagonists inhibited the migration of both tumour cells and macrophages[56]. In line with these results, our team described that soluble factors produced by human macrophages promoted gastric and colorectal cancer cell invasion, motility, migration and proteolysis[57]. These results were described to be dependent on matrix metalloproteinase (MMP)-9 and 2 activities and on the activation of EGFR (at the residue Y^{1086}), PLC-γ (phospholipase C-gamma), Gab1 (GRB2-associated binding protein-1), cSrc (Cellular Homologue of Rous sarcoma virus protein) and ERK1/2 (Extracellular regulated MAP kinase1/2). When EGF was depleted from the medium, macrophage-mediated cancer cell invasion and motility was impaired, suggesting EGF as one of the major pro-motile and pro-invasive factors produced by macrophages. Further, macrophages also induced phosphorylation of Akt (v-AKT murine thymoma viral oncogene homologue), and increased RhoA (Ras homolog gene family, member A) and Cdc42 (Cell division cycle protein 42)

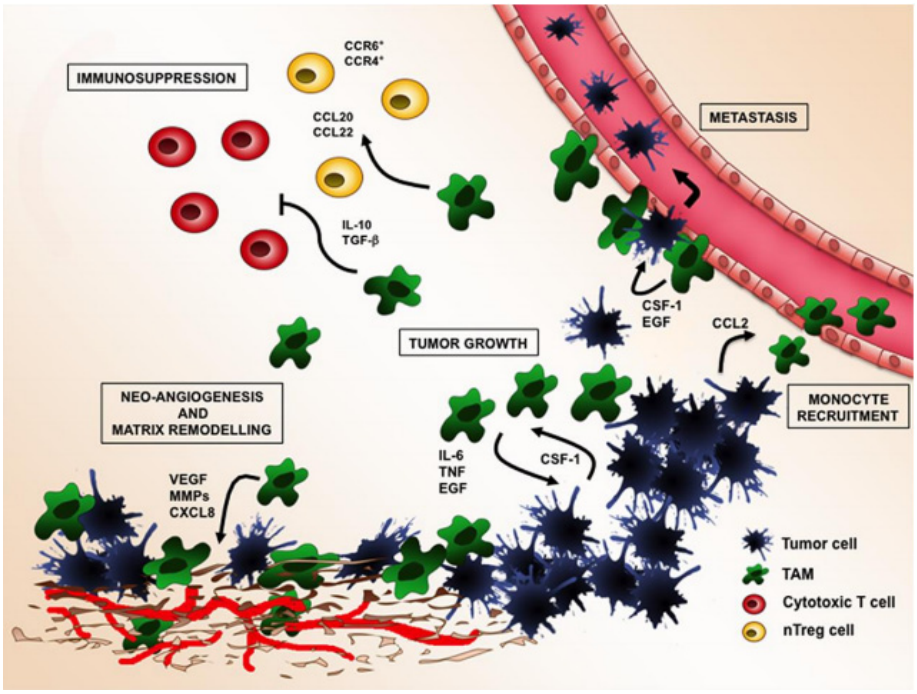

Figure 2. TAMs facilitate tumour cell survival and growth, migration and invasion, angiogenesis, metastasis and immune suppression. TAMs produce cytokines and growth factors (IL-6, low concentrations of TNF-α and EGF) that support tumour growth and survival. TAMs produce high levels of MMPs, favouring degradation of extracellular matrix and facilitating local tumour cell invasion, blood vessels intravasation and metastatic dissemination. Tumour invasion is tightly linked to the CSF1-EGF loop that occurs between macrophages and tumour cells. In addition, TAMs induce neoangiogene through the secretion of pro-angiogenic factors, such as VEGF and CXCL8. Additionally, macrophage-mediated immune suppression is correlated to their ability to counteract cytotoxic T cell function, through the release of IL-10 and TGF-β, and to recruit regulatory T cells (Tregs) through the release of chemokines such as CCL20 and CCL22. Adapted from Marelli et al. (2015) *Cancer Research Frontiers.*

activity. Interestingly, Akt phosphorylation seemed to be induced independently of EGFR activation (Figure 3)[57].

Macrophage are major contributors to tissue and matrix remodelling in tumours, being great producers of MMPs[57-59] and of other proteolytic enzymes (e.g. osteonectin (SPARC)[60], cathepsin proteases[61]). Secreted MMPs degrade the ECM releasing trapped pro-invasive, pro-motile and pro-angiogenic factors and opening paths for cell migration[62]. This favours local cancer cell invasion, intravasation into blood/lymph vessels and spreading[63]. Our group demonstrated that IL10-stimulated macrophages are more efficient in stimulating gastric and colorectal cancer cell migration, invasion and angiogenesis than their LPS-stimulated counterparts. Interestingly, these differences seemed to be related to the enhanced MMP-2 and MMP-9 activities of IL-10-stimulated macrophages and not to differences in the activation of the EGFR-signalling pathway, which is identical in both

macrophage populations[58]. The process of invasion may also involve macrophage-derived TGF-β, that promotes epithelial to mesenchymal transition (EMT)[64], a mechanism that promotes the invasive and metastatic behaviour of epithelial cancer cells[65].

Yet, the molecular mechanisms that drive cancer cell invasion and metastasis as well as the contribution of the cellular and non-cellular components of the tumour microenvironment remain poorly understood and constitute still major challenges in the cancer research field.

3.1.3. Angiogenesis

Macrophages increase the density of blood vessels at the tumour site, providing oxygenation and nutrients to tumour cells, in a process referred as "angiogenic switch"[66]. TAMs favour neoangiogenesis through the production of angiogenic factors such as VEGF-A, CXCL8, PIGF and prokineticin[67]. The genetic depletion of macrophage VEGF attenuated angiogenesis[68], while depletion of macrophages impaired tumour angiogenesis which was only restored via ectopic overexpression of VEGF[69]. The combination of increased migration and angiogenesis induced by macrophages facilitates cancer cell intravasation, facilitating metastasis[70].

3.1.4. Immunosuppression

TAMs suppress the anti-tumour adaptive immune responses. In fact, TAMs can directly inhibit the role of effector cells (e.g. natural killer cells [NK], conventional $CD4^+$ T cells [Tconvs] and CTL) of the adaptive immune response by expressing the programmed cell death protein 1 (PDL1) and the co-stimulatory molecules CD80/CD86, which engage the receptor cytotoxic T-lymphocyte antigen 4 (CTLA-4)[71] and/or by releasing IL-10 and TGF-β[72]. Additionally, TAMs are able to shape the type of leukocyte infiltrate at the tumour site through the release of chemokines (e.g., CCL17, CCL18, and CCL22) that will recruit immune suppressive cells, such as Tregs[42], inhibiting the proliferation and function of effector cells and favouring tumour immune escape[70]. Additionally, M2-like macrophages have been implicated in *de novo* generation and clonal expansion of Tregs, as well as in the inhibition of IL-17-producing $CD4^+$ T cells (Th17), further assisting the formation of a high anti-inflammatory microenvironment.

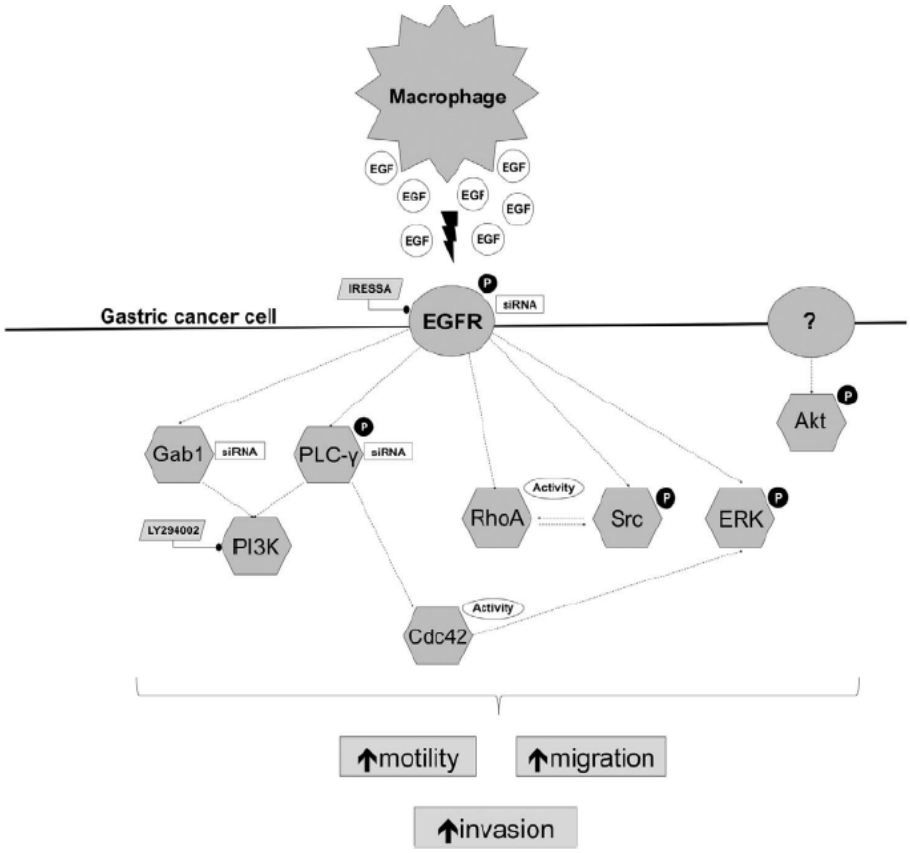

Figure 3. Model proposal for the macrophage-mediated invasion pathway. Soluble factors produced by macrophages, namely EGF, lead to EGFR phosphorylation in cancer cells. By siRNA experiments, EFGR-interacting partners such as Gab1 and PLC-y were demonstrated to be required for macrophage-mediated cancer cell invasion. Other molecules such as cSrc, ERK, Akt, and the small GTPAses Cdc42 and RhoA were demonstrated to be phosphorylated/activated. Silencing of EGFR demonstrated that macrophage-mediated cancer cell c-Src and ERK but not Akt occur downstream of EGFR signalling. Dashed arrows indicate putative interactions described in the literature. Closed circles indicate inactivation by pharmacological inhibitors. Unshaded rectangles indicate transient knocked-out expression by siRNAs. Black circles indicate increased protein phosphorylation. Elipses indicate increase in the GTP-bound form of the protein. Adapted from Cardoso *et al* (2013) *Oncogene*.

3.2. Macrophages in colorectal cancer

In line with the findings mentioned above, TAMs infiltration is frequently associated with poor prognosis[73]. However, in CRC the prognostic value of such infiltration is still contradictory[74]. While some studies associate massive macrophage infiltration with poor prognosis[75,76] others correlate high density of TAMs with improved outcome[73,77,78]. However, some of these studies lack TAMs phenotypic characterization[77], solely using a lineage-macrophage marker (e.g. CD68), without discriminating macrophage subpopulations. Due to the plasticity of these cells, one critical aspect in macrophage characterization is the discrimination between

M1 and M2 subpopulations[79]. Several studies use inadequate M1- or M2-like markers[78,80]. For instance, inducible nitric oxide synthetase 2 (iNOS2), used as a M1-like marker[78], was described to be a specific marker for these macrophages in mice, but not in humans. Further, the use of HLA-DR, frequently used as a M1-like marker, was also questioned[80]. Nevertheless, TAMs location at different tumour regions appears to be crucial for prognostic prediction, since accumulation of TAMs at the tumour invasive front, a region less affected by cancer cells, was associated with increased patients' disease-free survival[73,77]. Our group is assessing macrophage infiltration in CRC specimens and has observed interesting results: stronger infiltration of M1-like macrophages (positive for CD80) at normal colonic mucosa in contrast to M2-like (positive for CD163) macrophage accumulation at normal colonic mucosa, tumour nest and invasive front (MLPinto, unpublished data). Future work includes correlation of these results with the clinicopathologic data of patients, to evaluate possible clinical associations.

4. Regulatory T cells

Regulatory T cells (Tregs) are known to develop and maintain peripheral self-tolerance (recognition and unresponsiveness to self-constituents), and control immune responses to non-self-antigens[81,82].

Tregs derive from the thymus[83] and from thymic emigrants that were induced into Tregs in the periphery[84] and include $CD4^+$, $CD8^+$ T cells and $CD4^-CD8^-$ double negative subtypes[85]. The majority of Tregs comprise a small subset of $CD4^+$ T lymphocytes in mice and human (5-10%)[86] and are characterized by high cell surface expression of the interleukin-2 receptor α-chain (IL-2Rα) (CD25)[86], required for Treg survival and IL-2 absorption[87] and by the expression of Forkhead box protein 3 (Foxp3)[88]. FoxP3 is an essential Treg lineage-specifying transcription factor required for Treg development and suppressive competence[89]. Among other factors, demethylation of the Treg-specific demethylated region (TSDR), a FoxP3 locus, was shown to be crucial to maintain stable and high the expression of FoxP3[90]. Tregs molecular signature requires additional nuclear factors and is dependent on several molecules and signals such as IL-2, TGF-β, and co-stimulatory molecules such as CD28, triggered by its ligands CD80/CD86, expressed in APCs[91]. Treg cells display a distinct T cell receptor (TCR) repertoire, with increased affinity with self-antigen compared with that of Tconvs[92].

Currently, FoxP3 is one of the selected markers to identify Tregs, but its nuclear localization requires permeabilization of cellular and nuclear membranes, inhibiting the

isolation of viable Tregs[93]. Although the majority of FoxP3-expressing $CD4^+$ T cells are considered to be suppressive Tregs in mice, $CD4^+FoxP3^+$ T cells in humans display a heterogeneous phenotype and function[92]. For instance, $CD4^+CD25^-$ Tconvs can transiently upregulate the expression FoxP3 without acquiring suppressive competence[94]. Furthermore, not all $CD4^+CD25^+FoxP3^+$ T cells in PBMCs possess suppressive competence[95]. It is imperative to identify distinct human $FOXP3^+$ subpopulations to better understand Treg subpopulations in normal and disease states and to specifically target them to control pathological immune responses. To delineate $FoxP3^+$ T cell populations several cell surface molecules were investigated: IL-7 receptor α-chain (CD127), glucocorticoid induced TNFR family-related protein (GITR), CTLA-4, CD45RA (or CD45RO) and sialyl Lewis x (CD15s)[92,96-98]. These markers are expressed at different levels and reflect differential functional stages of the heterogeneous Treg population. However, these markers still carry some drawbacks and have to be used in concert. For instance, CD25 expression forms a continuum being difficult to accurately define a $CD25^{high}$ population and can be upregulated by Tconvs[92].

Miyara *et al.*[95], described that $CD4^+CD25^+FoxP3^+$ T cells can be divided into three phenotypically and functionally distinct subpopulations: 1) naïve or resting Tregs as $CD25^+CD45RA^+FOXP3^{low}$ (rTreg), 2) effector or activated Tregs as $CD25^{high}CD45RA^-FOXP3^{high}$ (aTreg), and 3) non-suppressive $CD4^+$ T cells as $CD25^+CD45RA^-FOXP3^{low}$ ($FOXP3^+$ non-Treg). *In vitro* and *in vivo* studies demonstrated that rTregs proliferate upon TCR stimulation and convert into terminally differentiated aTregs, which are hyporesponsive and highly apoptotic after activation and suppression. On the other hand, non-Tregs abundantly secrete pro-inflammatory cytokines, such as IL-17, are less active in FoxP3 expression and do not suppress Tconvs proliferation *in vitro*[95]. In addition, *in vitro* and *in vivo* studies demonstrated that previously suppressive $FoxP3^+$ Tregs lost their suppressive ability under Th1 and Th17-polarizing environments and acquire the ability to produce pro-inflammatory cytokines[99]. Altogether these data show the heterogeneity but also the plasticity of Treg populations in different microenvironments.

Additionally, Tregs can also be induced (iTregs) from Tconvs/naïve via TCR stimulation in the presence of IL-10 and TGF-β, generating Type-1 regulatory T cells (Tr1) and Th3, respectively. Tr1 express high levels of IL-10 in the absence of FoxP3 expression[100]; Th3, are a TGF-β-secreting Treg subset characterized by low IL-10 and intermediate levels of FoxP3 expression[101].

Tregs are able to suppress activation, proliferation and function of distinct immune cells, including $CD4^+$ and $CD8^+$ T lymphocytes, NK and NKT cells, and antigen-presenting cells (APCs) (Dendritic cells [DCs] and macrophages) and B cells[70,102]. Treg-mediated suppression can occur by cell-to-cell contact or in a cytokine dependent manner, via multiple mechanisms. The activated mechanisms may depend on the local microenvironment, the suppressed target cell or on the state of activation of Tregs (Figure 4)[102]. Tregs inhibit T cells through release of inhibitory cytokines, such as IL-35, IL-10 or TGF-1β[102,103], but a direct cell contact between Tregs and Tconvs is required[118,119]. In turn, these inhibitory cytokines induce other types of Tregs from $CD4^+$ T cells[104]. The high levels of IL-2R chain at Tregs surface can lead to competitive consumption of IL-2, scavenging it from other T cells and consequently inhibiting their proliferation; Tregs can generate and secrete adenosine, degrade tryptophan and transfer cAMPs to other T cells, leading to their metabolic disruption[105]. Via perforin and granzyme-dependent pathways Tregs can directly elicit effector T cell apoptosis. Finally, Tregs can indirectly affect Tconvs by hampering APCs function. CTLA-4, highly expressed at the surface of Tregs, binds to co-stimulatory molecules, such as CD80/CD86 from the surface of APC, leading to their removal[106]. The direct interaction established between Tregs and APC prevents the stable contacts between APC and the co-stimulatory molecule CD28 of $CD4^+$ T cells, inhibiting T cell activation[106].

4.1. Tregs in cancer

Tregs are mediators of peripheral tolerance to self-antigens and innocuous environmental antigens[81]. Tumour-associated antigens are modified or aberrantly expressed self-antigens. It is, therefore, expected that Tregs are the major precursors of tumour immune evasion[107]. In fact, Tregs were described to recognize a broad range of tumour-associated self-antigens and to suppress the response of tumour-antigen-specific effector T cells[108]. Additionally, Tregs have more self-reactive TCR repertoires and thus present higher ability to recognize self-tumour antigens than other $CD4^+$ T cells[92].

Previous studies have reported that during tumour initiation Tregs are enriched in the tumour tissue and in advance-stage disease their number increase systemically, in comparison to healthy individuals[109]. Tregs accumulate at the tumour microenvironment by recruitment, expansion and *de novo* generation. Tumour cells and stroma components produce and secrete several factors that are chemoattractants for Tregs, recruiting them to

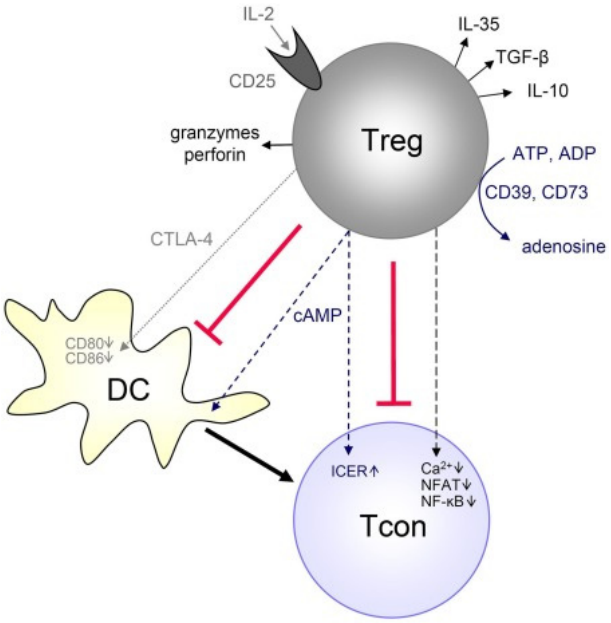

Figure 4. Mechanisms of Treg-mediated suppression. Tregs suppress directly or indirectly conventional T cells (Tcon) via different mechanisms, depending on the local immune environment, in the target cell or even according to Tregs status. Tregs secrete immunosuppressive adenosine or transfer cAMP to Tconvs, produce immunosuppressive cytokines (IL-10, TGF-β, IL-35), suppress Tconvs by IL-2 consumption or induce effector cell death via granzyme and perforin. Furthermore, Tregs can suppress Tconvs indirectly by downregulating costimulatory molecules on APCs (such as DCs) via CTLA-4. Adapted from Schmidt et al. (2012), *Frontiers in immunology*.

the tumour site. For instance, in colorectal cancer, CCL20 secreted by TAMs induces the recruitment of $CCR6^+$ nTreg cells[110] and, in ovarian cancer, TAMs are described to secrete CCL22 that mobilizes $CCR4^+$ nTreg cells[111]. After recruitment, Tregs are activated and expanded in the tumour. The high levels of TGF-β and IL-10 produced by tumour cells and TAMs favour pre-existing Tregs clonal expansion[101]. Furthermore, effector T cells were proposed to secret IL-2 that could induce the proliferation of Tregs[112]. The combined presence of TGF-β and IL-10 with DC or TAMs promotes the conversion of naïve or conventional T cells into suppressive Tregs, Th3 and Tr1[113,114]. Prostaglandin E2 (PGE2), indoleamine 2,3-dioxygenase (IDO), and TGF-β derived from the tumour have also been correlated with the conversion of iTregs from Tconvs/naïve[115,116].

The immunosuppressive role of Tregs was also indirectly correlated with metastatic advantages[117,118]. In breast cancer models, recruitment of Tregs to the primary tumour, increased CTL and NK cells' apoptosis and metastasis. Additionally, in the same model, the suppression of lung metastasis was accompanied by decrease of $CD4^+CD25^+$ T cells in the

primary tumour[121]. Additionally, systemic Treg depletion in patients induced regression of melanoma metastases[120].

4.1.1. Prognostic value of Tregs in colorectal cancer

The infiltration of Tregs into tumours has been reported to be associated with an unfavourable outcome in several human cancers, such as ovarian[119], breast, gastrointestinal, lung, liver, pancreatic cancer and melanoma[120]. Contrarily, in CRC the results are controversial with high densities of FoxP3$^+$ Tregs mostly correlating with favourable outcomes[121-125] Tregs infiltrate preferentially at the tumour nest (TN)[122,125]. In a cohort of 967 CRC specimens, high density of FoxP3$^+$ T cells at the TN was associated with better prognosis, whereas their accumulation at the surrounding healthy tissues was associated with worse prognosis[122]. Similar results were found by Frey *et al.* in a cohort of 1420 patients, where high FoxP3 infiltration at tumour site was an independent positive predictor of 5-years disease free survival in MMR-proficient patients, but not in MMR-deficient patients[121]. Even in a metastatic setting, higher levels of FoxP3$^+$ T cells, within the tumour of patients subjected to chemotherapy, was associated with better prognosis[126]. Ling and colleagues demonstrated that high levels of FoxP3$^+$ T cells correlated with a good prognosis in patients with low infiltration of CD8$^+$T cells[125]. Moreover, they described that accumulation of FoxP3 at the invasive front and TN alone are correlated with better prognosis, bearing strong prognostic information[125]. Additionally, higher intratumoural infiltration of Tregs than IL-17$^+$ T cells were associated with suppressed MMPs activities and decreased metastases score in CRC cancer upon resection[127]. Nevertheless, Treg-mediated suppression also involves interactions with APCs, and the prognostic role of the balance between macrophages and/or DCs and Tregs has not yet been performed in a CRC context.

The role of FoxP3$^+$ tumour-infiltrating lymphocytes in CRC may depend on the immune response found at the tumour. If the tumour microenvironment is infiltrated with immune cells that promote tumourigenesis and/or tumour progression, the immunosuppressive role of Tregs may be beneficial. However, if a Th1-like response, characteristic of a tumour antigen-specific immune response is dominant, the suppression by Tregs can be deleterious promoting tumour immune escape and progression[128]. The controversial results of FoxP3 infiltration can be further explained by the phenotypic and functional heterogeneity of FOXP3$^+$ T cell subpopulations[129]. The contribution of each Treg subpopulation (rTregs, aTregs and non-Tregs) at CRC microenvironment is still unknown.

A higher infiltration of non-Treg, capable of producing pro-inflammatory cytokines, could contribute to a better prognosis of FoxP3$^+$ T cells in CRC[130]. The controversial role of Tregs in cancer may also rely on the low inter-study comparability due to the use of different techniques, among others. The role and the prognostic significance of FoxP3$^+$ infiltration and FoxP3$^+$ subpopulation is still scarce. However, it seems that Tregs exert distinct influences at different inflammatory microenvironments, which may be reflected on different FoxP3$^+$ subpopulations[128]. The impact of Tregs in tumour progression may be determined by the type and location at the tumours as well as by the balance between Tregs and other immune populations within the tumour mass[22]. It is then imperative to clarify the role of FoxP3$^+$ T cells in the tumour microenvironment, so as to adopt adequate different strategies to manipulate Tregs, in order to improve patient survival.

5. Macrophage-Treg crosstalk

By cell-to-cell contact and in a cytokine-dependent way, Tregs exert a suppressive effect on monocyte/macrophage activation and effector function[131,132]. In humans, the inhibitory functions of Tregs on monocyte-derived macrophages were provided by *in vitro* autologous co-cultures between CD4$^+$CD25$^+$ T cells and monocytes[131]. These monocytes displayed a resting phenotype, producing lower levels of IFN-γ, TNF-α and IL-10 than when co-cultured with CD4$^+$CD25$^-$ T cells. When further challenged with LPS, Treg-educated macrophages were inhibited ofproducing IFN-γ, TNF-α and IL-6 and exhibited downregulation of CD86 when comparing with control monocytes. The different macrophage activation was reflected in the hampered APC function of Treg-educated macrophages[131]. Later, Tiemessen and colleagues[132], showed that Tregs steered macrophage differentiation towards an immunosuppressive phenotype[132], characterized by the upregulation of CD206 and CD163 and downregulation of HLA-DR and CD86. In addition, Treg-educated monocytes increased secretion of CCL18, enhanced phagocytic capacity and displayed a diminished capacity to respond to LPS, producing low levels of pro-inflammatory cytokines (IL1-β, IL-6, IL-8 TNF-α). The authors described that the upregulation of CD163 was dependent on IL-10. Contrarily, the upregulation of CD206 was cytokine-independent suggesting the need of cell-to-cell contact, which was further demonstrated using transwell assays[132]. Kryczek *et al.* reported a similar suppressive profile on human macrophages cultured with Tregs, but further described that the higher levels of IL-10 produced by Treg-educated macrophages induced the upregulation of the Tconvs cell inhibitory molecule B7-H4 on monocytes[133]. In

line with these reports, the presence of Tregs after myocardial infarction induced macrophages toward an anti-inflammatory profile, contributing to inflammation resolution and wound healing[135], in a mouse model. In the physiologic intestinal microenvironment, commensal microbiota promotes colonic Tregs differentiation, which in turn contribute to the immune homeostasis in the colon[136]. Tregs differentiation is also favoured by colonic DCs which repress the expression of LPS response genes, promoting microbiota protection, as well as, inhibiting macrophage activation due to hyporesponsiveness to TLR stimulation[136]. Nevertheless, the modulatory role of Tregs on macrophages phenotype and functions in a cancer context is still scarce.

Conversely, macrophages induce Tregs differentiation[113,114] and recruitment[137], extending their population within tumours and maintaining an immunosuppressive microenvironment that may favour tumour progression[138]. Along with cancer cells, TAMs are major source of TGF-β and directly induce Tregs by cell-to-cell interaction via membrane bound TGF-β[137]. In a colitis mouse model, macrophage-derived IL-10 was described to maintain FoxP3 expression in Tregs[139]. Further, in an immunocompetent mouse model with renal injury, IL-10/TGF-β–modified macrophages attenuated renal inflammation[140]. The suppression of $CD4^+$ T cells by IL-10/TGF-β–modified macrophages induced proliferation regulatory T cells from $CD4^+CD25^-$ T cells and increase Tregs in renal draining lymph nodes[140]. These results highlight the role of anti-inflammatory macrophages in *de novo* generation and recruitment of Tregs. Nevertheless, under pro-inflammatory conditions (e.g. rheumatoid arthritis), monocyte-derived IL-6, IFN-γ and IL-1β was described to induce aTregs to produce both pro-inflammatory (IL-17, IFN-γ, TNF-α) and anti-inflammatory (IL-10) cytokines, without losing their suppressive functions[141]. These data indicate that different macrophage subsets display distinct roles in the modulation of Tregs' properties, however the exact mechanisms underlying these modulation is still not completely understood. Furthermore, it is also likely that different Treg subpopulations could distinctly modulate macrophage inflammatory profiles.

Aim

Tumours are considered malignant when cancer cells invade the surrounding tissues, becoming prone to intravasate vessels and to metastasize. TAMs are considered obligate partners in the malignant transformation. Additionally, Tregs, which display immunosuppressive properties facilitate tumour immune escape, favouring cancer cell invasion. Given the modulatory role of Tregs on macrophage inflammatory phenotype, it is likely that Treg-educated macrophages may have enhanced pro-tumour activities. However, in CRC the role of TAMs and Tregs is controversial since their intratumoural infiltration is often correlated with good prognosis. Also, the influence of Tregs on monocyte/macrophage pro-invasive properties is presently unknown. Similarly, the phenotypic and functional profile of these immune cell populations and respective subpopulations in a CRC context remains to be elucidated.

Therefore, the main goal of this project is to better understand the role of Tregs on macrophages behaviour, uncovering their impact on CRC cell invasion. Specific objectives include:

1) Evaluate the impact of Tregs on monocyte-derived macrophage differentiation;
2) Assess the role of Tregs-educated macrophages on colorectal cancer cell invasion;
3) Investigate the mechanisms underlying Tregs modulation of macrophage-mediated cancer cell invasion, such as on MMPs proteolytic activity and the activation of the EGFR-invasion related signalling pathway;
4) Characterize FoxP3^{+} T cell infiltration in human CRC specimens.

Materials and methods

Cell line culture

The RKO (CRL-2577) and SW620 (CCL-227) stablished cancer cell lines, derived from human colon carcinomas, were obtained from the American Type Culture Collection (ATCC, Manassas, VA, USA) in 2012. RKO and SW620 cells were maintained at 37ºC, under a 5% CO_2 humidified-atmosphere, in complete RPMI1640-GLUTAMAX medium (Invitrogen, Merelbeke, Belgium) or in DMEM+F12 medium (Invitrogen), respectively. Media were supplemented with 10% fetal bovine serum (FBS) (Lonza, Basel, Switzerland), 100 U/ml penicillin and 100 mg/ml streptomycin (Invitrogen).

Immune cells isolation

Human monocytes and regulatory T cells were isolated from healthy blood donors' buffy coats, provided by the Immunohemotherapy Department, Hospital São João, Porto, Portugal. For an autologous setting, the same blood donor was used to isolate $CD14^+$ monocytes and $CD4^+CD25^+$ T cells. To combine monocyte with BD regulatory T cell isolation (BD Biosciences, Madrid, Spain), buffy coats were initially divided. Alternatively, to combine monocyte isolation with the StemCell regulatory T cell isolation kit (StemCell Technologies, Grenoble, France), peripheral blood mononuclear cells (PBMCs) collected from buffy coats were divided.

$CD14^+$ monocyte isolation

Monocytes were isolated using the Human Monocyte Enrichment Cocktail (StemCell Technologies), which consists in a negative selection of $CD14^+$ cells. From our previous work using this isolation system, over 80% of isolated monocytes were found to be CD14-positive[57]. Briefly, buffy coats were centrifuged at 1200 xg, without brake, for 20 minutes at room temperature (RT). The whitish layer containing PBMCs was then collected and used to isolate $CD14^+$ monocytes. PBMCs were incubated for 20 minutes under rotation with the RosetteSep™ Human Monocyte Enrichment Cocktail (StemCell Technologies), according to manufacturer's instructions. The enriched mixture was diluted (1:1 ratio) in phosphate buffered saline (PBS) supplemented with 2% FBS (Lonza), gently layered over equal volume of Histopaque®-1077 (Sigma-Aldrich, Madrid, Spain) and centrifuged at 1200 xg, without break, for 20 minutes at RT. The interface layer, enriched in human $CD14^+$ monocytes, was

collected, washed with PBS and centrifuged at 98 xg, with brake, for 17 minutes at 4ºC. The supernatant was discarded and the pellet with the isolated cells were resuspended with complete RMPI1640-GLUTAMAX medium supplemented with 10% FBS, 100 U/ml penicillin and 100 mg/ml streptomycin. For the *in vitro* studies, monocytes were seeded in the same culture medium, according to the experimental set up.

Human $CD4^+CD25^{high}$ T cell isolation

The Human Regulatory T Lymphocyte Separation Set (BD Biosciences) or the Regulatory T cell Isolation Kit (StemCell Technologies) were used to isolate the broadest phenotypic variety of Tregs. Isolations consisted in a negative ($CD4^+$) followed by a positive ($CD25^+$) selection of cells.

1. Human Regulatory T Lymphocyte Separation Set (BD Biosciences)

To isolate PBMCs, blood from buffy coats were gently layered over Histopaque®-1077 and centrifuged at 1200 xg, without brake, for 20 minutes at RT. The whitish layer containing PBMCs was then collected, washed with PBS, centrifuged at 18 xg for 10 minutes and the supernatant discarded. Then, PBMCs were resuspended in the Human Regulatory T Lymphocyte Separation Cocktail for 15 minutes at RT. The labelled cells were washed in 1x BD IMag™ buffer (1:10 ratio), centrifuged at 300 xg for 8 minutes, and the supernatant discarded. For $CD4^+$ T lymphocytes enrichment, cell pellet was resuspended in BD IMag™ Streptavidin Particles Plus – DM and incubated for additional 30 minutes at RT. The labelled cell suspension was brought to $60x10^6$ cells/mL with 1x BD IMag™ buffer, transferred to 5 mL round-bottom polystyrene tube (BD Falcon) and placed on the EasySep® magnet for 7 minutes. The supernatant (enriched fraction) was transferred to a new sterile tube. The enrichment step was repeated twice. The tube containing the combined enriched fraction was placed on the magnet for 7 minutes and the supernatant was removed to a new tube for a twice-enriched fraction containing $CD4^+$ T lymphocytes. For the positive selection of $CD4^+CD25^+$ T cells, the twice-enriched fraction was centrifuged, as previously, and the cell pellet was resuspended in the BD IMag™ Anti-APC Particles – DM and incubated for 30 minutes at RT. The labelled cell suspension was brought to $60x10^6$ cells/mL with 1X BD IMag™ buffer, transferred to 5 mL round-bottom tube and placed on the magnet for 8 minutes. With the tube on the magnet, supernatant was discarded. After two wash steps, the tube was removed from the magnet and isolated $CD4^+CD25^+$ T cells were resuspended in complete RMPI1640-GLUTAMAX medium supplemented with 10% FBS, 100 U/mL penicillin, 100 mg/mL streptomycin and 50 ng/mL anti-CD3 (OKT3, Abcam, UK).

2. Regulatory T cell Isolation Kit (StemCell Technologies)

Buffy coats were centrifuge at 1200 xg, without brake, for 20 minutes at RT. The whitish layer containing PBMCs was then collected and used to isolate $CD4^+CD25^+$ T cells. PBMCs were incubated for 20 minutes under rotation with RosetteSep® Human $CD4^+$ T Cell Enrichment Cocktail, following manufacturer's instructions. The enriched mixture was diluted (1:2 ratio) in PBS + 2% FBS, gently layered over Histopaque®-1077 and centrifuged, as previously. The interface layer, enriched in $CD4^+$ cells, was collected, washed with PBS + 2% FBS, centrifuged at 1200 xg, with brake, for 17 minutes at 4ºC and the supernatant was discarded. The enriched sample was transferred to a 5 mL round-bottom polystyrene tube and incubated under rotation with EasySep® Positive Selection Cocktail, for 15 minutes. Then, EasySep® Magnetic Nanoparticles were added to the suspension, for 10 minutes, following manufacturer's instruction. The cell suspension was brought to a volume of 2.5 mL with PBS + 2% FBS, resuspended and place into the magnet for 5 minutes. The supernatant fraction was then discarded while the magnetically labelled cells remained inside the tube. The positively selected cells were resuspended with complete RMPI1640-GLUTAMAX medium supplemented with 10% FBS, 100 U/mL penicillin, 100 mg/ml streptomycin and 50 ng/mL anti-CD3 (Abcam). For the *in vitro* studies Tregs were seeded in the same culture medium. A fraction of $CD4^+CD25^+$ T cells was analysed by flow cytometry to evaluate the efficiency and purity of the cell separation procedure. Isolation resulted in 77% $CD4^+CD25^+$ T cells with 94% expressing FoxP3.

Mono-culture of human $CD14^+$ monocytes or of $CD4^+CD25^+$ T cells

Isolated human $CD14^+$ monocytes from two different healthy blood donors were seeded in 58 cm^2 tissue-culture petri dishes (Greiner, Frickenhausen, Germany) at a density of $1x10^7$ monocytes per plate and maintained at 37ºC, under a 5% CO_2 humidified-atmosphere for 24 hours. Then, monocytes were transferred to three different substrates: 6-well tissue culture-treated plates (Falcon, Durham, USA) at a density of $1,2x10^6$ monocytes per well ($0,13\ x10^6$ monocytes/cm^2); 6-well tissue culture-nontreated plates at a density of $1,2x10^6$ monocytes per well ($0,13\ x10^6$ monocytes/cm^2) (Falcon); and 24-well tissue culture-treated plates (Falcon) with coverslips (Deckglasser, Lauda-Konigshofen, Germany) at a density of $5x10^5$ monocytes per well ($0,26\ x10^6$ monocytes/cm^2). Non-treated plates are hydrophobic polystyrene surfaces whereas treated plates are hydrophobic polystyrene surfaces that where chemically treated to become hydrophilic, usually by increasing their negative charge,

in order to improve cell attachment. The initial cell density seeded on 6- and 24-well plates relies on previous work performed in our laboratory[57,58]. Cultures were maintained at 37ºC, under a 5% CO_2 humidified-atmosphere to allow monocyte to macrophage differentiation for 3 and 7 days, as commonly performed in macrophage studies. At the third day, the culture medium was renewed. Morphology, density and adhesion of cells were examined at the third and seventh days, using a Olympus CKX41 (SC30) optical microscope and photographed with the anaySYSgetIT, 5.1 Software.

After $CD4^+CD25^+$ T cells isolation with Regulatory T cell Isolation Kit from SC, $3.6x10^6$ cells from the enriched $CD4^+$ mixture were collected to assess cell purity by FACS. In the end of the isolation procedure, $CD4^+CD25^+$ T cells were seeded with anti-CD3 (50 ng/mL) in 6-well tissue culture-nontreated plates at a density of $1x10^6$ cells/well ($0,11 x10^6$ monocytes/cm^2) and incubated at 37ºC, under a 5% CO_2 humidified-atmosphere. At day 3 and 7, cells were collected to assess cell purity by FACS, using specific anti-CD4-FITC (ImmunoTools) and anti-FoxP3-PE (BD Pharmingen) antibodies. The morphology, adhesion and confluence of Treg cells were examined in the third and seventh days using a Olympus CKX41 (SC30) optical microscope and photographed with the anaySYSgetIT, 5.1 Software. For 7 days cultures, cells were nourished on day 3 by changing 1/5 of the medium and keeping the same concentration of anti-CD3 mAb (OKT3). Tregs isolation was performed twice using whole buffy coats from two distinct healthy blood donors.

Flow cytometry

The purity of $CD4^+CD25^+FoxP3^+$ T cells was determined by fluorescence-activated cell sorting (FACS), using the cell surface receptors $CD4^+$ and $CD25^+$ for Tregs. Isolated $CD4^+CD25^+$ T cells were further characterized for intracellular FoxP3 expression, a lineage-defining transcription factor (Table 1). For this, cells were collected and centrifuged at 288xg during 5 minutes at 4°C. The supernatant was discarded and the pellet was resuspended with FACS staining buffer (PBS supplemented with 2% FBS [Lonza] and 1% sodium azide [Sigma-Aldrich]). Cells were divided and plated in ice into FACS-staining-U-bottom plates at a density of $5x10^5$-$1x10^6$ cells/condition. The plate was centrifuged at 242 xg during 3 minutes at 4°C, and the supernatant was removed by discarding it by a single fast movement. For cell surface receptors, cells were stained with anti-human CD4-FITC (ImmunoTools) and anti-human CD25-APC (BD Biosciences) diluted in FACS buffer (1:10 ratio), for 30 minutes, on ice and in the dark. After this time, cells were washed in FACS

buffer and centrifuged. After staining for cell surface molecules, cells were fixed in 4% paraformaldehyde (PFA) (Sigma-Aldrich) for 10 minutes at RT. For intracellular staining of FOXP3 cells were permeabilized in 0,2% Triton X-100 (Sigma-Aldrich) for 5 minutes at RT and stained with anti-human anti-FoxP3-PE (BD Pharmingen) diluted in FACS staining buffer (1:1 ratio) for 30 minutes at RT. After this period, cells were centrifuged as previously, supernatants were discard, the pellet was washed, resuspended in PBS 1x, collected into a FACS tube, and stored until acquisition at 4ºC, protected from light. Isotype-matched antibodies, IgG2a-FITC, IgG1,k-APC and IgG1-PE were used as negative control, to define background staining (Table 1).

Cells were acquired on BD Accuri™ C6 Flow cytometer BD CSampler (BD Biosciences), using BD Accuri™ C6 Software (collecting 10 000 cells). Analysis was performed with the same software. Percentage of positive cells was obtained by subtracting the respective isotype control.

Table 1. Antibodies used for monocytes and $CD4^+CD25^+$T cell phenotyping by FACS

Antigen	*Format*	*Clone*	*Isotype*	*Stain*	*Specificity*	*Manufacturer*	*Cat no.*
CD4	FITC	MEM-241	IgG2a	Surface	Lymphocyte	ImmunoTools	21278043
CD25	APC	2A3	IgG1,k	Surface	Tregs	BD Biosciences	340907
FoxP3	PE	259D/C7	IgG1	Intracellular	Tregs	BD Pharmingen	560046

Co-cultures of human $CD14^+$ monocytes and $CD4^+CD25^+$ Tregs

Isolated human $CD14^+$ monocytes and $CD4^+CD25^+$ T cells mono-cultures and co-cultures (1:1 or 2:1 ratios, Mac:$CD25^+$ T cell) were performed in 24-well tissue culture-treated plates (Falcon) with glass coverslips (Deckglasser) for 3 and 7 days in an autologous setting and in the presence of 50 ng/mL of soluble anti-CD3 monoclonal antibody. After this time, cultures were used for invasion assays with RKO or SW620 CRC cell lines, conditioned media (CM) stored for enzyme-linked immunosorbent assays (ELISA) and zymography analysis, cell viability assays and to assess morphology and macrophage molecular profile by immunocytochemistry (ICC). As controls, each cell population was cultured alone. The experimental design is illustrated in supplementary figure 1a. For 7 days cultures, cells were nourished on day 3 by changing 1/5 of the medium and keeping the same concentration of anti-CD3 mAb.

Cell viability and metabolic assays

The trypan blue-exclusion assay, based on cell membrane integrity, was used to estimate the number of viable immune cells present in mono or co-cultures, after 3 and 7 days. For this, culture supernatants were removed, diluted (1:1 ratio) in trypan blue dye (Sigma-Aldrich) and cells were counted in a Neubauer chamber. Additionally, to assess the viability of adherent cells, coverslips were incubated in complete RPMI medium with trypan blue dye (1:1 ratio) for 3 minutes, washed in PBS, and visualized through an Olympus CKX41 (SC30) optical microscope. To estimate total adherent live and dead cells, 6 random areas within each coverslip were considered and divided by the total area of the coverslip (diameter 12mm). Since trypan blue is a membrane impermeable molecule, the number of viable cells was estimated upon subtraction of the blue stained dead cells. Results are presented as the percentage of viable cells, present in suspension in the medium or adhered to the coverslip, over the total number of cells [(Total of live cells/Total of cells) x 100].

To complement this qualitative data, immune cells metabolic activity was determined though the resazurin reduction assay. Briefly, after 3 or 7 days of seeding, cells were incubated with resazurin redox dye (0.01 mg/mL) (Sigma-Aldrich) for 4 hours at 37°C and 5% CO_2, after which 200 µL/well were transferred to a 96-well black plate (MICROTEST™, Falcon). Wells containing only complete RPMI medium with resazurin were used as blank. Two technical replicates were performed. Fluorescence intensity was measured (530 nm Ex/590 nm Em), using the multi-mode microplate reader Synergy MX (BioTek). Results are presented as relative fluorescence units (RFU) per $1x10^5$ cells and represent the differences in fluorescence intensity ($fluorescence_{sample}$–$fluorescence_{blank}$).

Immunocytochemistry

Coverslips with cells fixed in 4% PFA were washed in PBS and quenched with 50 mM NH_4Cl for 10 minutes. After washing with PBS under agitation, cells were permeabilized with 0.2% Triton X-100 for 5 minutes. Cells were washed as previously, blocked for 45 minutes with 5% bovine serum albumin (BSA) (Sigma-Aldrich) and incubated for 1h30 with the monoclonal mouse primary antibodies anti-human CD80 (DAKO, PG-M1) or anti-human CD163 (Cell Marque,163M-16) or anti-human α-tubulin (Fisher Scientific, MAC 387). After washing with PBS, coverslips were incubated for 1 hour with goat anti-mouse AlexaFluor-594-conjugated secondary antibodies (Invitrogen, 927075) and washed. For actin staining coverslips were incubated with phalloidin-FITC for 15 minutes at RT. After the final wash,

coverslips were mounted on Vectashield with 6-diamidino-2-phenylindole (DAPI, Vector Laboratories, Burlingame, CA, USA). Cells were visualized with a Zeiss Axiovert 200M fluorescence microscope (Carl Zeiss, Aalen, Germany).

Enzyme-linked immunosorbent assay (ELISA)

Levels of IFN-γ, IL-6, IL-10 and total transforming growth factor (tTGF-β1) cytokines present in CM from cultures, prior and/or after invasion assays, were measured by ELISA, according to manufacturer's instructions (BioLegendMAX, San Diego, CA, USA). For IFN-γ and IL-6, 16 hours prior the ELISA, capture antibodies, diluted in coating buffer, were added to 96-well plates, sealed and incubated overnight (ON) at 4ºC. Then, wells were incubated with assay diluent at RT for 1 hour, with agitation, to block non-specific binding. From here the procedure was similar for all ELISA Kits. Briefly, after washing, samples were incubated in 96-well plates pre-coated with a capture antibody, specific for the cytokine in analysis, during 2 hours at RT with agitation. After washing, a detection antibody solution was added and incubated for 1 hour at RT with agitation. Then, wells were washed, incubated with Avidin-HRP D solution for 30 minutes at RT with agitation. Wells were washed again, incubated with substrate solution F or TMB substrate solution at RT, with agitation, until the colour develops according to the amount of cytokine bound. According to the cytokine, standard dilutions were prepared from 1000pg/mL to 7.8 pg/mL. The reaction was stopped with stop solution and the absorbance was read at 450 nm and 57 0nm on a SynergyMx fluorometer (Biotek) and using the Gen5by software. Finally, the values obtained at 570 nm were subtracted to the values obtained at 450 nm.

Invasion Assays

3D-coated matrigel invasion assays monitor cell movement through a barrier consisting of extracellular matrix components (collagen type IV, fibronectin, proteoglycans amongst other), which mimics the basement membrane that cancer cells have to cross to invade and metastasize. This *in vitro* assay has been successfully used to quantify the capability of cells to penetrate basement membranes in response to factors present in the medium[57,142].

Therefore, 8-µm-pore-size matrigel coated-inserts (BD Biosciences) were allowed to rehydrate in complete RPMI medium for 2 hours at 37ºC and 5% CO_2. After this time, a suspension of $0.5x10^6$ RKO or SW620 cells was incubated in the upper compartment of each insert in the absence (-) or in the presence of macrophages (Mac), $CD4^+CD25^+$ T cells

(CD25$^+$T) or both (Mac:CD25$^+$T to 1:1 and 2:1 ratio) in the lower compartment (Figure S1b). The immune cells were already seeded in the 24-well plate for 3 or 7 days. To guarantee the contact between the insert and the conditioned medium, the final volume of the lower compartments was brought to 750 µL by adding 250 µL of complete medium supplemented with anti-CD3 antibody (50 ng/mL). For control condition (-), 750 µL of complete medium supplemented with anti-CD3 (50 ng/mL) was placed in the lower compartment. After 24 hours of indirect culture at 37ºC and 5% CO_2, inserts were removed, washed in PBS, fixed in 4% PFA, mounted in Vectashield with DAPI and visualized through a Zeiss Axiovert 200M fluorescence microscope. To cover all the filter area, invasive cells were scored in 13 microscopic fields with 20x objective when DAPI-counterstained nuclei passed through the filter pores. The invasion assays were performed with 5 different donors for RKO and 3 donors for SW620 cell line. After matrigel invasion assays, CM were stored for ELISAs, zymography and coverslip were used to assess macrophage molecular profile by ICC.

Zymography

Conditioned media from macrophage, CD4$^+$CD25$^+$ Treg cells or co-cultures after invasion assays were analysed by gelatin zymography to evaluate MMP9 and 2 activity. Protein content was determined by Dc Protein kit (Bio-Rad, Amadora, Portugal) and 16 µg of protein were mixed with sample buffer (10% sodium dodecyl sulfate, 4% sucrose and 0.03% bromophenol blue in 0.5 M Tris–HCl, pH 6.8) to a final volume of 15 µL, loaded and separated on 10% polyacrylamide gels containing 0.1% gelatin (Sigma-Aldrich) as substrate, at 80 V and 120 mA. After electrophoresis, gels were washed twice with 2% triton X-100 and once with deionized water. Gelatin gels were subsequently incubated for 16 hours at 37ºC in appropriate MMP2 and MMP9 substrate buffer [50 mM Tris–HCl, pH 7.5 and 10 mM $CaCl_2$]. After this time, gels were washed in deionized water and stained with 0.1% Coomassie Brilliant Blue R-250 (Sigma-Aldrich) for 30 minutes. MMPs molecular weight and activity were estimated by densitometric analysis (QuantityOne, Bio-Rad).

Western blot

RKO cells, at approximately 80% confluency, were serum-starved ON and treated with CM from macrophages (CM(mac)), CD4$^+$CD25$^+$ T cells (CM(CD25$^+$T)) or co-cultures at 1:1 (CM(1:1)) and 2:1 ratios (CM(2:1)), or with complete RPMI as control (CM(RPMI)) for 1 hour. Then, monolayers were washed in PBS and cell lysates prepared in cold lysis RIPA

buffer [50 mM Tris-HCl-pH 7.5, 1% NonidetP-40, 150 mM NaCl], supplemented with proteases and phosphatases (2 mM ethylenediaminetetraacetate [EDTA], 3 mM sodium orthovanadate [Na_3VO_4], 20 mM sodium fluoride [NaF], 1 mM phenylmethylsulfonyl fluoride [PMF], 10 µg/mL aprotinin and leupeptin) for 15 minutes. Then, cells were scraped, collected and centrifuged for 10 minutes at 4ºC at 392 xg. Protein concentration was determined as previously described and 35 µg of protein mixed with sample buffer (Laemmeli 4x, β-mercaptoethanol [Biorad], bromophenol blue 0.25%) were loaded on 10% sodium dodecyl sulfate (SDS)-polyacrylamide gel. After electrophoresis, bands were transferred onto hybond nitrocellulose membranes (Amersham) in a blot cassette submerged in transfer buffer supplemented with methanol and SDS 10%, ON at 100 V 120 mA. Membranes were incubated with Ponceau Red Solution (Sigma-Aldrich) to allow the visualization of transferred bands and washed twice in deionized water. After blocking with 4% BSA in PBS+0.5% Tween-20 (Sigma-Aldrich) for 30 minutes, membranes were incubated for 1 hour with rabbit polyclonal antibodies against phospho-EGFR(Y^{1086}) (ThermoFisher, 36-9700), Akt (Cell Signaling, 9272S), phospho-Src(Y^{416}) (Cell Signaling, 2102S), Src (Cell Signaling, 2108S) or α-tubulin (Sigma-Aldrich, T5168) or with mouse monoclonal antibodies against EGFR (BD Transduction, 610016) or phospho-Akt (S^{473}) (Cell Signaling, 9246S). Donkey anti-rabbit or sheep anti-mouse-HRP-conjugated secondary antibodies (GE Healthcare) were used followed by ECL-Detection (GE Healthcare). Bands of phosphorylated proteins were quantified by densitometric analysis (QuantityOne-BioRad) and compared with the levels of the respective total proteins and of α-tubulin, as loading controls.

Immunohistochemistry

34 tissues samples from Hospital São João Tissue and Tumour Bank (gently provided by Professor Fátima Carneiro) were immunohistochemically stained for FoxP3 expression. Similarly to most published studies addressing the prognostic value of Tregs in cancer we used clone 236A/E7 (Abcam, ab20034), that was showed to detect mostly $CD4^+CD25^+$ T cells[88]. 3 µm-thick tissue sections were prepared from formalin-fixed, paraffin-embedded specimens. After deparaffinization, in clear-rite, and rehydration, using graded alcohol washes, slides were boiled at 98ºC in 10 mM citrate buffer (pH 6) for 10 minutes, for antigen retrieval. Subsequently, slides were allowed to cool down for 20 minutes and washed in 0.02% PBS(1x)-Tween (PBS-$t^{0.02\%}$). Endogenous peroxidase activity was blocked by incubation with 3% H_2O_2 solution in methanol for 10 minutes at RT in the dark, followed by new washing step with PBS-$t^{0.02\%}$. Tissue sections were limited with a hydrophobic pen and

Ultra V Block (Thermo) was applied for 30 minutes in a humidified chamber to block unspecific antigens. For immunostaining, slides were incubated with the mouse monoclonal anti-human FOXP3 antibody diluted with Large Volume Ultra AB Dilutent (Dako) to 1:100, for 1h30 at RT. After incubation with primary antibody, slides were washed with PBS-$t^{0.02\%}$ and incubated with labelled polymer horseradish peroxidase rabbit/mouse secondary antibody for 30 minutes (Envision Plus Detection System; Dako). Following a new washing step, antigen detection was performed by incubation with 3,3-Diaminobenzidine (DAB+ chromogen, DakoCytomation, Glostrup, Denmark) for 6 minutes, and washed 10 minutes in running water. Then, sections were counterstained with hematoxylin (AppliChem, Germany) for 1 minute, washed in running water for 15 minutes, rehydrated through graded alcohol incubations followed by 10 minutes in clear-rite and mounted with Entellan (Thermo Scientific). Tissue section from lymph nodes and tonsil were used as positive control.

Measurement of FoxP3 density

Foxp3-positive cells were quantified in three distinct regions: the normal colonic mucosa (NCM), tumour nest (TN) and tumour invasive front (IF). The NCM was defined as the region most far away from the outline of the tumour. The tumour nest was defined as the area apart from the tumour outline toward the center of the tumour. The invasive front was defined as the most advanced front of the tumour in the interface of the tumour and normal adjacent mucosa or, in an advanced stage, the submucosa. FoxP3-positive cells were manually counted in 10 high-power field of each region and the average number of cells in each region was considered for 30 tissue samples. In the remaining 4 tissue samples, the three areas could not be distinguished, therefore, were not considered.

Statistical Analysis

Data were analysed with Mann–Whitney test for comparisons between two groups or with Kruskal-Wallis test followed by a correction with Dunn's multiple comparison test when more than 3 conditions were compared at the same time. All statistical analysis were performed using GraphPad Prism v6, GraphPad Software, (San Diego, CA, USA -trial version), and expressed as mean values of at least three independent experiments ± standard deviation (SD). Differences in data values were considered significant at a P-value of <0.05.

Results

Macrophages display higher levels of adhesion and differentiation in 24-well plates with glass coverslips

Human monocyte isolation from peripheral blood and buffy coats was already established in our laboratory[57]. Previous experiments using FACS analysis revealed that on average 80-85% of the RosetteSep isolated monocytes expressed CD14, a monocyte/macrophage lineage marker. To optimize *in vitro* culture conditions, isolated human $CD14^+$ monocytes were seeded, in the absence of exogenous stimuli, on three different substrates: 6-well tissue culture-treated and -non-treated plates, at a density of $0{,}13x10^6$ monocytes/cm^2, or on 24-well tissue culture-treated plates containing glass coverslips/well, at a density of $0{,}26x10^6$ monocytes/cm^2. *In vitro* cultures were maintained for 3 and 7 days to allow purified monocyte differentiation into macrophages, and their density, adhesion and morphology were analysed. At day 3, monocytes exhibited low levels of differentiation and adhesion to the three substrates, while adherent monocyte-derived macrophages displayed very small round morphology (Figure 5, left panels). At day 7, macrophage density, adhesion and morphology between substrates differed (Figure 5, right panels). On 6-well tissue culture-treated plates, loss of cellular density and low levels of differentiation were observed, with macrophages displaying a small and round morphology (Figure 5, upper panel). In contrast, on 6-well tissue culture-non-treated plates (Figure 5, middle panel) and 24-well tissue culture-treated plates with glass coverslips inserted (Figure 5, lower panel) a higher cellular density was observed. Additionally, adherent/differentiated macrophages displayed a heterogeneous morphology and the most elongated exhibited long protrusions (Figure 5, lower panel, and arrowheads), suggesting higher levels of differentiation on this substrate. Looking into more detail for monocytes cultured on 24-well tissue culture-treated plates with glass coverslips, the number of adherent macrophages seemed to be higher in comparison to other substrates. For this reason, all subsequent experiments with monocytes were performed using 24-well tissue culture-treated plates with glass coverslips.

Isolation of $CD4^+CD25^+$ T cells with StemCell isolation kit allows an autologous setting between $CD14^+$ monocytes and $CD4^+CD25^+$ T cells

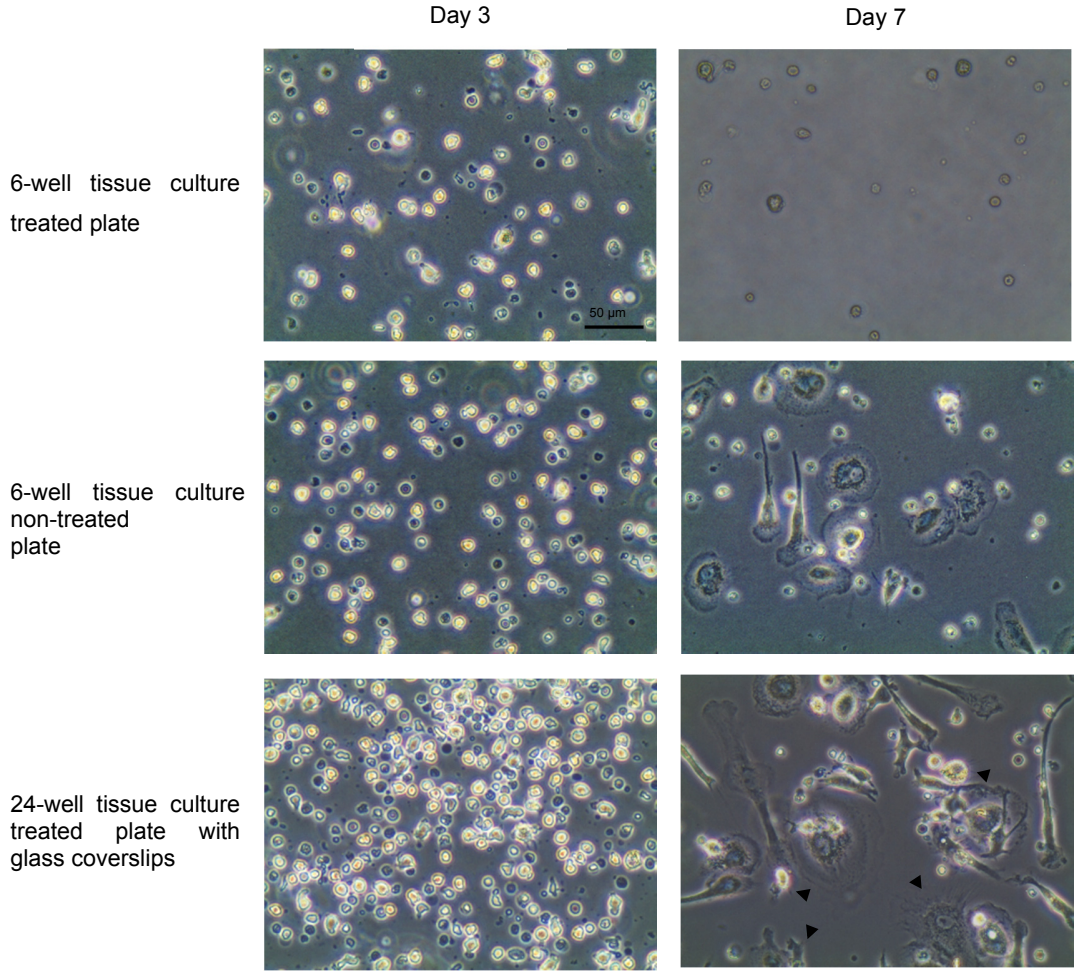

Figure 5. Macrophage display higher levels of adhesion and differentiation on 24-well plates with glass coverslips. Monocyte isolation was performed by negative selection using RosetteSep monocyte enrichment kit. Monocytes were seeded on three different substrates: 6-well tissue culture-treated plates (upper panels), 6-well tissue culture-non-treated plates (middle panels) and 24-well tissue culture-treated plates with glass coverslips inserted (lower panels), for 3 (left panels) or 7 days (right panels), to allow monocyte to macrophage differentiation. After this time, macrophage morphology and adhesion were examined. Cells were visualized and photographed at 200x magnification with an Olympus CKX41 (SC30) microscope. Arrowheads indicate macrophage long protrusions. Scale bar represents 50 µm. Experiments were performed with 2 donors.

Human $CD4^+CD25^+$ Tregs cells were isolated through a negative selection ($CD4^+$ T cells) followed by a positive selection ($CD25^+$ T cells) procedure. To optimize cell isolation, two commercially available regulatory T cell isolation kits were tested: the Human Regulatory T Lymphocyte Separation Set from BD Biosciences (BD) and the Regulatory T cell Isolation Kit from StemCell Technologies (SC). Since our main goal was to perform monocyte-Treg co-cultures, an autologous setting was designed and a sample from the same blood donor

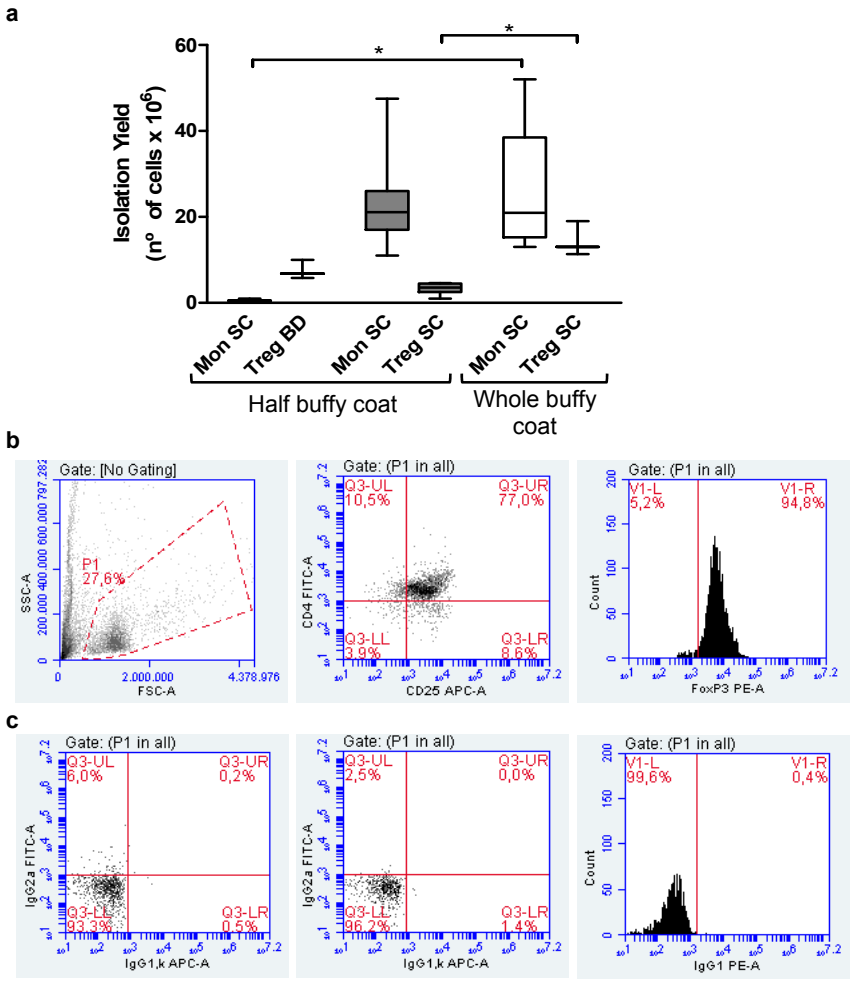

Figure 6. Isolation of Tregs with StemCell isolation kit allows an autologous setting between CD14$^+$ monocytes and CD4$^+$CD25$^+$ T cells. For an autologous setting the same blood donor was used to isolate CD14$^+$ monocytes and CD4$^+$CD25$^+$ Tregs. **a)** Monocyte (Mon SC) isolation was combined with BD regulatory T cell isolation (Tregs BD) or with StemCell regulatory T cell isolation Kit (Tregs SC). Buffy coats or PBMCs were first divided to isolate both immune cells. Non-divided PBMCs were also used to isolate only monocytes or only Tregs with SC Kit. Results are presented as the number of isolated cells x10^6. The purity of CD4$^+$CD25$^+$ T cells isolated with SC Kit was assessed by FACS. **b)** Cell aspect-ratio (left panel) and CD4$^+$CD25$^+$FoxP3$^+$ (middle and right panels) triple-staining immediately after purification. **c)** Respective IgGs were used to subtract background staining. Data are presented as box and whisker plots: white and grey boxes extend from the 25th to the 75th percentile, with a black line at the median; whiskers extend to show the highest and lowest values. For isolations with 3 distinct donors only the median value and range are shown. Experiments were performed at least with 3 distinct donors. *, significantly different at P<0.05.

was used to isolate both immune cell populations. Therefore, to combine monocyte isolation with BD regulatory T cell isolation Kit, buffy coats were initially divided, whereas to combine monocyte isolation with SC regulatory T cell isolation Kit, PBMCs were first collected from buffy coats and then divided for immune cell isolation. These differences resulted from specifications of the isolation protocols, as provided by the manufacturers. Our results

showed that when the buffy coat was initially divided to isolate these immune populations the yield of Tregs was sufficient ($7.53x10^6$±2.19 $CD4^+CD25^+$ T cells) but the yield of monocytes was very low ($0.50x10^6$±0.50 $CD14^+$ monocytes), compromising their isolation and seeding (Figure 6a). When the whole buffy coats' blood was centrifuged to obtain PBMCs and further divided to isolate $CD14^+$ monocytes and $CD4^+CD25^+$ T cells with the SC isolation kit, the yield of $CD4^+CD25^+$ T cells was lower ($3.32x10^6$±1.26 $CD4^+CD25^+$ T cells) but the monocyte isolation was successful ($23.62x10^6$±11.68 $CD14^+$ monocytes). When comparing isolation from half or whole PBMCs, the yield of monocytes was similar (Non-parametric Mann-Whitney Test; P=0.83), although the yield of $CD4^+CD25^+$ T cells was significantly different (Non-parametric Mann-Whitney Test; $P<0.05$) (Figure 6a). Altogether, our results evidence that SC isolation of $CD4^+CD25^+$ T cells represents the best compromise to purify both $CD14^+$ monocytes and $CD4^+CD25^+$ T cells, and to further perform an autologous setting between these immune populations. For this reason, all subsequent Treg isolations were performed using the SC kit.

To assess the purity of the SC isolated $CD4^+CD25^+$ T cells, FACS was performed immediately after isolation (Figure 6b and c). The population of interest was selected and gated based on cell aspect ratio (Forward scatter (FSC-A), for size, and side scatter (SSC-A), for cell complexity). Along our experiments, the yield of isolated T cells was, on average, 77% for $CD4^+CD25^+$ T and 94% for FoxP3. These results indicate that the majority of the isolated cells expressed Treg characteristic markers, although the presence of a residual fraction of $CD4^+CD25^{mid/low}$ T cells could not be ruled out. For this reason we decided to designate this population as $CD4^+CD25^+$ T cells.

Isolated T cells modify their morphology and FoxP3 expression profile after 3 and 7 days of culture

For a better analysis of $CD4^+CD25^+$ T morphology, cells were isolated using the SC kit and seeded on 6-well tissue culture-non-treated plates, at a density of $1x10^6$ cells/well. To guarantee Treg cell activation and function[143], soluble anti-CD3 monoclonal antibody was added to all cultures. *In vitro* cultures were maintained for 3 and 7 days and $CD4^+CD25^+$ T cells density, adhesion and morphology were subsequently analysed. Generally, $CD4^+CD25^+$ T cells displayed a small round morphology and very low levels of adhesion (Figure 7a). At day 3, and especially at day 7 after seeding, $CD4^+CD25^+$ T cells became a heterogeneous population, with some elongated cells, while the majority remained rounded

but smaller. Through smooth plate agitation, we observed that cells were more adhered at day 7 than at day 3. Additionally, through microscopic observation, cellular confluency remained similar at all time points. However additional quantitative testes are required to confirm this observation.

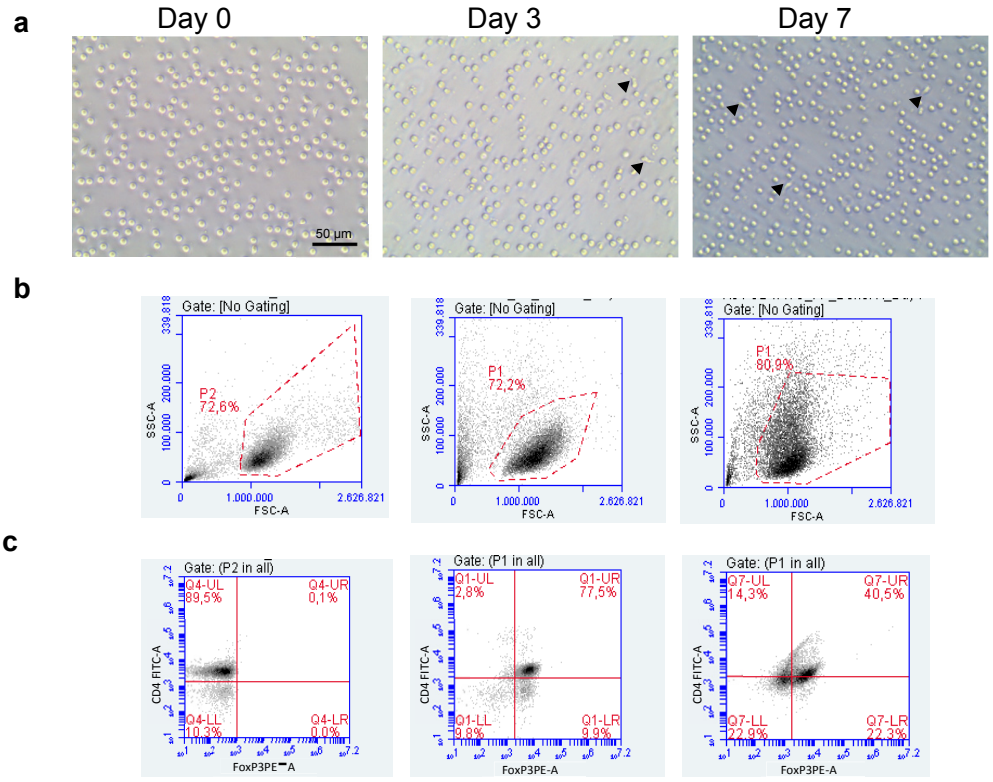

Figure 7. Isolated T cells modify their aspect ratio and FoxP3 expression profile after 3 and 7 days of culture. $CD4^+CD25^+$ T isolation was performed by negative selection followed by a positive selection using the SC kit. Cells were seeded in the presence of anti-CD3 mAb on 6-well tissue culture-non-treated plates at the density of $1x10^6$ cells. **a)** Morphologic evaluation of $CD4^+CD25^+$ T at day 0, 3 and 7 after isolation. Cells were visualized at 200x magnification. **b)** Aspect ratio and **c)** population purity by CD4 (activated T cell marker), immediately after purification (day 0, left panels), and CD4 and FoxP3 (Treg lineage marker) double staining at days 3 and 7 (middle and right panels) after seeding. Respective IgGs were used to subtract background staining. Experiments were performed with only one blood donor. Arrowheads indicate elongated cells. Scale bar represents 50 µm.

To assess cell purity, $CD4^+CD25^+$ T cells phenotype was evaluated by FACS for CD4 cell surface expression immediately after isolation and for CD4 and FoxP3 intracellular marker expression, at days 3 and 7 after isolation (Figure 7b, c and d). The population of interest was selected and gated (Figure 7b) based on cell aspect ratio. In concert with the previous morphological analyses, immediately after isolation, T cells displayed a well-defined aspect ratio, restricted in size and complexity. However at day 3 and especially at

day 7, the aspect ratio of the seeded population reduced in size (FSC-A) and increased in complexity (SSC-A). Regarding purity, isolation resulted in an average of 89% $CD4^+$ T cells (Figure 7c, left panel). At day 3, 77.5% of the population was $CD4^+FoxP3^+$ (Figure 7c, middle panel) while at day 7 two populations could be distinguished: one $CD4^+FoxP3^-$ (14.3%), and another $CD4^+FoxP3^+$ (40.5%) (Figure 7c, right panel). These results demonstrate loss of FoxP3 expression upon long-time culture.

Macrophages and $CD4^+CD25^+$ T cell-educated macrophages are viable and metabolically active while $CD4^+CD25^+$ T cells are viable but less active

The impact of Tregs on macrophage morphology and viability was assessed in *in vitro* cell cultures. Isolated human $CD14^+$ monocytes and $CD4^+CD25^+$ T cells mono- and co-cultures (1:1 or 2:1 ratios, Mac:$CD25^+$T) were performed using 24-well tissue culture-treated plates with glass coverslips, for 3 and 7 days, in an autologous setting. To ensure T cell activation, an anti-CD3 mAb was added to all conditions. Co-stimulation of CD28 was provided by the presence of monocytes in the culture plate. To assess cell morphology by actin/tubulin cytoskeleton organization, F-actin and α-tubulin staining was performed. Lower levels of adhesion and differentiation were observed at day 3 than at day 7 after seeding, especially in $CD4^+CD25^+$ T cells mono-cultures. At day 3, macrophages displayed preferentially a round morphology whereas when co-cultured with $CD4^+CD25^+$ T cells a higher number of elongated macrophages were observed, particularly at the 1:1 ratio (Figure 8a, upper panel). This was further confirmed at day 7, where macrophages at 1:1 ratio were more elongated than at 2:1 ratio and macrophage mono-cultures (Figure 8a, lower panel). In $CD4^+CD25^+$ T cells mono-cultures, at day 3, cells displayed a round morphology, while at day 7 the population became heterogeneous, presenting both elongated and small rounded cells, which is in concert with previous analyses. To rule out that co-cultures did not affect the sustainability of each immune population, cell viability was assessed by trypan blue-exclusion assay (Figure 8b) and cell metabolic activity by resazurin reduction assay (Figure 8c). No differences in terms of cell viability were observed between the distinct conditions (>80%) (Figure 8b). Regarding metabolic activity, macrophages ($0.28\pm0.08\times10^4$ RFUs per 1×10^6 cells) and macrophage-$CD4^+CD25^+$ T co-cultures (1:1 ratio: $0.31\pm0.08\times10^4$ RFUs per 1×10^6 cells; 2:1 ratio: $0.36\pm0.12\times10^4$ RFUs per 1×10^6 cells) presented slightly lower levels of activity at day 3 than at day 7 after seeding (macrophages: $0.36\pm0.14\times10^4$ RFUs per 1×10^6

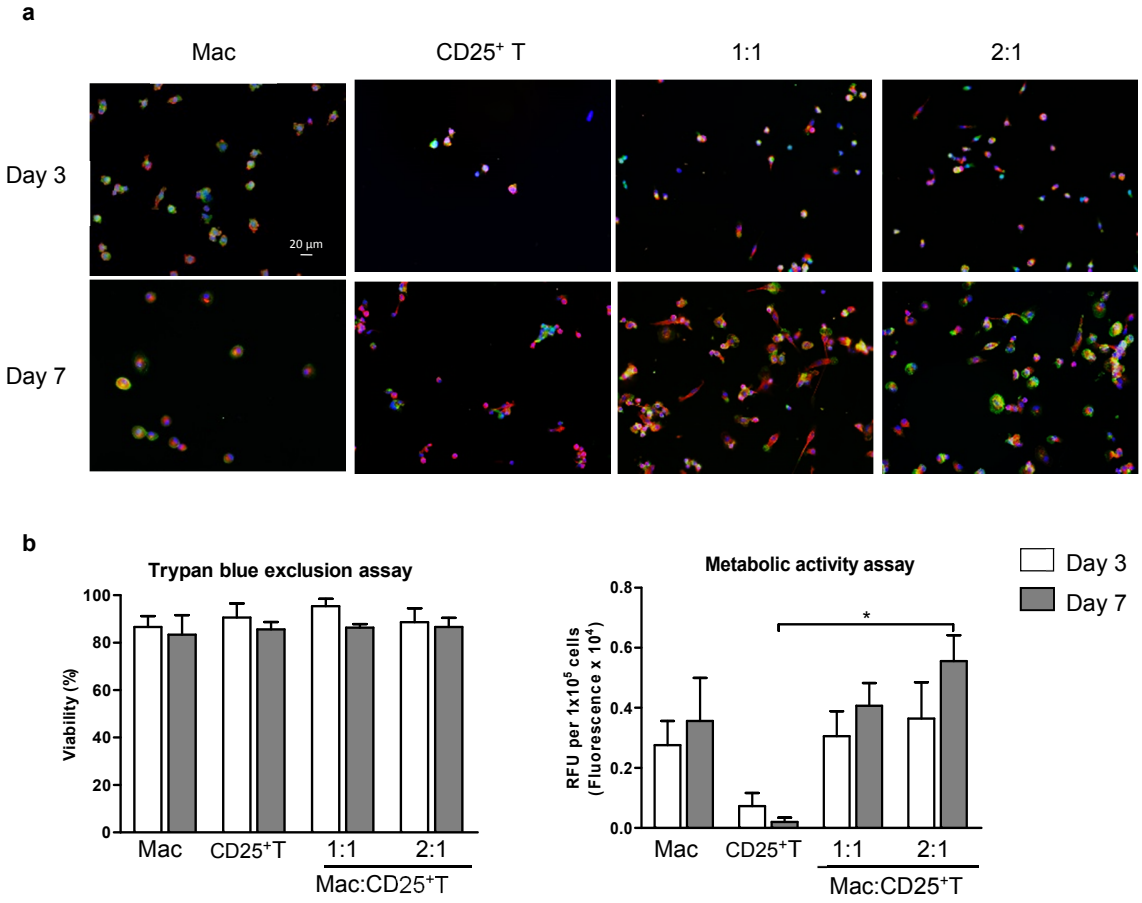

Figure 8. Macrophage and CD4⁺CD25⁺ T-educated macrophages are viable and metabolically active while CD4⁺CD25⁺ T cells are viable but less active. Monocytes and CD4⁺CD25⁺ Treg cells were isolated from buffy coats and seeded as single or co-cultures (1:1 and 2:1, Mon:CD4⁺CD25⁺ T ratio) with an anti-CD3 mAb, on 24-well tissue culture-treated plates with glass coverslips. Cells were fixed in 4% PFA and **a)** stained for actin and tubulin at day 3 (upper panels) and 7 (lower panels) after seeding. F-actin was stained with phalloidin-FITC (green), α–tubulin with a specific monoclonal antibody followed by incubation with AlexaFluor594 secondary antibody (red) and nuclei were counterstained with DAPI (blue). **b)** For trypan blue exclusion assay cells in the medium and in the coverslips were incubated with trypan blue and then counted in a Neubauer chamber. Cells exhibiting blue-stained nuclei were considered dead and results are expressed as percentage of viability (%), calculated through ($Total_{live\ cells}/Total_{cells}$)x100 for day 3 (open bars) and day 7 (grey bars). **c)** Metabolic activity was assessed by resazurin reduction over 4h. Results are expressed in relative fluorescence units (RFU) per $1x10^5$ cells for day 3 (open bars) and day 7 (grey bars). Bars represent mean values of independent experiments, performed with three distinct donors, and flags indicates SD. *, significantly different at $P<0.05$. Scale bar represents 20 µm.

cells; 1:1 ratio: $0.41\pm0.08x10^4$ RFUs per $1x10^6$ cells; 2:1 ratio: $0.56\pm0.09x10^4$ RFUs per $1x10^6$ cells). In contrast, CD4⁺CD25⁺T mono-cultures seemed to have low levels of activity at both days, but especially at day 7 ($0.07\pm0.04x10^4$ RFUs per $1x10^6$ cells, at day 3; $0.02\pm0.01x10^4$ RFUs per $1x10^6$ cells, at day 7). Interestingly, after 7 days, only CD4⁺CD25⁺ T cell-educated macrophages ratio 2:1 exhibited significantly higher metabolic activity than CD4⁺CD25⁺ T cell mono-cultures (Non-parametric Kruskal-Wallis Test; $P<0.05$), as

demonstrated by their higher ability to reduce resazurin to resorufin (Figure 8c). These results suggest that macrophages and $CD4^+CD25^+$ T cell-educated macrophages were viable and active after 3 and 7 days of culture while $CD4^+CD25^+$ T cells were viable but metabolically less active.

Co-cultures with isolated $CD4^+CD25^+$ T cells express CD163, but not CD80

One of our goals was to determine the effect of $CD4^+CD25^+$ T cells on macrophage inflammatory profile. Therefore, monocyte-derived macrophages were cultured, for 3 and 7 days, in the presence of Tregs and further characterized regarding CD80 (pro-inflammatory marker) and CD163 (anti-inflammatory marker) cell surface receptor expression (Figure 9a and b, respectively) and for IL-6, TGF-β and IFN-γ cytokines secretion profile (Figure 9 c and d, respectively). At day 3, mono- and co-cultures displayed lower levels of differentiation and consequently, the expression of macrophage cell surface markers was lower than at day 7. As expected from a naïve macrophage population, monocyte-derived macrophages, cultured alone and in the absence of exogenous stimuli, are a heterogeneous population expressing both CD80 and CD163 markers. Accordingly, macrophages alone secreted low levels of the distinct cytokines. Our results evidenced that since day 3 the presence of $CD4^+CD25^+$ T cells abrogated macrophage CD80 expression and reduced CD163 expression, especially in 1:1 ratio co-cultures. However, conditioned media (CM) from co-cultures of macrophages with $CD4^+CD25^+$ T cells (CM(1:1) and CM(2:1)) revealed slightly higher levels of IL-6 than from macrophages (CM(Mac)) alone (Figure 9c). The levels of tTGF-β remained similar in all conditions (Figure 9d). None of the cultures secreted detectable levels of IFN-γ after 3 or 7 days of seeding (data not shown). Overall, these results suggested that $CD4^+CD25^+$ T cells are inhibiting the expression of a pro-inflammatory receptor without fully inducing an anti-inflammatory profile. Of note, only one experiment was performed to evaluate the levels of cytokines available in the condition medium (CM) of the distinct conditions. Therefore, these results can be misleading regarding the general pattern of cytokine secretion of macrophage, $CD4^+CD25^+$ T cells and macrophage-$CD4^+CD25^+$ T cell co-cultures.

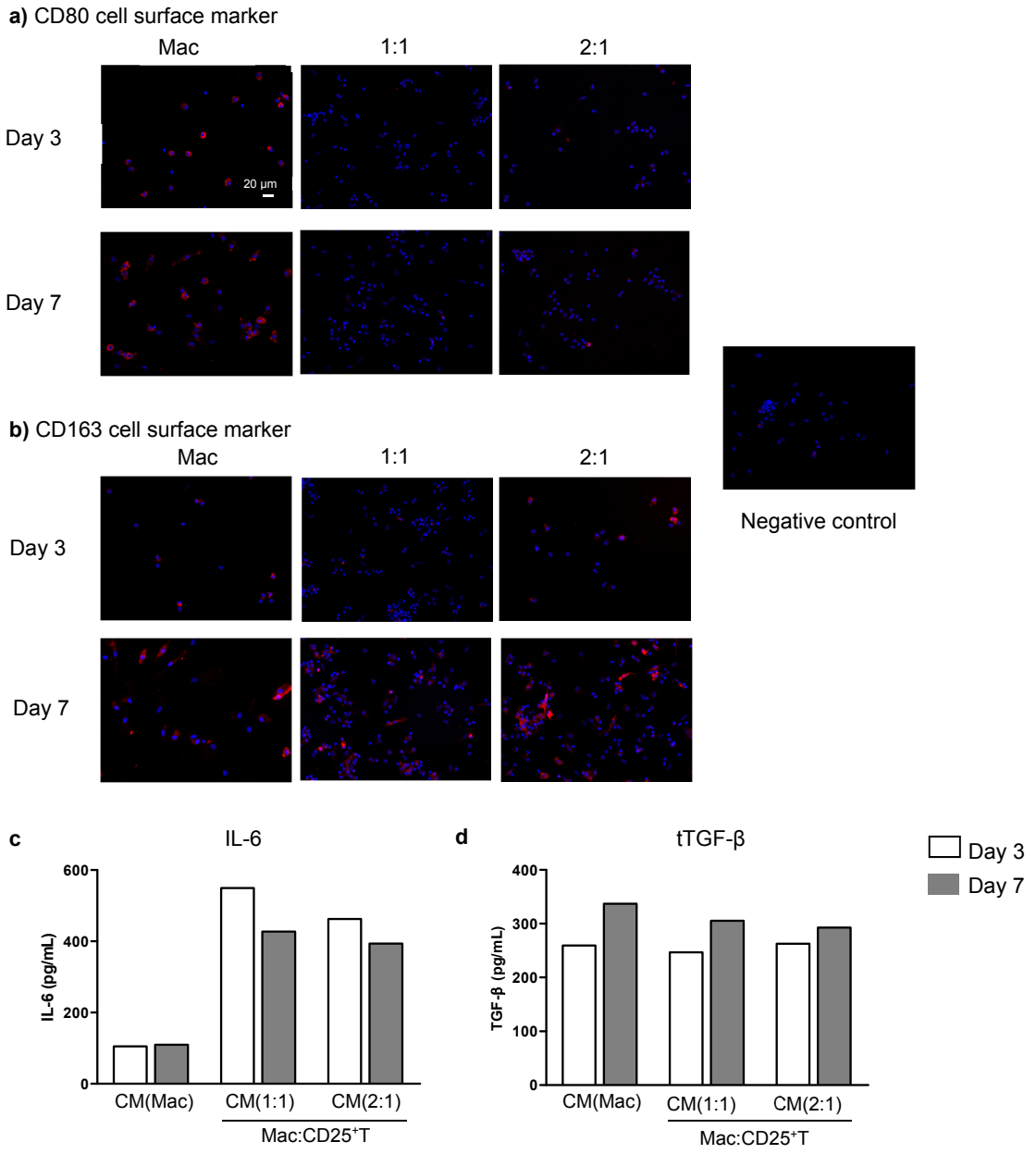

Figure 9. Co-cultures with isolated CD4$^+$CD25$^+$ T cells express CD163, but not CD80. The phenotype of monocyte-derived macrophages cultured alone or in the presence of CD4$^+$CD25$^+$ T cells (1:1 or 2:1, Mac:CD25$^+$ T ratio) was characterized by cell surface receptor expression of **a)** CD80 and **b)** CD163 for 3 (upper panel) and 7 days (lower panels) after culture, and by secretion of **c)** IL-6 and **d)** tTGF-β cytokines measured by ELISA in conditioned media collected at day 3 (white bars) and 7 (grey bars) after seeding. Negative control was used to subtract background staining. ICC analyses are representative of 3 experiments and ELISA resulted from conditioned media of a single experiment. CD80 and CD163 were stained with specific monoclonal antibodies followed by incubation with AlexaFluor594 secondary antibody (red) and nuclei were counterstained with DAPI (blue). Scale bar represents 20 µm.

Macrophages and CD4$^+$CD25$^+$ T cell-educated macrophages significantly induce RKO but not SW620 cancer cell invasion

We have previously demonstrated that soluble factors produced by macrophages promote gastric and CRC cell invasion[57]. To clarify the role of CD4$^+$CD25$^+$ T cells on macrophage pro-invasive activity, macrophages or CD4$^+$CD25$^+$ Treg-educated macrophages were cultured for 3 or 7 days and further confronted with CRC cells, using 3D-matrigel invasion assays. In these experiments, two different cell lines were used: RKO, isolated from a primary colon adenocarcinoma, and SW620, isolated from a colorectal cancer lymph node metastasis. For control purposes, each cell population was cultured alone during the same time points. RKO displayed higher ability to invade the matrigel (106.3±40.73 invasive cells) than SW620 (12.30±7.96 invasive cells) (Figure 10a and b, respectively). Our results

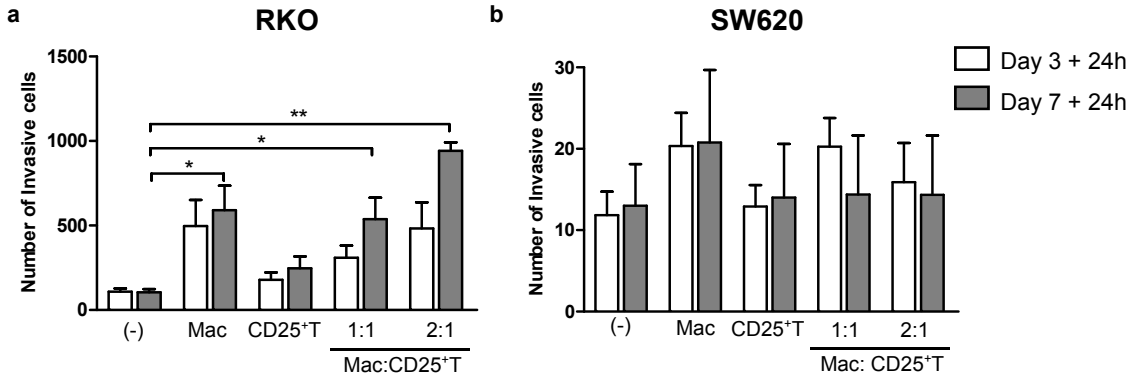

Figure 10. **Macrophages and CD4$^+$CD25$^+$ T-educated macrophages significantly induce RKO but not SW620 cancer cell invasion.** RKO or SW620 human colon cancer cells CD4$^+$CD25$^+$ T cells were incubated for 24 h at the upper compartment of matrigel-coated invasion chambers, in the presence of: RPMI medium (-), macrophages (Mac), CD4$^+$CD25$^+$ T cells (CD25$^+$T), Mac and CD4$^+$CD25$^+$ T cells co–cultured at 1:1 or 2:1 (Mac:CD25$^+$T) ratio, during 3 (white bars) or 7 (grey bars) days. Bars represent mean values of independent experiments ± SD. RKO invasion assay was performed with an n=5 and SW620 was performed with an n=3. *, significantly different at P<0.05, ** significantly different at P<0.01.

evidenced that RKO cancer cell invasion was significantly promoted by macrophages (Non-parametric Kruskal-Wallis Test; P<0.05) and by CD4$^+$CD25$^+$ T cell-educated macrophages at 2:2 (Non-parametric Kruskal-Wallis Test; P<0.05) and especially at 2:1 ratios (Non-parametric Kruskal-Wallis Test; P<0.01), upon 7 days of differentiation. Interestingly, SW620 cancer cell invasion was not significantly promoted by macrophages or by macrophages and CD4$^+$CD25$^+$ T cell co-cultures. Since significant differences were only found with RKO invasion, the remaining indirect co-cultures were only established with this cancer cell line and not with SW620 CRC cells.

$CD4^+CD25^+$ T cell-educated macrophages in indirect contact with RKO cells express CD163, but not CD80, and display a "mixed" cytokine secretion profile

We have previously described that IL-10-stimulated macrophages (anti-inflammatory-like profile) displayed higher pro-invasive activity than LPS-stimulated macrophages (pro-inflammatory-like profile)[58]. Here, we aimed to understand if the observed pro-invasive activity induced by $CD4^+CD25^+$ T cell-educated macrophages was associated with the acquisition of an anti-inflammatory profile upon indirect co-culture with RKO cancer cells. Therefore, macrophage and $CD4^+CD25^+$ T cell-educated macrophages cell surface receptor (CD80 and CD163) expression and cytokine (IL-6, IFN-γ, tTGF-β and IL-10) secretion profiles were assessed, upon 24h of indirect co-cultures.

In the presence of RKO, at day 3 + 24h, macrophages in mono-cultures expressed low levels of CD80 (Figure 11a) and intermediated levels of CD163 (Figure 11b). However, at day 7 + 24h, the expression of these markers was upregulated in almost all macrophages (Figure 11a and b), resembling a heterogeneous population. At day 3 + 24h with RKO, $CD4^+CD25^+$ T cell-educated macrophages expressed low levels of CD80, whereas at day 7 + 24h the expression of this pro-inflammatory marker was completely suppressed (Figure 11a). Regarding CD163, at day 3 + 24h with RKO, the expression of this marker on $CD4^+CD25^+$ T cell-educated macrophages was negative at 1:1 and low at 2:1 ratios (Figure 11b). However, at day 7 + 24h, the levels of CD163 on $CD4^+CD25^+$ T cell-educated macrophages were heterogeneous at 1:1 and at 2:1 ratios (Figure 11b), suggesting an up-regulation of this anti-inflammatory marker in long-term co-cultures.

Regarding the cytokine secretion profile (Figure 12), our results showed that when $CD4^+CD25^+$ T cell-educated macrophages were co-cultured in the presence of RKO cells (CM(1:1+RKO) and CM(2:1+RKO)) the levels of secreted IL-6, IFN-γ and IL-10 were higher than those of each immune population cultured with RKO cells (CM(Mac+RKO) and CM($CD4^+CD25^+$ T+RKO)), at both 3 + 24h and 7 + 24h days. Interestingly, none of these cytokines was detected in CM(RKO) and CM(Treg+RKO), but low levels of IL-6 and IL-10 were detected in CM(Mac+RKO). These results suggest that the high levels of the cytokines present in macrophage-$CD4^+CD25^+$ Treg population derived from the immune cell populations, rather than from RKO cancer cells. Interestingly, the levels of tTGF-β were similar in all conditions (Figure 12). At day 3 + 24h with RKO, 1:1 co-cultures (CM (1:1+RKO)) secreted significantly more IL-6, IL-10 and IFN-γ to the culture medium than

$CD4^+CD25^+$ T cells (CM($CD4^+CD25^+$ T+RKO)) (Non-parametric Kruskal-Wallis Test; $P<0.05$) and more IFN-γ than macrophages (CM(Mac+RKO)) (Non-parametric Kruskal-Wallis Test; $P<0.05$). In 2:1 ratio (CM(2:1+RKO)), IL-10 secretion was significantly higher than in CM($CD4^+CD25^+$ T+RKO) (Non-parametric Kruskal-Wallis Test; $P<0.05$), whereas IFN-γ was only higher than CM(Mac+RKO) at day 7+24h (Non-parametric Kruskal-Wallis Test; $P<0.05$).

Our results suggest that the more pro-invasive activity of $CD4^+CD25^+$ T cell-educated macrophages occurs in parallel with the loss of a pro-inflammatory marker (CD80) without the acquisition of a classical anti-inflammatory profile (mixed expression of pro- and anti-inflammatory cytokines is observed).

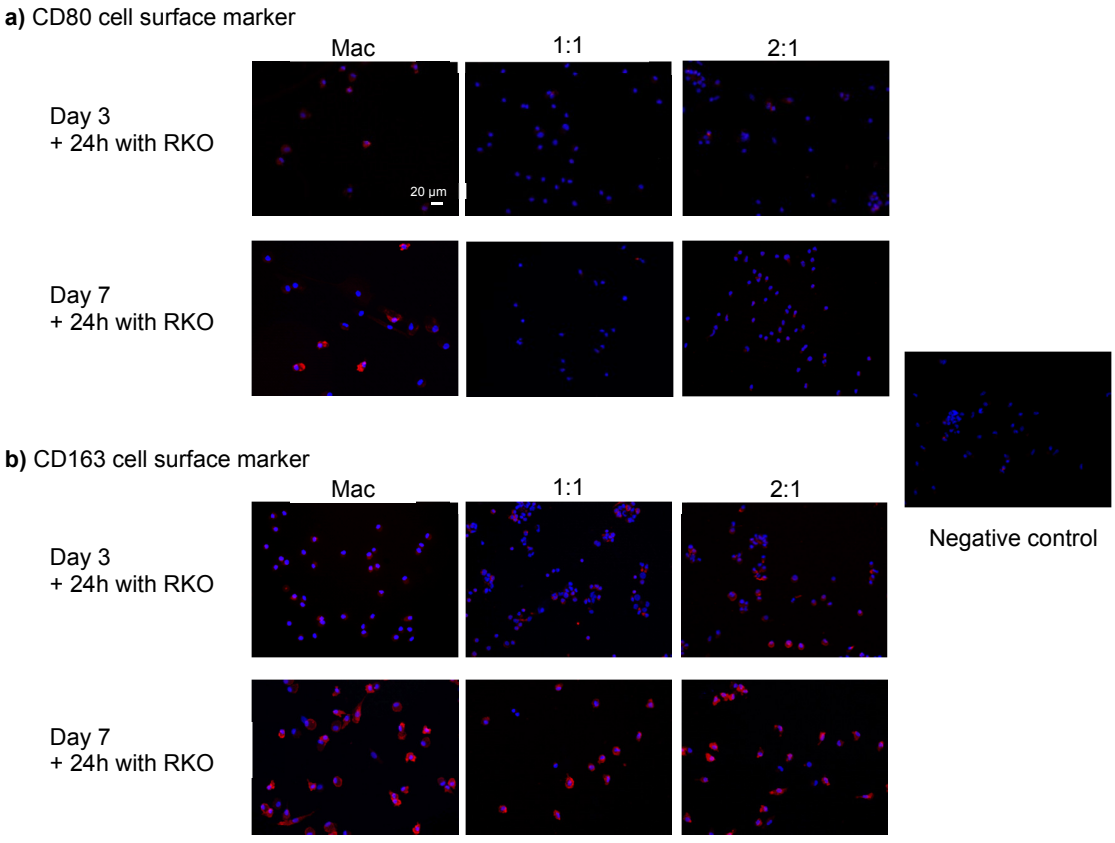

Figure 11. **$CD4^+CD25^+$ T-educated macrophages in indirect contact with RKO cells express CD163, but not CD80.** Upon indirect co-cultures with RKO cancer cells, the profile of macrophages cultured alone or in the presence of $CD4^+CD25^+$ T cells (1:1 or 2:1, Mac: $CD4^+CD25^+$ T cell ratio) was characterized by cell surface receptor expression of: **a)** CD80 and **b)** CD163, for 3 days + 24h with RKO (upper panel) and 7 days + 24h with RKO (lower panels). Negative control was used to subtract background staining. Experiments were performed with three distinct donors. CD80 and CD163 were stained with specific monoclonal antibodies followed by incubation with AlexaFluor594 secondary antibody (red) and nuclei were counterstained with DAPI (blue). Scale bar represents 20 µm.

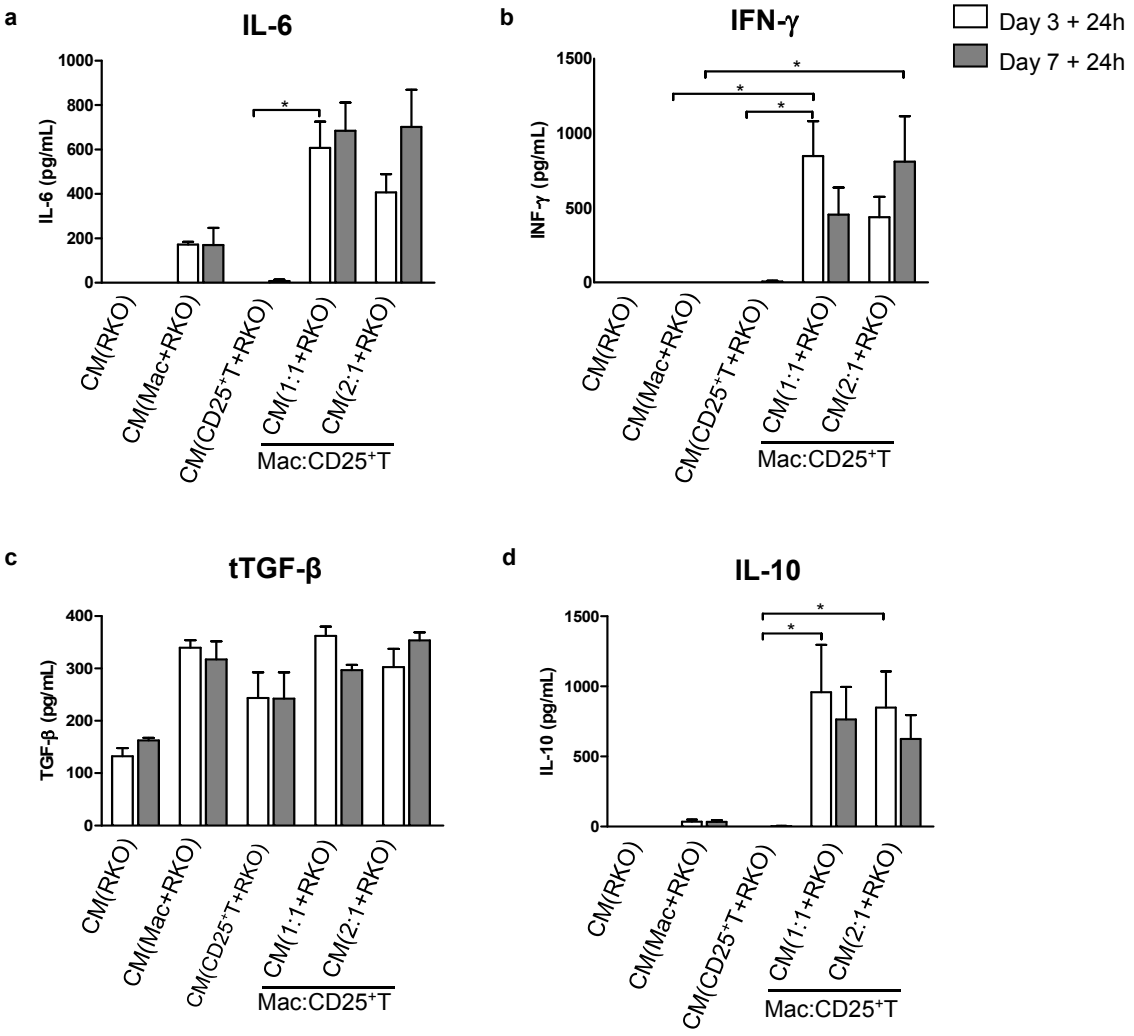

Figure 12. **CD4$^+$CD25$^+$T-educated macrophages in indirect contact with RKO cells display a "mixed" cytokine secretion profile.** Upon indirect co-cultures with RKO cancer cells, the profile of macrophages cultured alone or in the presence of CD4$^+$CD25$^+$ T (1:1 or 2:1, Mac:CD25$^+$T ratio) was characterized by secretion of: **a)** IL-6, **b)** IFN-γ, **c)** tTGF-β and **d)** IL-10 cytokines measured through ELISA, in conditioned media collected at day 3 + 24h with RKO (white bars) and 7 + 24h with RKO (grey bars). Bars represent mean values of 3 independent experiments ± SD. *, significantly different at P<0.05.

Pro-MMP9 activity is higher in CM of macrophage and macrophage co-cultures

The activity of MMPs has been previously implicated in macrophage-pro-invasive activity[57]. Furthermore, the higher ability of IL-10-stimulated macrophages, rather than its LPS-stimulated counterparts, to stimulate invasion was correlated to their higher ability to induce

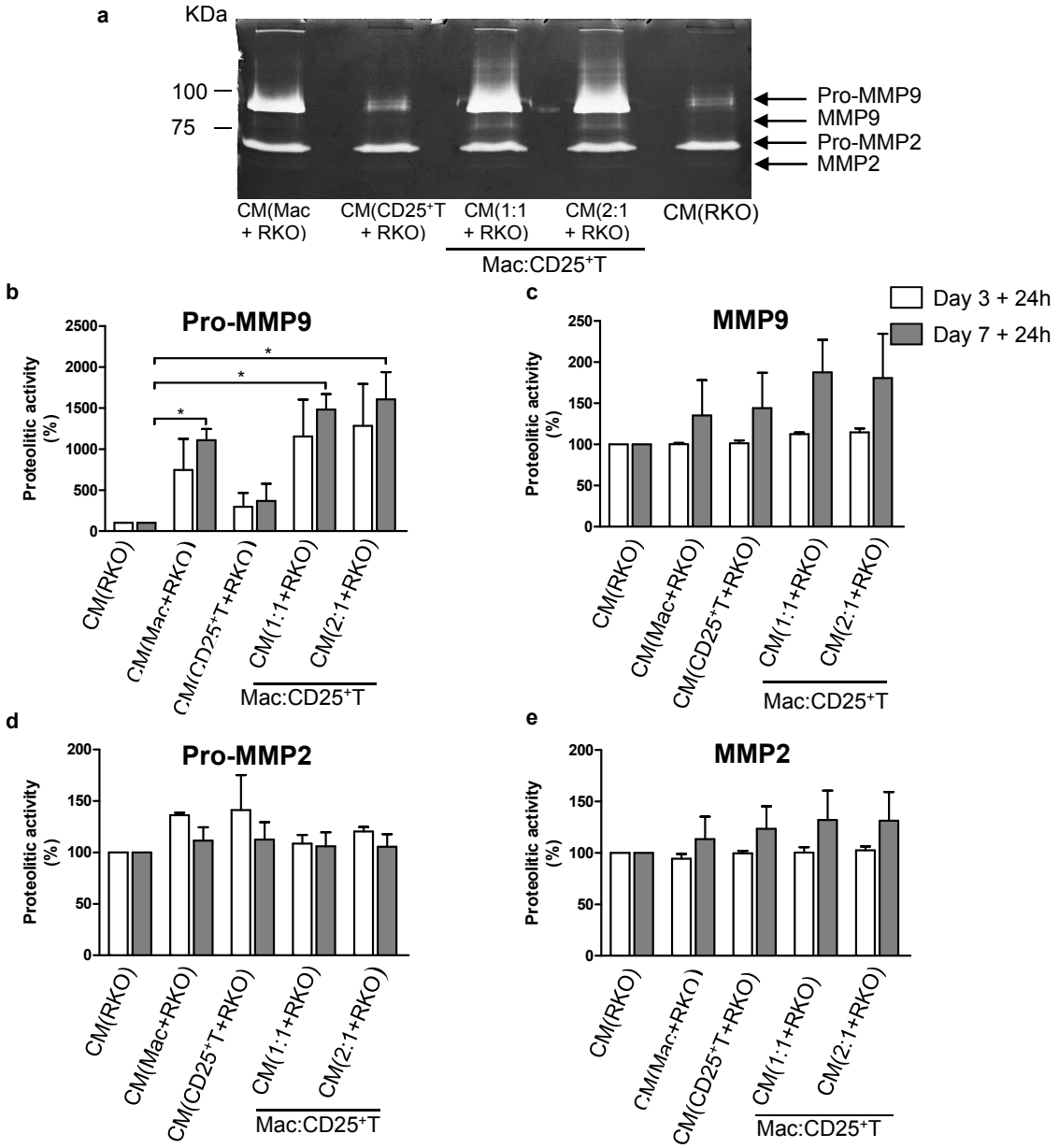

Figure 13. **Pro-MMP9 activity is higher in CM of macrophage and macrophage co-cultures**. Macrophage, $CD4^+CD25^+$ T cells and macrophage- $CD4^+CD25^+$ T cell co-cultures (1:1 and 2:1) were maintained for 3 or 7 days. Then, matrigel invasion assays were performed for 24h with RKO as an indirect co-cultures and **a)** CM from matrigel invasion assays containing RPMI and RKO (CM(RKO)), macrophages and RKO (CM(Mac+RKO)), $CD4^+CD25^+$ T cells and RKO (CM($CD25^+$T+RKO)), Macrophage-Treg cultured at 1:1 with RKO (CM(1:1+RKO)) or at 2:1 ratio with RKO (CM(2:1+RKO)) were analysed on gelatin zymograms. **b)** Proteolytic bands were revealed in white on a Coomassie Blue-stained background. Densitometry analysis using the QuantityOne software (BioRad) allowed quantification of **b)** pro-MMP9, **c)** MMP9 **d)** pro-MMP2 and **e)** MMP2 gelatin proteolytic activity. Results are expressed as percentage (%) of proteolytic activity in comparison with the activity present in RPMI culture medium and RKO (CM(RPMI+RKO)) at day 3 + 24h with RKO (white bars) or at day 7 + 24h with RKO (grey bars). Bars represent mean values of independent experiments ± SD (n=3). *, significantly different at $P<0.05$.

MMP2 and MMP9 proteolytic activities[58]. To investigate the possible mechanisms underlying

$CD4^+CD25^+$ T cells modulation of macrophage-mediated RKO cancer cell invasion, the proteolytic profile of gelatinases (MMP2 and MMP9) on CM derived from invasion assays was assessed by gelatin zymography (Figure 13a). Our results showed that, at day 7 + 24h, the CM from macrophage (CM(Mac+RKO)) and macrophage-$CD4^+CD25^+$ Treg co-cultures with RKO cells (CM(1:1+RKO) and CM(2:1+RKO)) presented higher pro-MMP9 proteolytic activity than the CM from negative control (CM(RPMI+RKO)) or from $CD4^+CD25^+$ T cells cultured alone with CRC cells (CM($CD25^+$T+RKO)) (Non-parametric Kruskal-Wallis Test; $P<0.05$) (Figure 13b). Although less evident, the proteolytic activity of gelatinases MMP9 and MMP2 were also higher on $CD4^+CD25^+$ T-macrophage co-cultures than when these immune populations were cultured apart with the colorectal cancer cells. However, the levels of pro-MMP2 were very similar between all the conditions at both days (Figure 13c, e and d, respectively). These results suggest that pro-MMP9 is associated with the enhanced pro-invasive activity of RKO in the presence of macrophages and of $CD4^+CD25^+$ T cell-educated macrophages. However, this does not explain the slightly higher pro-invasive ability of $CD4^+CD25^+$ T cell-educated macrophages in 2:1 ratio. This suggests that the differences found in the invasion profile of RKO did not exclusively rely on the proteolytic activity of these MMPs.

Conditioned media from macrophages and from $CD4^+CD25^+$ T cell-educated macrophages induce phosphorylation of EGFR in RKO cancer cells

EGFR and its related signalling molecules have been implicated in macrophage-mediated cancer cell invasion[57,58]. Therefore, to further explore the possible mechanisms involved in the pro-invasive activities of macrophages and $CD4^+CD25^+$ T cell-educated macrophages on RKO cell invasion, EGFR-signalling pathway was tested by western blot (Figure 14). Our hypothesis was that similarly to macrophages, $CD4^+CD25^+$ T cell-educated macrophages would stimulate cancer cell invasion through the activation of EGFR and of its associated downstream partners. For further investigation, RKO cells were incubated for 1 h with RPMI, as negative control (-), with CM from macrophage (CM(Mac)) or with CM from 3 and 7 days of $CD4^+CD25^+$ T-macrophage co-cultures (CM(1:1) and CM(2:1)). Our results indicate that, after 1 hour of treatment, CM from macrophages and CM from $CD4^+CD25^+$ T cell-educated macrophages similarly enhanced the phosphorylation levels of cancer cell EGFR (Y^{1086}) in comparison with the negative control (Figure 14). The differences obtained in the

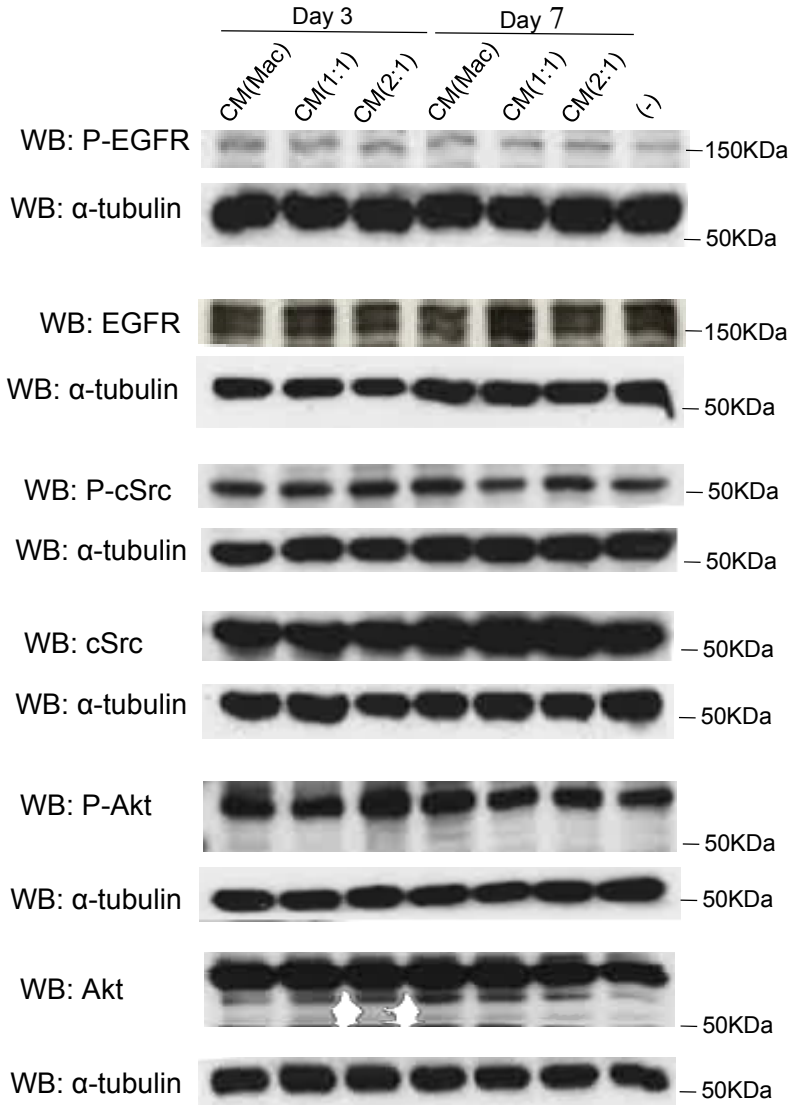

Figure 14. Conditioned media from macrophages and $CD4^+CD25^+$ T cell-educated macrophages induce phosphorylation of EGFR in RKO cancer cells. RKO cells were treated, during 1h, with RPMI (-), CM from macrophages (Mac) and from macrophage-$CD4^+CD25^+$ T cell co-cultures (1:1 or 2:1 ratios) from 3 and 7 days. Cell lysates were analysed by western blot for phosphorylated EGFR (Y^{1086}) (P-EGFR), cSrc (Y^{416}) (P-cSrc), AKT (S^{473}) (P-AKT). α–tubulin was used as a loading control and total EGFR, cSrc and AKT was used to rule out that changes in the phosphorylated form was not related with differences in the expression of the respective total pair. Results are representative of independent experiments performed with CM collected from two different donors and using RKO cells from different cellular passages.

phosphorylation levels of cancer cell cSrc (Y^{416}) and AKT (T^{202}/Y^{204}) were not fully concordant between distinct donors and between conditions. However, at day 7, at 1:1 ratio cSrc-phosphorylation seems to be decreased in comparison with macrophages and Treg-educated macrophages at 2:1 ratio. Altogether, these results suggest that similarly to macrophages, $CD4^+CD25^+$ T cell-educated macrophages may stimulate colorectal cancer

cell invasion through the activation of the EGFR pathway. Once more, the slightly differences in the ability of macrophage and of Treg-educated macrophages at 2:1 ratio to stimulate invasion cannot be explained by the EGFR-mediated signalling pathway.

FoxP3-positive cells infiltrate preferentially at the tumour nest and invasive front on human CRC specimens

Human CRC specimens obtained from a well characterized tissue and tumour data bank (Centro Hospitalar do Porto, Hospital de São João) were characterized by IHC for FoxP3$^+$ Tregs infiltration at 3 distinct regions, including the adjacent normal colonic mucosa (NCM), the tumour invasive front (IF) and the tumour nest (TN), using an anti-FOXP3 antibody (Figure 15). For this analysis only cases presenting the three regions within the same histological section were considered. The selection didn't have in consideration the patients' clinicopathological data, but the various cancer stages are represented. From the thirty specimens analysed, a significantly higher number of FoxP3-positive cells were found at both the TN (Non-parametric Mann-Whitney Test; P=0.007) and at the IF (Non-parametric Mann-Whitney Test; P=0.0002), comparing with NCM. These results suggest that, although not abundant, FoxP3$^+$ cells, most probably Tregs, are preferentially located within the tumour and invasive front than in the normal colonic mucosa. This is precisely the region were we previously observed more anti-inflammatory macrophages (data not shown), suggesting that the immune activity of these populations might be modulated by the existent cancer cells or even by FoxP3$^+$ cells.

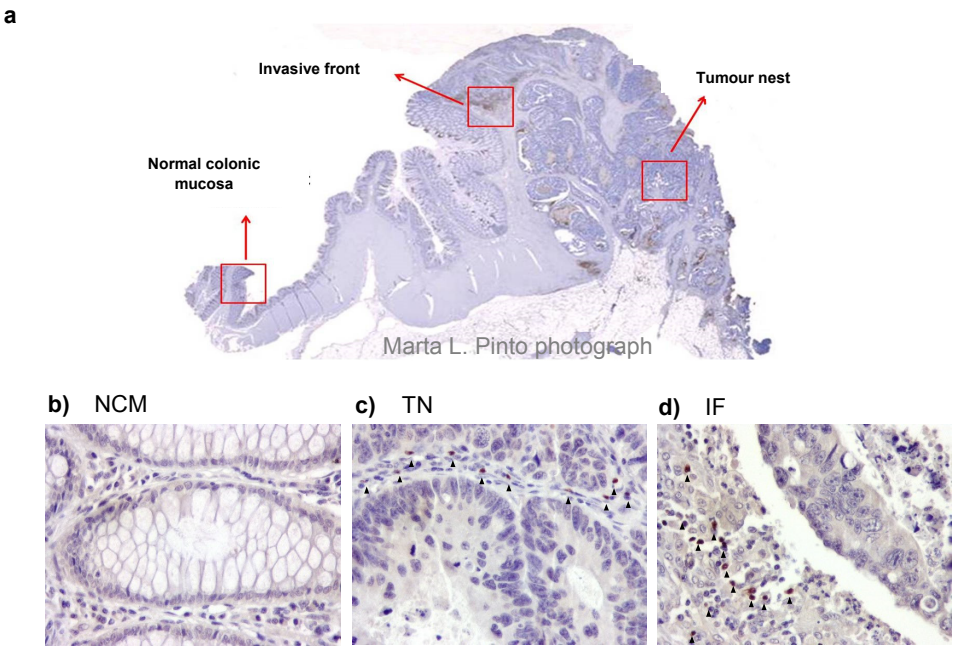

Figure 15. FoxP3–positive cells infiltrate preferentially the tumour nest and invasive front on human CRC specimens. **a) CRC** histologic section with the distinct regions analyzed: adjacent normal colon mucosa (NCM), tumour nest (TN) and Invasive front (IF).Immunohistochemically staining of FoxP3, a Treg lineage marker, on one representative case of CRC in the **b)** NCM, **c)** TN and **d)** IF. IHC staining of FoxP3 was visualized and counted at 400x magnification. Arrow heads indicate brown FoxP3-positive cells.

Table 1. Mean number of FoxP3 in normal colonic mucosa (NCM), tumour nest (TN) and invasive front (IF) from 30 different CRC cases. Foxp3=Forkhead box P3; SD=standard deviation.

Marker	NCM (Mean±SD)	TN (Mean±SD)	IF (Mean±SD)	NCM/TN (P value)	NCM/IF (P value)	TN/IF (P value)
FoxP3	3,40±4,66	8,47±7,11	11,46±7,97	NS	0,0002***	0,007**

, significantly different at P<0.01. *, significantly different at P<0.001.

Discussion

Tumour-associated macrophages and Tregs dominantly infiltrate tumours but their role on CRC fate is controversial. The impact of these immune populations on the regulation of each other cell activities and the relevance of such modulation on CRC progression are still to be unveiled. Therefore, we investigated the impact of $CD4^+CD25^+$ T cell populations on macrophage differentiation and the role of $CD4^+CD25^+$ Treg-educated macrophages on colorectal cancer cell invasion, dissecting the underling pro-invasive mechanisms. With this work, we demonstrated that: 1) macrophages alone constitute an heterogeneous population whereas, in the presence of $CD4^+CD25^+$T cells, macrophage pro-inflammatory phenotype was reduced, without achieving a full anti-inflammatory profile; 2) both macrophages and $CD4^+CD25^+$ T cell-educated macrophages induced RKO cancer cell invasion, being Treg-educated macrophages at 2:1 ratio the most efficient condition to promote invasion; 3) the pro-invasive activity of macrophages and $CD4^+CD25^+$ T cell-educated macrophages was concomitant with similar increase on pro-MMP9 proteolytic activity; 4) similarly to macrophages, $CD4^+CD25^+$ T cell-educated macrophages at 2:1 ratio, stimulate cancer cell EGFR phosphorylation and 5) $FoxP3^+$ cells accumulated preferentially at the tumour nest and at the invasive front than at the normal colonic mucosa of colorectal cancer human specimens.

Activation and differentiation of human monocytes into macrophages can be critically affected by culture conditions. Adherence is frequently considered an activation signal for monocytes[144] and the surface to which monocytes adhere can affect cell survival, morphology and ability to form adherent macrophage monolayers[145]. The seeding of monocytes on tissue culture treated polystyrene culture substrates contributed to poor cell survival and adherence, whereas polystyrene tissue culture non-treated and glass substrates favoured survival and monocyte-derived macrophage differentiation. The slight different levels of differentiation between these last conditions can be due to differences in cultured cell density: 6-well plates have $0{,}13 \times 10^6$ monocytes/cm^2 whereas in 24-well plates $0{,}26 \times 10^6$ monocytes/cm^2 were seeded, indicating that cells on 24-well plates have the possibility to establish more cell-to-cell contacts and to secrete autocrine factors that may favour differentiation and adhesion. Monocyte-derived macrophages differentiated, in the absence of exogenous stimuli, on 24-well plates with glass coverslips, became elongated and exhibited cell protrusions, resembling the *in vitro* anti-inflammatory like morphology also characteristic of non-stimulated heterogeneous macrophage populations[146].

In humans, regulatory T cells are phenotypically and functionally heterogeneous, but no specific cell surface markers have yet been described and their isolation still relies on the selection of $CD4^+CD25^{high}$ or sorting of $CD4^+CD25^{high}CD127^{low}$T cells from PBMCs[92]. In this study the limited access to the cell sorter infrastructure led us to rely on the selection of the $CD4^+CD25^{high}$ population and on its further characterization regarding FoxP3 expression. As assessed by FACS, isolation with regulatory T cell isolation kit from StemCell indicated that the majority of the isolated population expressed Treg markers. However the presence of a small $CD4^+CD25^{mid/low}$ T cell population could not be ruled out. The most reasonable explanation for this is the lack of defined boundaries between high and intermediated levels of CD25 expression cells during the magnetic selection of $CD25^{high}$ cells[92], leading to the inclusion of activated Tconvs that upregulate the expression of CD25 and FoxP3. Despite our reported high levels of $FoxP3^+$ T cells, a very small percentage of $CD4^+CD25^{mid/high}Fox3^{low}CD45RA^-$ non-Tregs and $CD4^+CD25^{mid/high}FoxP3^{low}CD45RA^+$ rTregs can also be present[92,95]. The most rigorous approach to discriminate functional $CD4^+CD25^+$Treg cells would be to sort this population further combining the cell surface marker CD127[96], which inversely correlates with intracellular expression of FoxP3, and also according to their active or resting state, taking advantage of CD45RA[95] and CD15s[98] cell surface markers. Interestingly, after seven days of culture, the reduced size and irregular morphology presented by the $CD4^+CD25^+$ T cell population was accompanied by FoxP3 expression reduction. These results are supported by other reports where long-term cultures decreased FoxP3 expression and suppressive properties of former potent Treg suppressor cells initially sorted as $CD4^+CD25^{high}CD45A^-$ T cell population[147].

In addition, our results showed that, in comparison with macrophages and co-cultures, the isolated $CD4^+CD25^+$ T cells display lower ability to reduce resazurin to resorufin but cell viability was not affected. This is not unexpected since, besides TCR stimulation by anti-CD3, the full activation of Tregs also requires CD28 co-stimulation. Anti-CD28 was not added in Tregs mono-cultures based on previous reports describing that macrophage also expressed low levels of this receptor[148]. Therefore, the addition of anti-CD28 to cultures could affect macrophage inflammatory profile. Additionally, $CD4^+CD25^+$ Treg cells are described to be hyporesponsive *in vitro*, as a result of their high susceptibility to apoptosis after activation and suppression[95]. Alltogether our results indicate that Tregs affected macrophage adhesion but not viability or metabolic activity. To further confirm these results more accurate viability assays and Tregs activation, by *in vitro* suppression assays, should be performed. The higher metabolic activity in 2:1 ratio, after 7 days of culture, can result

from a higher activity from both macrophages and $CD4^+CD25^{high}$ T cells. The level of anti-CD3 and CD28 co-stimulation provided by CD80/CD86 molecules on macrophages was the same in 1:1 and 2:1 ratios, however the stimuli per T cell is higher in 2:1 ratio due to the lower number of $CD4^+CD25^{high}$ T cells, potentiating their activity.

As expected[131], unstimulated macrophages resembled a naïve heterogeneous population, expressing both pro- and anti-inflammatory cell surface markers and secreting low levels of cytokines. In contrast, along time, $CD4^+CD25^+$ Treg-educated macrophages decreased CD80, a marker preferentially expressed by pro-inflammatory macrophages, and increased CD163, a marker of anti-inflammatory macrophages. These results suggest that $CD4^+CD25^+$ T cells induced macrophage polarization towards a more anti-inflammatory profile. However, the cytokine profile resembles of an active heterogeneous population with high levels of both pro- and anti-inflammatory cytokines. These results must be carefully analysed since only one experiment was used to evaluate conditioned medium cytokine levels. Nevertheless, these results suggest a pivotal role of $CD4^+CD25^+$ T cells in the modulation of macrophage towards a more anti-inflammatory-like phenotype. The loss of CD80 co-stimulatory molecule observed in co-cultures, represent a well-known mechanism of suppression where CTLA-4, highly expressed in Tregs, binds to CD80/CD86 in APCs leading to their downregulation, and consequently, affecting Tconvs and APCs cell-cell interactions[106]. In previous work reporting the skewing of monocyte/macrophages by Tregs towards an anti-inflammatory profile, the levels of the anti-inflammatory cell surface marker CD163 and especially of CD206 were upregulated[132]. Here, CD163 expression levels are still lower than in macrophages mono-culture although increasing along time. These results suggest that the increase of CD163 expression in co-cultures is slower than in macrophages mono-cultures and/or that this T cell population is not completely skewing macrophages towards an anti-inflammatory profile. The CD163 upregulation is dependent on IL-6 and IL-10 cytokines and is downregulated by IFN-γ, and TGF-β[149,150]. Interestingly, in our experiments, the levels of tTGF-β were similar in all conditions, suggesting that slight differences in CD163 expression were not dependent on this cytokine. These equal levels of tTGF-β are expected since the antibodies in tTGF-β ELISA do not permit to discriminate between cytokine active and inactive forms. Unexpectedly, the enhanced expression of IL-6 and the absence of IFN-γ in our co-cultures were not accompanied by an upregulation of CD163. On the other hand, $CD4^+CD25^+$ T cell-educated macrophages are described to display lower levels of IL-6 and IFN-γ than macrophages alone[132]. These results suggest that in Treg-macrophage co-cultures CD163 upregulation is associated with other factors,

such as IL-10, frequently secreted in these co-cultures. The unexpected high levels of both pro- (IL-6) and anti-inflammatory (tTGF-β) molecules obtained can be explained by the mixed profile presented by macrophages, secreting both pro- and anti- inflammatory cytokines, and/or by the heterogeneous FoxP3^{+} and FoxP3^{-} T cell populations. One of the possible origins for this FoxP3^{-} population are the CD4^{+}CD25^{-}FoxP3^{low} conventional T cells that, when freshly isolated expressed CD25$^{mid/low}$. Upon TCR in vitro stimulation these Tconvs are described to present a transient expression of FoxP3, but after long-term *in vitro* culture are able to revert to their conventional T cell phenotype[143,151]. This population is described to produce high levels of both pro- and anti-inflammatory cytokines after co-culture with monocytes, in comparison with their CD4^{+}CD25^{+}CD127^{low} counterparts[131,132]. Alternatively, but not exclusively, pro-inflammatory cytokines can derive from isolated CD4^{+}CD25^{+}FoxP3^{low}CD45RA^{-} non-Treg cell population or from FoxP3^{+} aTregs, which decreased FoxP3 expression and were induced to produce pro- and anti-inflammatory cytokines in co-culture with macrophages[95,152]. These hypotheses should be confirmed by re-purifying macrophages after co-culture and re-assess their inflammatory profile. The same procedure should be followed for CD4^{+} T cells, where the inflammatory profile and the immunosuppressive functions of T cells should be assessed.

Recently, macrophages were described to promote gastric and colorectal cancer cell invasion through the release of soluble pro-invasive factors[57,58]. Although the role of Tregs in cancer progression is not clear, based in breast, melanoma and pancreatic mouse cancer models, these immune cells seem to have an indirect role in cancer cell metastasis by favouring tumour immune evasion and tumour-promoting activities on other immune cells[117,118]. To our knowledge this was the first time that the pro-invasive properties of macrophages, differentiated in the presence of CD4^{+}CD25^{+} T cells, was assessed. We showed that, after long-term culture, RKO invasion was promoted by macrophages and by CD4^{+}CD25^{+} T cell-educated macrophages, but not by CD4^{+}CD25^{+} T cells alone. This indicates that CD4^{+}CD25^{+} T cell have no direct role on RKO cancer cell invasion but that, at 2:1 ratio, macrophage pro-invasive properties were enhanced. In contrast, SW620 invasion was not stimulated. Differences on the basal levels of invasiveness between RKO and SW620 cells may be related with intrinsic features of these cell lines. Due to the putative indirect role of Tregs and the reported direct role of macrophages on cancer cell invasion we sought to search for the underlying pro-invasive mechanisms mediated by macrophages on RKO cells.

Macrophage pro-invasive properties were described to be enhanced in anti-inflammatory macrophages rather than in their pro-inflammatory counterparts[58]. We hypothesized that, in the presence of Tregs and RKO, macrophages would acquire an anti-inflammatory profile, explaining their higher pro-invasive activity. Interestingly, Edin and collaborators described that macrophages stimulated with M-CSF and supernatant of RKO CRC cells, had more similarities with anti-inflammatory macrophages regarding cell surface markers while their cytokine secretion profile seemed to be of a "mixed" pro- and anti-inflammatory population[153]. Of note, M-CSF-derived macrophages are more active and tend to resemble *per si* an anti-inflammatory profile[153]. Our experiments are in agreement with this study, since $CD4^+CD25^+$ T cell-educated macrophages exhibited loss of the pro-inflammatory CD80 and maintained CD163 anti-inflammatory cell surface receptor. In contrast, cytokine expression revealed characteristics of a heterogeneous pro- and anti-inflammatory profile. mRNA expression pattern of different phenotypic markers as other cytokines and chemokines, and additional flow cytometry analysis, involving other cell surface receptors should be assessed to further confirm these results. Regarding cancer cell secretion profile, RKO did not seem to contribute to the high levels of cytokines detected in $CD4^+CD25^+$ T- macrophage cultures with RKO. To confirm this, macrophage-$CD4^+CD25^+$ T co-cultures, without indirect contact with RKO, should be considered in parallel. The limited number of isolated $CD4^+CD25^+$ T cells impaired this analysis. Importantly, these results also highlight that the secretion profile of 1:1 ratio at day 3 was only achieved by 2:1 cultures at day 7 (for IL-6, IFN-γ and TGF-β), indicating that the evolution of co-cultures was dependent on the proportion of T cells. Interestingly, IFN-γ, a factor involved in host defence, was not detected in mono- and co-cultures before invasion assay but was highly secreted when macrophage-$CD4^+CD25^+$ T cells were co-cultured with RKO, suggesting that factors produced by the cancer cells primed a pro-inflammatory response. This suggests that naïve macrophages could not initiate pro-inflammatory response, within the time points analysed, whereas the previous activation of macrophages by $CD4^+CD25^+$ T cells may induce a faster recognition and response to these factors[58].

The expression and activity of proteolytic enzymes, such as MMPs, have a crucial role on the modulation of cancer cell invasion, as they degrade the ECM releasing trapped pro-invasive and pro-motile factors, opening paths for cell migration[62]. MMP2 and MMP9 proteases are involved in colorectal cancer progression and are produced by macrophages, reinforcing their pro-invasive activities[57,58,154]. In this work only pro-MMP9 seems to explain the higher levels of invasion of RKO cells in indirect contact with macrophages and

macrophage-$CD4^+CD25^+$ T cells cultures. These results are consistent with our previous reports indicating that macrophages are major MMP9 producers and that macrophage-mediated cancer cell invasion was essentially related to MMP9 proteolytic activity[19]. Since $CD4^+CD25^+$ T cells and RKO produced low levels of these gelatinases, this study further suggests macrophages as the major pro-MMP9 producers and principal proteolysis contributors. Although not significant, the levels of pro-MMP9 seem to be higher in co-culture than in macrophage mono-cultures, in line with the higher invasive profile obtained in 2:1, but not in 1:1 ratio. The differences found between day 3 and 7 may rely on the higher immune cell differentiation status but also on the higher activity of MMP9 and MMP2 at day 7.

Cancer cells-derived CSF1 recruits and stimulates macrophages to produce EGF, which in turn activates cancer cells EGF receptor enhancing their invasion capability and motility[35]. The CFS1-EGF loop was highly described in breast cancer. Additionally, in *in vitro* colon cancer models, macrophage-derived EGF activated cancer cell EGFR phosphorylation, stimulating their invasion, motility and migration[57]. Our results also demonstrated that macrophages in mono- and co-cultures induced cancer cell EGFR tyrosine residue (Y^{1086}) phosphorylation, a cSrc docking and binding site[155]. The subsequent phosphorylation and activation of cSrc and of AKT were not fully validated. Nevertheless, $CD4^+CD25^+$ T cell-educated macrophages in 1:1 co-cultures seemed to induce low levels of RKO cells cSrc phosphorylation, which suggests that one of the differences between the ratios analysed, and respective ability to induce invasion, may underlie on EGFR-pathway activation. However, studies in further detail need to be perform to characterize other signalling pathways and factors possibly involved in the promotion of cancer cell invasion. Of note, the explanation for the different ability of macrophages and of $CD4^+CD25^+$ T-educated macrophages at 2:1 ratio to induce RKO cell invasion remains unclear. These findings provide support for the modulatory role of $CD4^+CD25^+$ T cells on the modulation of the macrophage profile and of the macrophage ability to induce cancer cell invasion and EGFR phosphorylation.

The role of Tregs on colorectal cancer is mostly correlated with favourable outcomes[121-125]. Here we reported that FoxP3-positive cells accumulate preferentially at the invasive front and at the tumour nest rather than at the normal colonic mucosa. Nevertheless, the reduced number of cases analysed did not allow us to establish any relation with patients' clinicopathological data and to assess their clinical relevance. As mentioned above, in humans, FoxP3 can be expressed in non-regulatory T cells or in

Tconvs[92]. Therefore, although FoxP3 is still referenced marker for IHC staining to characterize Tregs, the single use of this marker may overestimate their number. In CRC, the intratumoural accumulation of FoxP3$^+$ T cells has been correlated with good prognosis. The discordant results of Tregs prognosis significance may rely on different Tregs subpopulations (rTregs, aTregs, non-Tregs)[95] that accumulate at the tumour site. In melanoma tissues, higher accumulation of aTregs has been associated with worst prognosis[156]. In this sense, in CRC, the accumulation of non-Tregs cells would be correlated with better prognostic[129]. To further investigate the role of Tregs in CRC, other markers (such as CD4, CD25 and/or CD45RA+) should be combined with FoxP3 to assess active and resting Tregs infiltration at different tumour regions. Interestingly, our group previously observed anti-inflammatory, but not pro-inflammatory, macrophages at the tumour nest and invasive front of the same set of CRC specimens (MLPinto, unpublished results). Together with our results, we envisage that, in a colorectal cancer context, FoxP3$^+$ T cells and anti-inflammatory macrophages infiltrate at the same tumour region, interacting and modulating each other phenotype and functions. Therefore, the characterization of FoxP3$^+$ T cells subpopulations should be crossed with TAMs differentiation profile at the same CRC specimen and further correlated with patients' clinicopathological information.

Conclusions and future perspectives

In conclusion, this work suggests that $CD4^+CD25^+$ Tregs were successfully isolated, although a small population of $CD4^+CD25^{mid/low}$ T cells could not be ruled out. This stands out the need for a more rigorous Treg isolation method, for instance sorting this rare and heterogeneous population combining more Treg cell surface markers to specifically isolate suppressive Tregs from non-Tregs and Tconvs. To further assess Treg purity and function, the suppressive ability of Tregs on Tconvs proliferation and cytokine secretion *in vitro* should be investigated. This would allow to highlight the role of highly pure suppressive Treg subpopulation on macrophage differentiation.

Our *in vitro* co-culture findings provided support for the modulatory role of $CD4^+CD25^+$ T cells on macrophage morphology, adhesion, inflammatory profile and pro-invasive properties. $CD4^+CD25^+$ Tregs induced macrophage differentiation towards a more anti-inflammatory profile despite displaying a “mixed” cytokine secretion. However, these results should be further confirmed using quantitative analyses (FACS) of macrophage pro- and anti-inflammatory markers. Also, a broader range of cytokines/chemokines and a larger sample size should be analysed. Further, $CD4^+CD25^+$ T cells do not seem to display direct pro-invasive properties but they induced, at the 2:1 ratio, macrophage pro-invasive properties. These results were concomitant with an increase of pro-MMP9 proteolytic activity and EGFR-phosphorylation on macrophages and on Treg-educated macrophages co-cultured. However, the distinct role of different $CD4^+CD25^+$ T cells ratios on macrophage invasion related pathways remains to be elucidated. Nevertheless, it should be emphasized that the 2:1 ratio seems to be the most appropriated, since it better reflects the peripheral blood macrophage-Treg proportion. The higher ability of $CD4^+CD25^+$ T cell-educated macrophages, at 2:1 ratio, to induce RKO cell invasion, comparing with macrophage mono-cultures, should be further analysed. For this, other invasion-related pathways as well as factors reported to be involved in the promotion of cancer cell invasion should be examined, and a higher number of donors should be considered. In the future, we expect to further explore the putative modulatory role of Tregs on macrophage pro-tumoural properties, contributing to the design of novel therapeutic strategies targeting macrophages and/or Tregs. Of note, our work also demonstrated that $FoxP3^+$ cells accumulate preferentially at the intratumoural region and invasive front rather than at the normal colonic mucosa of colorectal cancer human specimens. Now, we intent to increase the number of cases analysed, further characterize $FoxP3^+$ subpopulations and cross this characterization on

CRC specimens with TAMs phenotypic profile and patients' clinicopathological information, to evaluate possible clinical associations.

Supplementary Data

a

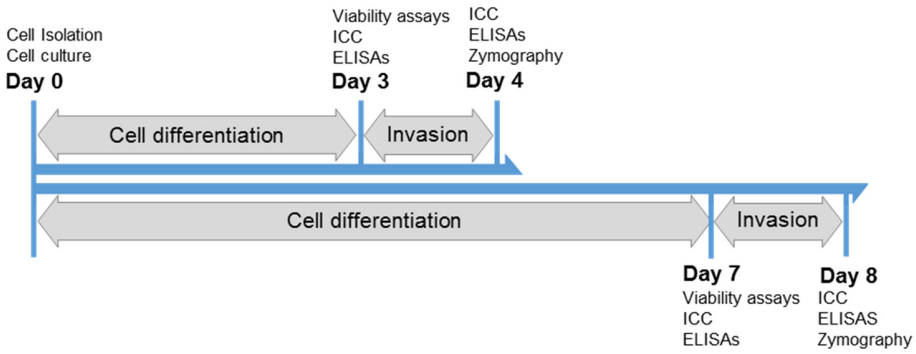

b

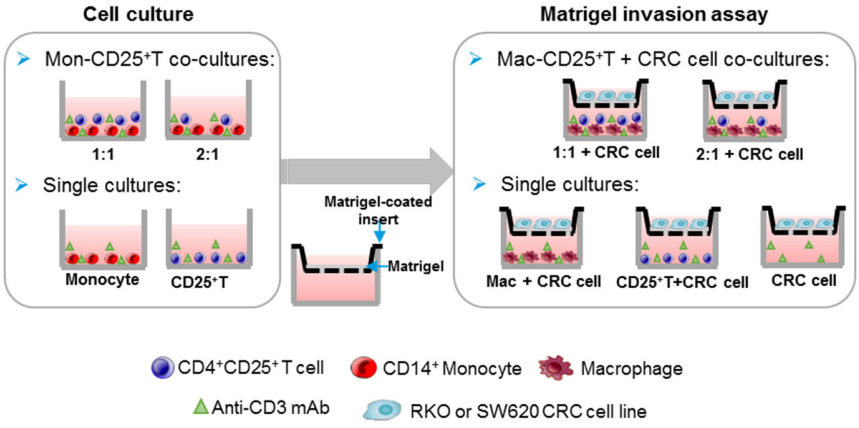

Figure S1. ***In vitro*** **experimental set-up performed to dissect CD4$^+$CD25$^+$ T-educated macrophages profile and pro-invasive properties. a)** Schematic time-line with methodology applied before or/and after invasion assays to assess cells viability, molecular phenotype by immunocytochemistry (ICC), secretion profile by enzyme-linked immunosorbent assays (ELISAs) and MMPs activity by zymography. At day 0 **b)** CD14$^+$ monocytes (Mon) and CD4$^+$CD25$^+$ T cells (CD25$^+$T) were isolated and seeded in co-cultures at 1:1 or 2:1 ratios or in single cultures for 3 or 7 days. After this time, RKO or SW620 human colon cancer cells (CRC cell) were incubated for 24h in the upper compartment of matrigel-coated invasion insert, in the presence of: RPMI medium (CRC cell), macrophages (Mac + CRC cell), CD4$^+$CD25$^+$ T cells (CD25$^+$ T + CRC cell), Mac and CD4$^+$CD25$^+$ T cells co–cultured at 1:1 or 2:1 ratio (1:1 + CRC cell or 2:1 + CRC cell).

Bibliography

1 Navin, N. *et al.* Inferring tumor progression from genomic heterogeneity. *Genome research* **20**, 68-80, doi:10.1101/gr.099622.109 (2010).
2 Dalerba, P. *et al.* Single-cell dissection of transcriptional heterogeneity in human colon tumors. *Nature biotechnology* **29**, 1120-1127, doi:10.1038/nbt.2038 (2011).
3 Elinav, E. *et al.* Inflammation-induced cancer: crosstalk between tumours, immune cells and microorganisms. *Nature reviews. Cancer* **13**, 759-771, doi:10.1038/nrc3611 (2013).
4 Siegel, R. L., Miller, K. D. & Jemal, A. Cancer statistics, 2015. *CA Cancer J Clin* **65**, 5-29, doi:10.3322/caac.21254 (2015).
5 Bishehsari, F., Mahdavinia, M., Vacca, M., Malekzadeh, R. & Mariani-Costantini, R. Epidemiological transition of colorectal cancer in developing countries: environmental factors, molecular pathways, and opportunities for prevention. *World journal of gastroenterology : WJG* **20**, 6055-6072, doi:10.3748/wjg.v20.i20.6055 (2014).
6 Wiseman, M. The second World Cancer Research Fund/American Institute for Cancer Research expert report. Food, nutrition, physical activity, and the prevention of cancer: a global perspective. *The Proceedings of the Nutrition Society* **67**, 253-256, doi:10.1017/S002966510800712X (2008).
7 Pernot, S. *et al.* Colorectal cancer and immunity: what we know and perspectives. *World journal of gastroenterology : WJG* **20**, 3738-3750, doi:10.3748/wjg.v20.i14.3738 (2014).
8 Cho, K. R. & Vogelstein, B. Genetic alterations in the adenoma--carcinoma sequence. *Cancer* **70**, 1727-1731 (1992).
9 Fearon, E. R. Molecular genetics of colorectal cancer. *Annual review of pathology* **6**, 479-507, doi:10.1146/annurev-pathol-011110-130235 (2011).
10 Fearnhead, N. S., Wilding, J. L. & Bodmer, W. F. Genetics of colorectal cancer: hereditary aspects and overview of colorectal tumorigenesis. *British medical bulletin* **64**, 27-43 (2002).
11 Rodriguez-Viciana, P. *et al.* Phosphatidylinositol-3-OH kinase as a direct target of Ras. *Nature* **370**, 527-532, doi:10.1038/370527a0 (1994).
12 Riley, T., Sontag, E., Chen, P. & Levine, A. Transcriptional control of human p53-regulated genes. *Nature reviews. Molecular cell biology* **9**, 402-412, doi:10.1038/nrm2395 (2008).
13 Grady, W. M. *et al.* Mutation of the type II transforming growth factor-beta receptor is coincident with the transformation of human colon adenomas to malignant carcinomas. *Cancer research* **58**, 3101-3104 (1998).
14 Lao, V. V. & Grady, W. M. Epigenetics and colorectal cancer. *Nature reviews. Gastroenterology & hepatology* **8**, 686-700, doi:10.1038/nrgastro.2011.173 (2011).
15 Jobin, C. Colorectal cancer: looking for answers in the microbiota. *Cancer discovery* **3**, 384-387, doi:10.1158/2159-8290.CD-13-0042 (2013).
16 Itzkowitz, S. H. & Yio, X. Inflammation and cancer IV. Colorectal cancer in inflammatory bowel disease: the role of inflammation. *American journal of physiology. Gastrointestinal and liver physiology* **287**, G7-17, doi:10.1152/ajpgi.00079.2004 (2004).
17 Nguyen, D. X., Bos, P. D. & Massague, J. Metastasis: from dissemination to organ-specific colonization. *Nature reviews. Cancer* **9**, 274-284, doi:10.1038/nrc2622 (2009).

18 Grivennikov, S. I., Greten, F. R. & Karin, M. Immunity, inflammation, and cancer. *Cell* **140**, 883-899, doi:10.1016/j.cell.2010.01.025 (2010).
19 Schreiber, R. D., Old, L. J. & Smyth, M. J. Cancer immunoediting: integrating immunity's roles in cancer suppression and promotion. *Science* **331**, 1565-1570, doi:10.1126/science.1203486 (2011).
20 Hanahan, D. & Coussens, L. M. Accessories to the crime: functions of cells recruited to the tumor microenvironment. *Cancer cell* **21**, 309-322, doi:10.1016/j.ccr.2012.02.022 (2012).
21 Junttila, M. R. & de Sauvage, F. J. Influence of tumour micro-environment heterogeneity on therapeutic response. *Nature* **501**, 346-354, doi:10.1038/nature12626 (2013).
22 Galon, J. *et al.* Type, density, and location of immune cells within human colorectal tumors predict clinical outcome. *Science* **313**, 1960-1964, doi:10.1126/science.1129139 (2006).
23 Balkwill, F. & Mantovani, A. Inflammation and cancer: back to Virchow? *Lancet* **357**, 539-545 (2001).
24 Allavena, P., Sica, A., Solinas, G., Porta, C. & Mantovani, A. The inflammatory micro-environment in tumor progression: the role of tumor-associated macrophages. *Crit Rev Oncol Hematol* **66**, 1-9 (2008).
25 Sica, A. & Mantovani, A. Macrophage plasticity and polarization: in vivo veritas. *The Journal of clinical investigation* **122**, 787-795, doi:10.1172/JCI59643 (2012).
26 De Kleer, I., Willems, F., Lambrecht, B. & Goriely, S. Ontogeny of myeloid cells. *Frontiers in immunology* **5**, 423, doi:10.3389/fimmu.2014.00423 (2014).
27 Ginhoux, F. & Jung, S. Monocytes and macrophages: developmental pathways and tissue homeostasis. *Nature reviews. Immunology* **14**, 392-404, doi:10.1038/nri3671 (2014).
28 Mantovani, A., Sozzani, S., Locati, M., Allavena, P. & Sica, A. Macrophage polarization: tumor-associated macrophages as a paradigm for polarized M2 mononuclear phagocytes. *Trends in immunology* **23**, 549-555 (2002).
29 Gordon, S. Alternative activation of macrophages. *Nature reviews. Immunology* **3**, 23-35 (2003).
30 Hazlett, L. D. *et al.* IL-33 shifts macrophage polarization, promoting resistance against Pseudomonas aeruginosa keratitis. *Investigative ophthalmology & visual science* **51**, 1524-1532, doi:10.1167/iovs.09-3983 (2010).
31 Pesce, J. *et al.* The IL-21 receptor augments Th2 effector function and alternative macrophage activation. *The Journal of clinical investigation* **116**, 2044-2055, doi:10.1172/JCI27727 (2006).
32 Sica, A., Schioppa, T., Mantovani, A. & Allavena, P. Tumour-associated macrophages are a distinct M2 polarised population promoting tumour progression: potential targets of anti-cancer therapy. *European journal of cancer* **42**, 717-727 (2006).
33 Noel, W., Raes, G., Hassanzadeh Ghassabeh, G., De Baetselier, P. & Beschin, A. Alternatively activated macrophages during parasite infections. *Trends in parasitology* **20**, 126-133, doi:10.1016/j.pt.2004.01.004 (2004).
34 Mantovani, A., Biswas, S. K., Galdiero, M. R., Sica, A. & Locati, M. Macrophage plasticity and polarization in tissue repair and remodelling. *The Journal of pathology* **229**, 176-185, doi:10.1002/path.4133 (2013).
35 Condeelis, J. & Pollard, J. W. Macrophages: obligate partners for tumor cell migration, invasion, and metastasis. *Cell* **124**, 263-266 (2006).

36 Martinez, F. O., Gordon, S., Locati, M. & Mantovani, A. Transcriptional profiling of the human monocyte-to-macrophage differentiation and polarization: new molecules and patterns of gene expression. *Journal of immunology* **177**, 7303-7311 (2006).
37 Medzhitov, R. & Horng, T. Transcriptional control of the inflammatory response. *Nature reviews. Immunology* **9**, 692-703, doi:10.1038/nri2634 (2009).
38 Mantovani, A. *et al.* The chemokine system in diverse forms of macrophage activation and polarization. *Trends in immunology* **25**, 677-686, doi:10.1016/j.it.2004.09.015 (2004).
39 Qian, B. Z. & Pollard, J. W. Macrophage diversity enhances tumor progression and metastasis. *Cell* **141**, 39-51, doi:10.1016/j.cell.2010.03.014 (2010).
40 Linde, N. *et al.* Vascular endothelial growth factor-induced skin carcinogenesis depends on recruitment and alternative activation of macrophages. *The Journal of pathology* **227**, 17-28, doi:10.1002/path.3989 (2012).
41 Giulia Marelli, P. A., Marco Erreni. Tumor-associated macrophages, multi-tasking cells in the cancer landscape. *Cancer Research Frontiers* **1**, 149-161, doi:10.17980/2015.149 (2015).
42 Coussens, L. M., Zitvogel, L. & Palucka, A. K. Neutralizing tumor-promoting chronic inflammation: a magic bullet? *Science* **339**, 286-291, doi:10.1126/science.1232227 (2013).
43 Chitu, V. & Stanley, E. R. Colony-stimulating factor-1 in immunity and inflammation. *Current opinion in immunology* **18**, 39-48, doi:10.1016/j.coi.2005.11.006 (2006).
44 Balkwill, F. Cancer and the chemokine network. *Nature reviews. Cancer* **4**, 540-550, doi:10.1038/nrc1388 (2004).
45 Balkwill, F. R. & Mantovani, A. Cancer-related inflammation: common themes and therapeutic opportunities. *Seminars in cancer biology* **22**, 33-40, doi:10.1016/j.semcancer.2011.12.005 (2012).
46 Jenkins, S. J. *et al.* Local macrophage proliferation, rather than recruitment from the blood, is a signature of TH2 inflammation. *Science* **332**, 1284-1288, doi:10.1126/science.1204351 (2011).
47 Schaper, F. & Rose-John, S. Interleukin-6: Biology, signaling and strategies of blockade. *Cytokine & growth factor reviews*, doi:10.1016/j.cytogfr.2015.07.004 (2015).
48 Coussens, L. M. & Werb, Z. Inflammation and cancer. *Nature* **420**, 860-867, doi:10.1038/nature01322 (2002).
49 Liu, Y., Li, P. K., Li, C. & Lin, J. Inhibition of STAT3 signaling blocks the anti-apoptotic activity of IL-6 in human liver cancer cells. *The Journal of biological chemistry* **285**, 27429-27439, doi:10.1074/jbc.M110.142752 (2010).
50 Balkwill, F. TNF-alpha in promotion and progression of cancer. *Cancer metastasis reviews* **25**, 409-416, doi:10.1007/s10555-006-9005-3 (2006).
51 Wyckoff, J. *et al.* A paracrine loop between tumor cells and macrophages is required for tumor cell migration in mammary tumors. *Cancer research* **64**, 7022-7029, doi:10.1158/0008-5472.CAN-04-1449 (2004).
52 Wyckoff, J. B. *et al.* Direct visualization of macrophage-assisted tumor cell intravasation in mammary tumors. *Cancer research* **67**, 2649-2656, doi:10.1158/0008-5472.CAN-06-1823 (2007).
53 Goswami, S. *et al.* Macrophages promote the invasion of breast carcinoma cells via a colony-stimulating factor-1/epidermal growth factor paracrine loop. *Cancer research* **65**, 5278-5283, doi:10.1158/0008-5472.CAN-04-1853 (2005).
54 Patsialou, A. *et al.* Invasion of human breast cancer cells in vivo requires both paracrine and autocrine loops involving the colony-stimulating factor-1 receptor. *Cancer research* **69**, 9498-9506, doi:10.1158/0008-5472.CAN-09-1868 (2009).

55 Lin, E. Y. *et al.* Macrophages regulate the angiogenic switch in a mouse model of breast cancer. *Cancer research* **66**, 11238-11246, doi:10.1158/0008-5472.CAN-06-1278 (2006).
56 Pignatelli, J. *et al.* Invasive breast carcinoma cells from patients exhibit MenaINV- and macrophage-dependent transendothelial migration. *Science signaling* **7**, ra112, doi:10.1126/scisignal.2005329 (2014).
57 Cardoso, A. P. *et al.* Macrophages stimulate gastric and colorectal cancer invasion through EGFR Y(1086), c-Src, Erk1/2 and Akt phosphorylation and smallGTPase activity. *Oncogene* **33**, 2123-2133 (2014).
58 Cardoso, A. P. *et al.* Matrix metalloproteases as maestros for the dual role of LPS- and IL-10-stimulated macrophages in cancer cell behaviour. *BMC cancer* **15**, 456, doi:10.1186/s12885-015-1466-8 (2015).
59 Hagemann, T. *et al.* Enhanced invasiveness of breast cancer cell lines upon co-cultivation with macrophages is due to TNF-alpha dependent up-regulation of matrix metalloproteases. *Carcinogenesis* **25**, 1543-1549, doi:10.1093/carcin/bgh146 (2004).
60 Sangaletti, S. *et al.* Macrophage-derived SPARC bridges tumor cell-extracellular matrix interactions toward metastasis. *Cancer research* **68**, 9050-9059, doi:10.1158/0008-5472.CAN-08-1327 (2008).
61 Quail, D. F. & Joyce, J. A. Microenvironmental regulation of tumor progression and metastasis. *Nature medicine* **19**, 1423-1437, doi:10.1038/nm.3394 (2013).
62 Hadler-Olsen, E., Winberg, J. O. & Uhlin-Hansen, L. Matrix metalloproteinases in cancer: their value as diagnostic and prognostic markers and therapeutic targets. *Tumour biology : the journal of the International Society for Oncodevelopmental Biology and Medicine* **34**, 2041-2051, doi:10.1007/s13277-013-0842-8 (2013).
63 Mantovani, A., Schioppa, T., Porta, C., Allavena, P. & Sica, A. Role of tumor-associated macrophages in tumor progression and invasion. *Cancer metastasis reviews* **25**, 315-322 (2006).
64 Bonde, A. K., Tischler, V., Kumar, S., Soltermann, A. & Schwendener, R. A. Intratumoral macrophages contribute to epithelial-mesenchymal transition in solid tumors. *BMC cancer* **12**, 35, doi:10.1186/1471-2407-12-35 (2012).
65 Kalluri, R. & Weinberg, R. A. The basics of epithelial-mesenchymal transition. *The Journal of clinical investigation* **119**, 1420-1428, doi:10.1172/JCI39104 (2009).
66 Hanahan, D. & Weinberg, R. A. Hallmarks of cancer: the next generation. *Cell* **144**, 646-674, doi:10.1016/j.cell.2011.02.013 (2011).
67 Motz, G. T. & Coukos, G. The parallel lives of angiogenesis and immunosuppression: cancer and other tales. *Nature reviews. Immunology* **11**, 702-711, doi:10.1038/nri3064 (2011).
68 Stockmann, C. *et al.* Deletion of vascular endothelial growth factor in myeloid cells accelerates tumorigenesis. *Nature* **456**, 814-818, doi:10.1038/nature07445 (2008).
69 Lin, E. Y. *et al.* Vascular endothelial growth factor restores delayed tumor progression in tumors depleted of macrophages. *Molecular oncology* **1**, 288-302, doi:10.1016/j.molonc.2007.10.003 (2007).
70 Noy, R. & Pollard, J. W. Tumor-associated macrophages: from mechanisms to therapy. *Immunity* **41**, 49-61, doi:10.1016/j.immuni.2014.06.010 (2014).
71 Noman, M. Z. *et al.* PD-L1 is a novel direct target of HIF-1alpha, and its blockade under hypoxia enhanced MDSC-mediated T cell activation. *The Journal of experimental medicine* **211**, 781-790, doi:10.1084/jem.20131916 (2014).
72 Sica, A. *et al.* Autocrine production of IL-10 mediates defective IL-12 production and NF-kappa B activation in tumor-associated macrophages. *Journal of immunology* **164**, 762-767 (2000).

73 Zhang, Q. W. *et al.* Prognostic significance of tumor-associated macrophages in solid tumor: a meta-analysis of the literature. *PloS one* **7**, e50946, doi:10.1371/journal.pone.0050946 (2012).
74 Erreni, M., Mantovani, A. & Allavena, P. Tumor-associated Macrophages (TAM) and Inflammation in Colorectal Cancer. *Cancer microenvironment : official journal of the International Cancer Microenvironment Society* **4**, 141-154 (2011).
75 Bailey, C. *et al.* Chemokine expression is associated with the accumulation of tumour associated macrophages (TAMs) and progression in human colorectal cancer. *Clinical & experimental metastasis* **24**, 121-130 (2007).
76 Kang, J. C., Chen, J. S., Lee, C. H., Chang, J. J. & Shieh, Y. S. Intratumoral macrophage counts correlate with tumor progression in colorectal cancer. *Journal of surgical oncology* **102**, 242-248 (2010).
77 Forssell, J. *et al.* High macrophage infiltration along the tumor front correlates with improved survival in colon cancer. *Clinical cancer research : an official journal of the American Association for Cancer Research* **13**, 1472-1479 (2007).
78 Edin, S. *et al.* The distribution of macrophages with a M1 or M2 phenotype in relation to prognosis and the molecular characteristics of colorectal cancer. *PloS one* **7**, e47045 (2012).
79 Edin, S., Wikberg, M. L., Oldenborg, P. A. & Palmqvist, R. Macrophages: Good guys in colorectal cancer. *Oncoimmunology* **2**, e23038, doi:10.4161/onci.23038 (2013).
80 Murray, P. J. *et al.* Macrophage activation and polarization: nomenclature and experimental guidelines. *Immunity* **41**, 14-20 (2014).
81 Sakaguchi, S. Naturally arising Foxp3-expressing CD25+CD4+ regulatory T cells in immunological tolerance to self and non-self. *Nature immunology* **6**, 345-352, doi:10.1038/ni1178 (2005).
82 Sakaguchi, S., Yamaguchi, T., Nomura, T. & Ono, M. Regulatory T cells and immune tolerance. *Cell* **133**, 775-787, doi:10.1016/j.cell.2008.05.009 (2008).
83 Hsieh, C. S., Lee, H. M. & Lio, C. W. Selection of regulatory T cells in the thymus. *Nature reviews. Immunology* **12**, 157-167, doi:10.1038/nri3155 (2012).
84 Paiva, R. S. *et al.* Recent thymic emigrants are the preferential precursors of regulatory T cells differentiated in the periphery. *Proceedings of the National Academy of Sciences of the United States of America* **110**, 6494-6499, doi:10.1073/pnas.1221955110 (2013).
85 Shevach, E. M. From vanilla to 28 flavors: multiple varieties of T regulatory cells. *Immunity* **25**, 195-201, doi:10.1016/j.immuni.2006.08.003 (2006).
86 Baecher-Allan, C., Brown, J. A., Freeman, G. J. & Hafler, D. A. CD4+CD25high regulatory cells in human peripheral blood. *Journal of immunology* **167**, 1245-1253 (2001).
87 Sakaguchi, S., Sakaguchi, N., Asano, M., Itoh, M. & Toda, M. Immunologic self-tolerance maintained by activated T cells expressing IL-2 receptor alpha-chains (CD25). Breakdown of a single mechanism of self-tolerance causes various autoimmune diseases. *Journal of immunology* **155**, 1151-1164 (1995).
88 Roncador, G. *et al.* Analysis of FOXP3 protein expression in human CD4+CD25+ regulatory T cells at the single-cell level. *European journal of immunology* **35**, 1681-1691 (2005).
89 Fontenot, J. D., Gavin, M. A. & Rudensky, A. Y. Foxp3 programs the development and function of CD4+CD25+ regulatory T cells. *Nature immunology* **4**, 330-336 (2003).
90 Huehn, J., Polansky, J. K. & Hamann, A. Epigenetic control of FOXP3 expression: the key to a stable regulatory T-cell lineage? *Nature reviews. Immunology* **9**, 83-89, doi:10.1038/nri2474 (2009).

91 Hoeppli, R. E., Wu, D., Cook, L. & Levings, M. K. The environment of regulatory T cell biology: cytokines, metabolites, and the microbiome. *Frontiers in immunology* **6**, 61, doi:10.3389/fimmu.2015.00061 (2015).
92 Sakaguchi, S., Miyara, M., Costantino, C. M. & Hafler, D. A. FOXP3+ regulatory T cells in the human immune system. *Nature reviews. Immunology* **10**, 490-500 (2010).
93 Zhou, X. *et al.* Isolation of purified and live Foxp3+ regulatory T cells using FACS sorting on scatter plot. *Journal of molecular cell biology* **2**, 164-169, doi:10.1093/jmcb/mjq007 (2010).
94 Allan, S. E. *et al.* Activation-induced FOXP3 in human T effector cells does not suppress proliferation or cytokine production. *International immunology* **19**, 345-354, doi:10.1093/intimm/dxm014 (2007).
95 Miyara, M. *et al.* Functional delineation and differentiation dynamics of human CD4+ T cells expressing the FoxP3 transcription factor. *Immunity* **30**, 899-911, doi:10.1016/j.immuni.2009.03.019 (2009).
96 Liu, W. *et al.* CD127 expression inversely correlates with FoxP3 and suppressive function of human CD4+ T reg cells. *The Journal of experimental medicine* **203**, 1701-1711, doi:10.1084/jem.20060772 (2006).
97 Baecher-Allan, C., Wolf, E. & Hafler, D. A. MHC class II expression identifies functionally distinct human regulatory T cells. *Journal of immunology* **176**, 4622-4631 (2006).
98 Miyara, M. *et al.* Sialyl Lewis x (CD15s) identifies highly differentiated and most suppressive FOXP3high regulatory T cells in humans. *Proceedings of the National Academy of Sciences of the United States of America* **112**, 7225-7230, doi:10.1073/pnas.1508224112 (2015).
99 Yurchenko, E. *et al.* Inflammation-driven reprogramming of CD4+ Foxp3+ regulatory T cells into pathogenic Th1/Th17 T effectors is abrogated by mTOR inhibition in vivo. *PloS one* **7**, e35572, doi:10.1371/journal.pone.0035572 (2012).
100 Vieira, P. L. *et al.* IL-10-secreting regulatory T cells do not express Foxp3 but have comparable regulatory function to naturally occurring CD4+CD25+ regulatory T cells. *Journal of immunology* **172**, 5986-5993 (2004).
101 Chen, W. *et al.* Conversion of peripheral CD4+CD25- naive T cells to CD4+CD25+ regulatory T cells by TGF-beta induction of transcription factor Foxp3. *The Journal of experimental medicine* **198**, 1875-1886 (2003).
102 Schmidt, A., Oberle, N. & Krammer, P. H. Molecular mechanisms of treg-mediated T cell suppression. *Frontiers in immunology* **3**, 51, doi:10.3389/fimmu.2012.00051 (2012).
103 Strauss, L. *et al.* A unique subset of CD4+CD25highFoxp3+ T cells secreting interleukin-10 and transforming growth factor-beta1 mediates suppression in the tumor microenvironment. *Clinical cancer research : an official journal of the American Association for Cancer Research* **13**, 4345-4354, doi:10.1158/1078-0432.CCR-07-0472 (2007).
104 Hall, B. M., Verma, N. D., Tran, G. T. & Hodgkinson, S. J. Distinct regulatory CD4+T cell subsets; differences between naive and antigen specific T regulatory cells. *Current opinion in immunology* **23**, 641-647, doi:10.1016/j.coi.2011.07.012 (2011).
105 Fallarino, F. *et al.* Modulation of tryptophan catabolism by regulatory T cells. *Nature immunology* **4**, 1206-1212, doi:10.1038/ni1003 (2003).
106 Schmidt, A. *et al.* Human regulatory T cells rapidly suppress T cell receptor-induced Ca(2+), NF-kappaB, and NFAT signaling in conventional T cells. *Science signaling* **4**, ra90, doi:10.1126/scisignal.2002179 (2011).
107 Zou, W. Regulatory T cells, tumour immunity and immunotherapy. *Nature reviews. Immunology* **6**, 295-307, doi:10.1038/nri1806 (2006).

108 Bonertz, A. *et al.* Antigen-specific Tregs control T cell responses against a limited repertoire of tumor antigens in patients with colorectal carcinoma. *The Journal of clinical investigation* **119**, 3311-3321, doi:10.1172/JCI39608 (2009).
109 Mougiakakos, D., Choudhury, A., Lladser, A., Kiessling, R. & Johansson, C. C. Regulatory T cells in cancer. *Advances in cancer research* **107**, 57-117, doi:10.1016/S0065-230X(10)07003-X (2010).
110 Liu, J. *et al.* Tumor-associated macrophages recruit CCR6+ regulatory T cells and promote the development of colorectal cancer via enhancing CCL20 production in mice. *PloS one* **6**, e19495, doi:10.1371/journal.pone.0019495 (2011).
111 Curiel, T. J. *et al.* Specific recruitment of regulatory T cells in ovarian carcinoma fosters immune privilege and predicts reduced survival. *Nature medicine* **10**, 942-949, doi:10.1038/nm1093 (2004).
112 Quezada, S. A., Peggs, K. S., Simpson, T. R. & Allison, J. P. Shifting the equilibrium in cancer immunoediting: from tumor tolerance to eradication. *Immunological reviews* **241**, 104-118, doi:10.1111/j.1600-065X.2011.01007.x (2011).
113 Ghiringhelli, F. *et al.* Tumor cells convert immature myeloid dendritic cells into TGF-beta-secreting cells inducing CD4+CD25+ regulatory T cell proliferation. *The Journal of experimental medicine* **202**, 919-929, doi:10.1084/jem.20050463 (2005).
114 Bergmann, C. *et al.* T regulatory type 1 cells in squamous cell carcinoma of the head and neck: mechanisms of suppression and expansion in advanced disease. *Clinical cancer research : an official journal of the American Association for Cancer Research* **14**, 3706-3715, doi:10.1158/1078-0432.CCR-07-5126 (2008).
115 Mougiakakos, D. Regulatory T cells in colorectal cancer: from biology to prognostic relevance. *Cancers* **3**, 1708-1731, doi:10.3390/cancers3021708 (2011).
116 Curti, A. *et al.* Modulation of tryptophan catabolism by human leukemic cells results in the conversion of CD25- into CD25+ T regulatory cells. *Blood* **109**, 2871-2877, doi:10.1182/blood-2006-07-036863 (2007).
117 Byrne, W. L., Mills, K. H., Lederer, J. A. & O'Sullivan, G. C. Targeting regulatory T cells in cancer. *Cancer research* **71**, 6915-6920, doi:10.1158/0008-5472.CAN-11-1156 (2011).
118 Kitamura, T., Qian, B. Z. & Pollard, J. W. Immune cell promotion of metastasis. *Nature reviews. Immunology* **15**, 73-86, doi:10.1038/nri3789 (2015).
119 Sato, E. *et al.* Intraepithelial CD8+ tumor-infiltrating lymphocytes and a high CD8+/regulatory T cell ratio are associated with favorable prognosis in ovarian cancer. *Proceedings of the National Academy of Sciences of the United States of America* **102**, 18538-18543 (2005).
120 Nishikawa, H. & Sakaguchi, S. Regulatory T cells in tumor immunity. *International journal of cancer. Journal international du cancer* **127**, 759-767, doi:10.1002/ijc.25429 (2010).
121 Frey, D. M. *et al.* High frequency of tumor-infiltrating FOXP3(+) regulatory T cells predicts improved survival in mismatch repair-proficient colorectal cancer patients. *International journal of cancer. Journal international du cancer* **126**, 2635-2643 (2010).
122 Salama, P. *et al.* Tumor-infiltrating FOXP3+ T regulatory cells show strong prognostic significance in colorectal cancer. *Journal of clinical oncology : official journal of the American Society of Clinical Oncology* **27**, 186-192, doi:10.1200/JCO.2008.18.7229 (2009).
123 Suzuki, H., Onishi, H., Morisaki, T., Tanaka, M. & Katano, M. Intratumoral FOXP3+VEGFR2+ regulatory T cells are predictive markers for recurrence and survival in patients with colorectal cancer. *Clinical immunology* **146**, 26-33, doi:10.1016/j.clim.2012.10.007 (2013).

124 Huang, Y. *et al.* Prognostic value of tumor-infiltrating FoxP3+ T cells in gastrointestinal cancers: a meta analysis. *PloS one* **9**, e94376, doi:10.1371/journal.pone.0094376 (2014).
125 Ling, A., Edin, S., Wikberg, M. L., Oberg, A. & Palmqvist, R. The intratumoural subsite and relation of CD8(+) and FOXP3(+) T lymphocytes in colorectal cancer provide important prognostic clues. *British journal of cancer* **110**, 2551-2559, doi:10.1038/bjc.2014.161 (2014).
126 Correale, P. *et al.* Regulatory (FoxP3+) T-cell tumor infiltration is a favorable prognostic factor in advanced colon cancer patients undergoing chemo or chemoimmunotherapy. *Journal of immunotherapy* **33**, 435-441, doi:10.1097/CJI.0b013e3181d32f01 (2010).
127 Wang, Q., Feng, M., Yu, T., Liu, X. & Zhang, P. Intratumoral regulatory T cells are associated with suppression of colorectal carcinoma metastasis after resection through overcoming IL-17 producing T cells. *Cellular immunology* **287**, 100-105, doi:10.1016/j.cellimm.2014.01.002 (2014).
128 Ladoire, S., Martin, F. & Ghiringhelli, F. Prognostic role of FOXP3+ regulatory T cells infiltrating human carcinomas: the paradox of colorectal cancer. *Cancer immunology, immunotherapy : CII* **60**, 909-918, doi:10.1007/s00262-011-1046-y (2011).
129 Nishikawa, H. Regulatory T cells in cancer immunotherapy. *[Rinsho ketsueki] The Japanese journal of clinical hematology* **55**, 2183-2189 (2014).
130 Nishikawa, H. & Sakaguchi, S. Regulatory T cells in cancer immunotherapy. *Current opinion in immunology* **27**, 1-7, doi:10.1016/j.coi.2013.12.005 (2014).
131 Taams, L. S. *et al.* Modulation of monocyte/macrophage function by human CD4+CD25+ regulatory T cells. *Human immunology* **66**, 222-230 (2005).
132 Tiemessen, M. M. *et al.* CD4+CD25+Foxp3+ regulatory T cells induce alternative activation of human monocytes/macrophages. *Proceedings of the National Academy of Sciences of the United States of America* **104**, 19446-19451, doi:10.1073/pnas.0706832104 (2007).
133 Kryczek, I. *et al.* Cutting edge: induction of B7-H4 on APCs through IL-10: novel suppressive mode for regulatory T cells. *Journal of immunology* **177**, 40-44 (2006).
134 Nakamura, K. *et al.* TGF-beta 1 plays an important role in the mechanism of CD4+CD25+ regulatory T cell activity in both humans and mice. *Journal of immunology* **172**, 834-842 (2004).
135 Weirather, J. *et al.* Foxp3+ CD4+ T cells improve healing after myocardial infarction by modulating monocyte/macrophage differentiation. *Circulation research* **115**, 55-67, doi:10.1161/CIRCRESAHA.115.303895 (2014).
136 Zeng, H. & Chi, H. Metabolic control of regulatory T cell development and function. *Trends in immunology* **36**, 3-12, doi:10.1016/j.it.2014.08.003 (2015).
137 Savage, N. D. *et al.* Human anti-inflammatory macrophages induce Foxp3+ GITR+ CD25+ regulatory T cells, which suppress via membrane-bound TGFbeta-1. *Journal of immunology* **181**, 2220-2226 (2008).
138 Zhou, J. *et al.* Increased intratumoral regulatory T cells are related to intratumoral macrophages and poor prognosis in hepatocellular carcinoma patients. *International journal of cancer. Journal international du cancer* **125**, 1640-1648 (2009).
139 Murai, M. *et al.* Interleukin 10 acts on regulatory T cells to maintain expression of the transcription factor Foxp3 and suppressive function in mice with colitis. *Nature immunology* **10**, 1178-1184, doi:10.1038/ni.1791 (2009).
140 Cao, Q. *et al.* IL-10/TGF-beta-modified macrophages induce regulatory T cells and protect against adriamycin nephrosis. *Journal of the American Society of Nephrology : JASN* **21**, 933-942, doi:10.1681/ASN.2009060592 (2010).

141 Walter, G. J. *et al.* Interaction with activated monocytes enhances cytokine expression and suppressive activity of human CD4+CD45ro+CD25+CD127(low) regulatory T cells. *Arthritis and rheumatism* **65**, 627-638, doi:10.1002/art.37832 (2013).
142 Oliveira, M. J. *et al.* Beta-casein-derived peptides, produced by bacteria, stimulate cancer cell invasion and motility. *The EMBO journal* **22**, 6161-6173, doi:10.1093/emboj/cdg586 (2003).
143 Dieckmann, D., Plottner, H., Berchtold, S., Berger, T. & Schuler, G. Ex vivo isolation and characterization of CD4(+)CD25(+) T cells with regulatory properties from human blood. *The Journal of experimental medicine* **193**, 1303-1310 (2001).
144 Shaw, R. J., Doherty, D. E., Ritter, A. G., Benedict, S. H. & Clark, R. A. Adherence-dependent increase in human monocyte PDGF(B) mRNA is associated with increases in c-fos, c-jun, and EGR2 mRNA. *The Journal of cell biology* **111**, 2139-2148 (1990).
145 Johnson, W. D., Jr., Mei, B. & Cohn, Z. A. The separation, long-term cultivation, and maturation of the human monocyte. *The Journal of experimental medicine* **146**, 1613-1626 (1977).
146 McWhorter, F. Y., Wang, T., Nguyen, P., Chung, T. & Liu, W. F. Modulation of macrophage phenotype by cell shape. *Proceedings of the National Academy of Sciences of the United States of America* **110**, 17253-17258, doi:10.1073/pnas.1308887110 (2013).
147 Hoffmann, P. *et al.* Loss of FOXP3 expression in natural human CD4+CD25+ regulatory T cells upon repetitive in vitro stimulation. *European journal of immunology* **39**, 1088-1097, doi:10.1002/eji.200838904 (2009).
148 Sandilands, G. P. *et al.* Were monocytes responsible for initiating the cytokine storm in the TGN1412 clinical trial tragedy? *Clinical and experimental immunology* **162**, 516-527, doi:10.1111/j.1365-2249.2010.04264.x (2010).
149 Sulahian, T. H. *et al.* Human monocytes express CD163, which is upregulated by IL-10 and identical to p155. *Cytokine* **12**, 1312-1321, doi:10.1006/cyto.2000.0720 (2000).
150 Pioli, P. A., Goonan, K. E., Wardwell, K. & Guyre, P. M. TGF-beta regulation of human macrophage scavenger receptor CD163 is Smad3-dependent. *Journal of leukocyte biology* **76**, 500-508, doi:10.1189/jlb.1203617 (2004).
151 Tran, D. Q., Ramsey, H. & Shevach, E. M. Induction of FOXP3 expression in naive human CD4+FOXP3 T cells by T-cell receptor stimulation is transforming growth factor-beta dependent but does not confer a regulatory phenotype. *Blood* **110**, 2983-2990, doi:10.1182/blood-2007-06-094656 (2007).
152 Voo, K. S. *et al.* Identification of IL-17-producing FOXP3+ regulatory T cells in humans. *Proceedings of the National Academy of Sciences of the United States of America* **106**, 4793-4798, doi:10.1073/pnas.0900408106 (2009).
153 Edin, S., Wikberg, M. L., Rutegard, J., Oldenborg, P. A. & Palmqvist, R. Phenotypic skewing of macrophages in vitro by secreted factors from colorectal cancer cells. *PloS one* **8**, e74982 (2013).
154 Foda, H. D. & Zucker, S. Matrix metalloproteinases in cancer invasion, metastasis and angiogenesis. *Drug discovery today* **6**, 478-482 (2001).
155 Lombardo, C. R., Consler, T. G. & Kassel, D. B. In vitro phosphorylation of the epidermal growth factor receptor autophosphorylation domain by c-src: identification of phosphorylation sites and c-src SH2 domain binding sites. *Biochemistry* **34**, 16456-16466 (1995).
156 Sugiyama, D. *et al.* Anti-CCR4 mAb selectively depletes effector-type FoxP3+CD4+ regulatory T cells, evoking antitumor immune responses in humans. *Proceedings of*

the National Academy of Sciences of the United States of America **110**, 17945-17950, doi:10.1073/pnas.1316796110 (2013).